CHAPTER 1

INTRODUCTION

1.1. General

The palm oil industry is notably one of the most important contributors to Malaysian's economy. Malaysia produces and exports 49.5% and 64.5% respectively, of the world's total palm oil and its products. In 2011, approximately 5.0 million hectares of land in Malaysia were under oil palm cultivation, accounting for 14.51 % of the total land area (Malaysian Palm Oil Board, 2011). Research has been intense on the palm oil itself as well as agricultural productivity, but sustainability concerns have inevitably led to many research topics on the by-products and treatment technologies. The process flow diagram of extraction of crude palm oil is depicted in Figure 1.1. After transportation of the fresh fruit bunches (FFB) to the mills for processing, they are sterilized at 140°C, 3 bar for 75-90 min. The wastewater from sterilizer condensate is the major source of liquid effluent (Thani *et al.*, 1999).

In the next stage, to strip the fruits from their bunches, the FFBs are fed to a rotary drum-stripper and then discharged into a digester. The fruits are mashed in the digester by the rotating arms. At this stage, the oil-bearing cells of the mesocarp are broken from the mashing of the fruits under heating. Twin screw presses are applied to extract the oil from the digested mash of fruit under high pressure. To increase the flow of the oil, hot water is added. The crude oil slurry for oil separation and purification is then fed to a clarification system (Thani *et al.,* 1999).

The crude palm oil (CPO) from the screw presses is then pumped to a clarification tank (horizontal or vertical) for oil separation. The clarified oil is skimmed-off from the top of the clarification tank. Before sending oil to the storage tank, it is passed through a high speed centrifuge and a vacuum dryer. Hydrocyclone is usually used to separate the kernels and shells. The last source of wastewater flow is a discharge

from this process (Chow and Ho, 2000). Figure 1.2 depicts the general mass balance of different products generated from a palm oil mill.

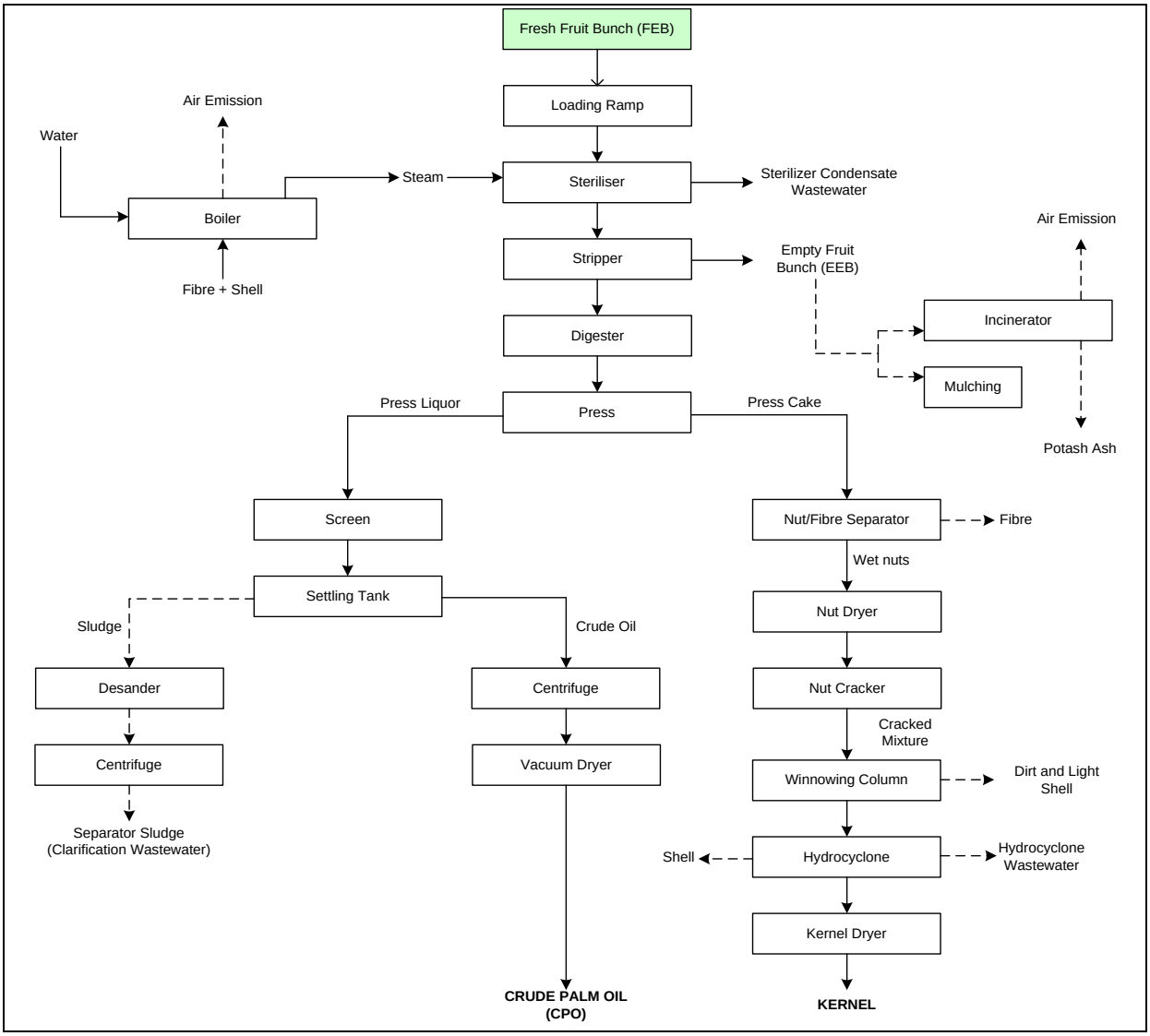

Figure 1.1. Typical palm oil extraction process and sources of wastewater production (Thani *et al.*, 1999)

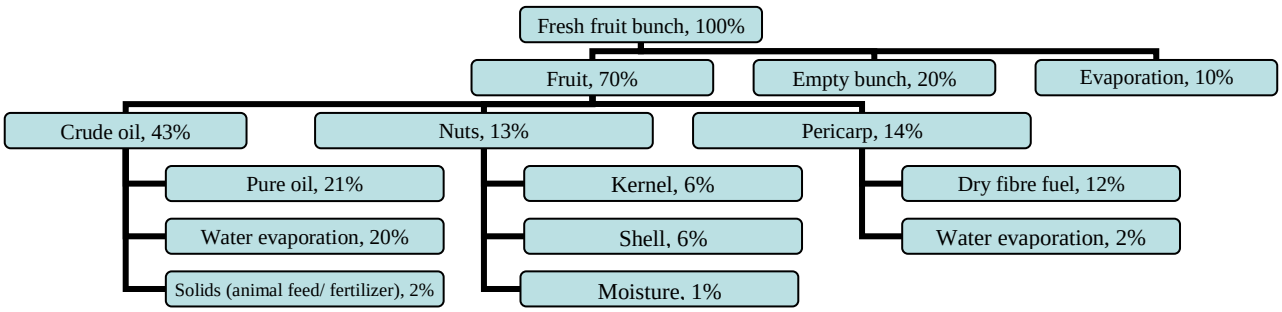

Figure 1.2. Characteristics fruit and generation composition chart of a palm oil mill (Muttamara *et al.*, 1987)

This industry generates large quantities of polluted wastewater commonly known as palm oil mill effluent (POME). It is estimated that 5-7.5 tonnes of water is required for each tonne of crude palm oil production; and more than 50% of the water becomes POME (Ahmad *et al.*, 2003; Zinatizadeh *et al.*, 2006). Based on palm oil production industry in Malaysia, 15.2 million tonnes of POME has been produced in 2005 alone (Malaysia Palm Oil Production Council, 2006). Three main sources of the POME are sterilization (36%), clarification (60%), and hydrocyclone (4%) units. Raw POME as a colloidal suspension contains 95–96% water, 0.6–0.7% oil and 4–5% total solids (Ma, 2000). It contains different suspended components including short fibres, cell walls, carbohydrates (from hemicellulose to simple sugars), free organic acids, nitrogenous compounds (from proteins to amino acids), and minor organic and mineral constituents (Ugoji, 1997). The fresh POME is a hot and acidic brownish wastewater. Table 1.1 shows the typical characteristics of POME.

Table 1.1. Typical characteristics of POME (Ma, 2000)

Parameter	**Average***	**Parameter**	**Average***
Chemical Oxygen Demand (COD)	50000	Phosphorous	180
Biochemical Oxygen Demand (BOD_5)	25000	Potassium	2270
Total Solids	40500	Magnesium	615
Suspended Solids	18000	Calcium	439
Total Volatile Solids	34000	Boron	7.6
Total Nitrogen	750	Iron	46.5
Ammoniacal Nitrogen	35	Manganese	2.0
Oil and Grease	4000	Copper	0.89
pH	4.7	Zinc	2.3

*All in mg/l except pH.

Nowadays, fossil fuels are the primary source of global energy requirements, with their foreseeable depletion due to limited fossil energy resource (Lin and Lay, 2004; Atif *et al.*, 2005; Ginkel *et al.*, 2005; Leite *et al.*, 2008; Zadariana *et al.*, 2009). With respect to global environmental impacts due to the usages of this energy resource,

such as greenhouse effect, ozone layer depletion and resource recovery, intensive search is going on worldwide towards renewable and non-polluting energy source. Hydrogen (H_2) is considered to be a promising fuel due to its high-energy yield (122 kJ/g) and eco-friendliness (Atif *et al.,* 2005; Cheong *et al.,* 2007; Mohan *et al.,* 2007; Wu and Chang, 2007; Younesi *et al.,* 2008; Zhang *et al.,* 2008 ; Leite *et al.,* 2008; Zadariana *et al.,* 2009; Antonopoulou et al., 2011). H_2 is generated mostly from fossil fuels, biomass and water. Thermo-catalytic and gasification processes using natural gas as a starting material, naphtha composition and heavy oils are the next largest source to produce the H_2 gas, followed by coal, and only 4% is produced from water using electricity (Li *et al.,* 2008). Most H_2 gas is presently generated from nonrenewable sources such as natural gas (50%), petroleum-derived napthenes and distillates (30%), coal (18%), or electricity produced from a variety of fuels (2%) (Lay, 2000). Anaerobic fermentation technology to produce H_2 has become a worldwide focus of research due to increasing demand for energy, cost saving and the protection of the environment.

The energy production potential of biomass has been estimated to be about 5% of Malaysian electricity demand (EPU, 1999). Thus, Malaysian government has identified renewable energy as the fifth fuel alternative (Energy Commission, 2002).

Several studies on biohydrogen production from POME have been accomplished using different reactors such as anaerobic contact filter (ACF), up-flow anaerobic sludge blanket (UASB) (Huang *et al.,* 2004), anaerobic sequencing batch reactor (ASBR), batch reactors (i.e. fermentors and serum bottles) (Atif *et al.,* 2005; Krishnan and Desa, 2006; Chong *et al.,* 2009; Prasertsan *et al.,* 2009; Suwnsaard *et al.,* 2009; Ismail *et al.,* 2010). The up flow anaerobic sludge blanket (UASB) reactor due to its ability to keep high microorganism concentration within and high rate of waste stabilization in the reactor, is an alternative bioreactor to generate biological hydrogen. The long start-up period (2-4 months), high and very low up-flow velocities, and granules washout at

hydraulic stresses are the major problems associated with UASB reactors. Therefore, the UASB process modification is needed to eliminate the existing problems as well as having high-performance hydrogen production from POME. In this study, a combination of up-flow anaerobic sludge blanket (UASB) and up-flow fixed film (UFF) in a single reactor was used as modified up-flow anaerobic sludge blanket-fixed film (UASB-FF) bioreactor.

Microbial granule formation is critical in a high rate reactor like UASB. The suspended solids in the POME, however, may present unfavorable impact towards granule formation and sludge bed stability when the up-flow velocity is high in the UASB. On the other hand, provision of a required up flow velocity is very importance to guarantee the granules stability. Therefore, to partially solve this problem and to balance between the favorable performance of the process and stable microbial granules population, an external settling tank is designed to settle out the suspended solids prior to recycling the effluent to the reactor.

1.2. Objectives of study

The objectives of this research are:

1. To study the performance of different pretreatment methods (heat-shock, chemical, acid, base, and freezing and thawing) to enrich hydrogen producing bacteria using different sludge for hydrogen production and chemical oxygen demand (COD) reduction from POME;
2. To determine the simultaneous effects of two independent operating variables i.e. feed flow rate (Q_F) and up-flow velocity (V_{up}) on biological hydrogen production from POME in the UASB-FF bioreactor;
3. To determine the kinetic parameters of the process;
4. To study the effects of three process variables i.e. influent COD concentration,

initial bicarbonate alkalinity (BA) and biomass concentration on fermentative hydrogen production, and mass transfer of the process using the granular sludge.

1.3. Purpose and scope of study

The different pretreatment methods (heat-shock, chemical, acid, base, and freezing and thawing) were studied in batch culture to obtain the best pretreatment method for enhancing hydrogen production from POME prior to starting main dark fermentative hydrogen production in UASB-FF bioreactor. Pre-treatment of sludge is required for anaerobic system to disable hydrogen consuming bacteria and to enhance the growth of hydrogen producing bacteria and their activities; concomitantly this helps to enrich this bacterial population number for enhanced H_2 generation goals.

Application of a modified UASB-FF bioreactor on biological hydrogen production from POME is the main focus of the present study. An UASB-FF bioreactor with working volume of 2.55 liter was designed and fabricated to study its potential and feasibility for microbial hydrogen production from POME. After reactor start-up, response surface methodology (RSM) was used to obtain optimum operating conditions for two variables i.e. Q_F (1.7-10.2 l/d) and V_{up} (0.5-3.0 m/h). The responses (outline these responses) were assessed and the steady state performance of the UASB-FF was modeled. The optimum operating conditions were obtained for biohydrogen production from pre-settled POME.

RSM was also used in the investigation of the interactive effects of three important process variables namely influent COD (COD_{in}), BA and MLVSS at 3000-10000 mg/l, 200-2000 mg $CaCO_3$/l and 2000-6000 mg/l respectively, on the biological hydrogen production in batch experiments. Intact and fragmented granules were used in order to study the effect of substrate mass transfer into the granules. The cumulative hydrogen production, specific hydrogen production rate were the responses studied.

CHAPTER 2

LITERATURE REVIEW

In this chapter, a review on the general concepts and mechanism of biological hydrogen production processes is presented. The review covers important environmental and operating factors in enhancing biohydrogen production, reactor types and technologies to produce biohydrogen and available options to enrich hydrogenic microbial population. The statistical experimental design i.e. response surface methodology (RSM) was used in this project in order to model and optimize the process. Lastly, the anaerobic process was modeled upon the kinetic information obtained from the experimental data.

2.1. Introduction

Emissions emanating from the combustion of fossil fuels lead to some adverse environmental impacts. These emissions contain COx, NOx, and SOx which are claimed to contribute to global warming, ozone layer depletion, and acidic deposition. In addition, fossil fuels are limited energy resources and non-renewable. Therefore, various researches are intensely focused on the renewable energy sources. Hydrogen (H_2) is one of such renewable energy sources known for its non-polluting and environmentally friendly nature, as its end combustion product is pure water (H_2O). Furthermore, hydrogen is a promising fuel due to its high energy yield (122kJ/g) which is 2.4, 2.8 and 4 times higher than energy yields of methane, gasoline and coal, respectively (Hart, 1997; Lay *et al.,* 1998; Misuno *et al.,* 2000; Pinto *et al.,* 2002; Yu *et al.,* 2002; Fan *et al.,* 2004; Lin and Lay, 2004; Atif *et al.,* 2005; Ginkel *et al.,* 2005; Leite *et al.,* 2008; Zadariana *et al.,* 2009; Han et al., 2012).

Recently, significant attention is directed towards the use of H_2 as an alternative and eco-friendly energy source throughout the world. Different hydrogen production methods have been reported; among others are fossil fuel reforming (Hameed and Gondal, 2005), biological processes of biomass (Chang *et al.,* 2002), and electrolysis of water (Zhou *et al.,* 2004). Biological production of H_2 is a less energy intensive alternative where processes can be operated at ambient temperature and pressure (Leite *et al.,* 2008; Kim and Kim, 2012).

The three main biological processes that have been applied are biophotolysis of water using algae and cyanobacteria, photo-decomposition of organic compounds by photosynthetic bacteria, and fermentative H_2 production from organic matters (Nandi and Sengupta, 1998; Das and Veziroglu, 2001; Hawkes *et al.,* 2002; Logan, 2004; Levin *et al.,* 2004; Cheong and Conly, 2006; Mohan *et al.,* 2007). Amongst aforementioned biological methods, fermentative hydrogen production became more favourable due to some outstanding advantages such as high hydrogen production rate (HPR), low energy requirement, relatively easy operation, and high sustainability (Wu and Chang, 2007; Zhang *et al.,* 2008). The dark hydrogen fermentation is carried out by fermentative hydrogen-producing microorganisms, such as facultative anaerobes and obligate anaerobes. In anaerobic conditions, hydrogen is produced during the breakdown of organic compounds by the microorganisms. When organic compounds are the only carbon and energy source for providing metabolic energy, the process is called dark hydrogen fermentation. Fermentative hydrogen generation is a common anoxic process where the bacteria degrade organic matters to produce the required electron in the anaerobic reaction. This technique provides a specific condition under which acidogens (hydrogen producing bacteria) and methanogens (hydrogen consuming bacteria) exhibit an imbalance in their activities resulting in accumulation of hydrogen (Leite *et al.,* 2008). Dark fermentation in the acidogenic phase utilizing obligate and facultative

anaerobes leads to H_2 production. This method usually achieves a much higher H_2 production rate than other biological processes (Das and Veziroglu, 2001; Levin *et al.*, 2004; Wu and Chang, 2007; Subadhi and Lal, 2011).

Previous studies described four fermentation reactions that take place in the anaerobic hydrogen production systems, *viz.* acetic acid fermentation, propionic acid fermentation, butyric acid fermentation, and ethanol fermentation as given respectively in equations 2.1-2.4 (Heuvel *et al.*, 1988; Fox and Pohland, 1994; Ren *et al.*, 1997; Himmi *et al.*, 2000; Li *et al.*, 2008). Among the fermentative reactions, hydrogen is generated from acetic acid (Eq. 2.1), butyric acid (Eq. 2.3), and ethanol fermentations (Eq. 2.4); however, the propionic acid fermentation (Eq. 2.2) may be more energetically favourable than other fermentation types due to the lower Gibbs free-energy change (ΔG^0) (Cohen *et al.*, 1979; Zoetemeyer *et al.*, 1982; Cohen, 1982; Cha and Noike, 1997; Ren *et al.*, 1997; Lay, 2000).

$$C_6H_{12}O_6 + 4H_2O + 2NAD^+ \rightarrow 2CH_3COO^- + 2HCO_3^- + 2NADH + 2H_2 + 6H^+$$

$$\Delta G^0 = -215.67 \text{ kJ/mol} \qquad (2.1)$$

$$C_6H_{12}O_6 + 2NADH \rightarrow 2CH_3CH_2COO^- + 2H_2O + 2NAD^+$$

$$\Delta G^0 = -357.87 \text{ kJ/mol} \qquad (2.2)$$

$$C_6H_{12}O_6 + 2H_2O \rightarrow CH_3CH_2CH_2COO^- + 2HCO_3^- + 2H_2 + 3H^+$$

$$\Delta G^0 = -261.46 \text{ kJ/mol} \qquad (2.3)$$

$$C_6H_{12}O_6 + 2H_2O + 2NADH \rightarrow 2CH_3CH_2OH + 2HCO_3^- + 2NAD^+ + 2H_2$$

$$\Delta G^0 = -234.83 \text{ kJ/mol} \qquad (2.4)$$

Hydrogen-producing bacteria can utilize various forms of substrates. Studies showed that glucose, sucrose and starch were mainly used as substrates for fermentative hydrogen production (Wang and Wan, 2009). However, numerous works also made use of waste as substrate due to its availability, low cost, high carbohydrate content and biodegradability in the biological processes of H_2 production (Kapdan, and Kargi, 2006;

Marone *et al.,* 2012). Additionally, use of wastewater is in line with "waste to energy" concept, and simultaneously contributes to the treatment of waste. In this regard, various types of waste including food and agricultural industry wastes, carbohydrate-rich industrial wastewaters, and surplus biomass from treatment plants have been utilized in biohyrogen production processes (Lay *et al.,* 1999; Das and Veziroglu, 2001; Kapdan, and Kargi, 2006; Cuetos *et al.,* 2007; Leite *et al.,* 2008; Zhang *et al.,* 2008; Ozmihci and Kargi, 2011). The Figure (2.1) shows fermentative hydrogen production pathway.

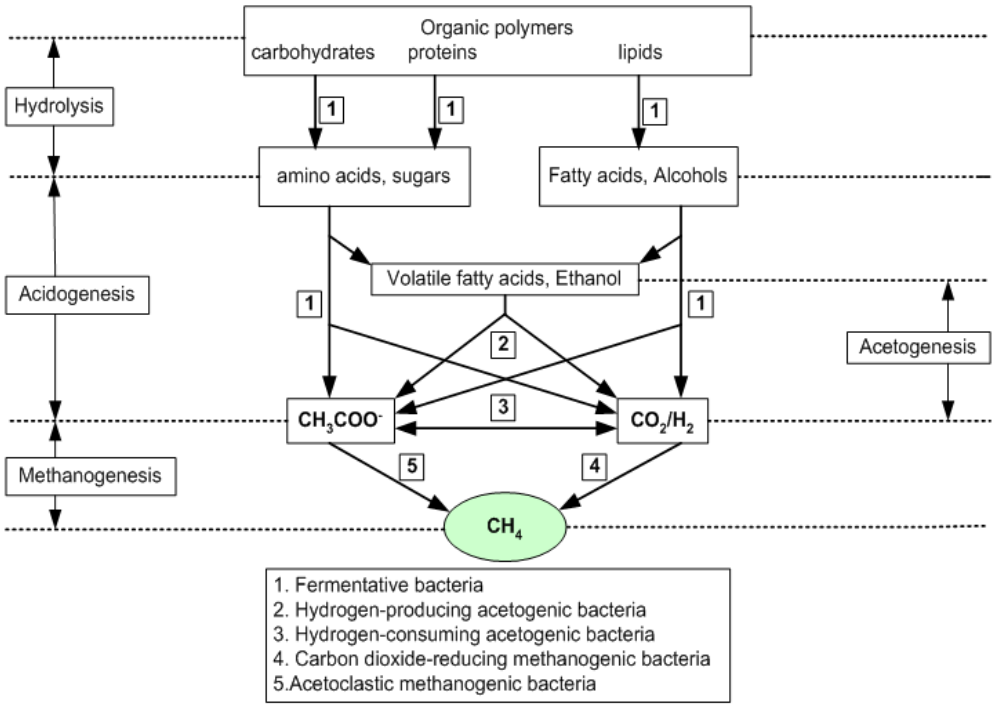

Figure 2.1. Anaerobic digestion and fermentative hydrogen production pathway

Diverse reactor designs have been introduced to accommodate hydrogenic microbial population and providing them with the required conditions to accomplish fermentative hydrogen production process. Some of them are: anaerobic sequencing batch reactor (AnSBR) (Mohan *et al.,* 2007; Bhaskar *et al.,* 2008), batch reactor fermentation (Pakarinen *et al.,* 2008; Chong *et al.,* 2009), up flow anaerobic sludge blanket (UASB) reactor (Huang *et al.,* 2004;Yu and Mu, 2006), granule-based complete mixed reactor (CMR) (Fang *et al.,* 2002), fixed or packed bed reactor (Rachman *et al.,*

1998; Chang *et al.*, 2002; Lee *et al.*, 2003; Mohan *et al.*, 2007; Leite *et al.*, 2008), anaerobic fluidized bed reactor (AnFBR) (Wu *et al.*, 2003; Zhang *et al.*, 2007), and trickling bio-filter (Oh *et al.*, 2004; Zhang *et al*., 2006). These reactors applied various environmental and operational conditions in order to achieve better efficiency in the anaerobic hydrogen production process. The studied conditions and affecting factors include temperature, pH, hydraulic retention time (HRT), type and concentration of substrate (e.g. organic matter, nitrogen, phosphorous, and metal ions), inocula and organic loading rate (OLR) (Das and Veziroglu, 2001; Hawkes *et al.*, 2007; Li and Fang, 2007; Show *et al.*, 2007; Das and Veziroglu, 2008; Wang and Wan, 2009).

This study reviewed the previous researches carried out on the fermentative hydrogen production, and specifically discussed the key environmental/operating variables in enhancing biohydrogen production. Hence, significant operating factors *viz.* OLR, HRT, temperature, and pH were investigated, and their influences on the hydrogen yield were graphically presented for a better comparison and discussion.

2.2. Effect of environmental and operational factors on fermentative hydrogen production

2.2.1. Organic loading rate (OLR)

Organic loading rate (OLR) as one of the most significant parameters was extensively studied to investigate the effects of various substrate loadings on the process when either a real or a synthetic wastewater was utilized as the substrate(s). Organic matters must be utilized by microorganisms to produce hydrogen (e.g. glucose was used in reactions 1-4), and it is measured by OLR (g/l.d) which represents magnitude of COD (g/L) fed through a certain time. With regard to the relationship defining the loading rate, two independent parameters *viz*. HRT and COD concentration can be considered to evaluate the effect of the loading rate (Wu *et al*., 2005; Show *et al*., 2007; Y. Bhaskar,

et al., 2008; Chookaew *et al.,* 2012). The presence of a minimum supply of organics is of importance for microorganism metabolism; however, the higher OLR does not necessarily lead to higher hydrogen yield but could lead to higher production rate. Therefore, optimization studies are essential to gain the higher production efficiency. Besides, optimization of OLR can only be implemented when the microbial populations are well acclimatized to the applied OLR. When the population is not yet acclimated with the substrate to produce hydrogen, the affinity of the bacterial consortium towards the substrate will not be at its highest (corresponding to the lowest attainable half-velocity substrate constant, K_s) (Wu *et al*., 2005; Yang *et al*., 2007). Thus, a stepwise introduction of microorganisms to the final OLR is usually of fundamental importance, and acclimatization is thoroughly achieved when experiments reach a steady state in hydrogen production rate (HPR).

On the other hand, with the same OLR, the waste composition is a vital factor affecting H_2 generation rate. As the refractory fraction of the COD content in the waste increases, the hydrogen yield decreases; for digestible wastes the trend follows Monod's relation: the hydrogen yield is increased by increasing the substrate concentration until the maximum specific growth rate (μ_{max}) is reached, thereafter the yield will remain constant or even decreases because of the substrate inhibition effect (Wu and Chang, 2007; Bhaskar *et al*., 2008). Increasing the HRT will also increase this undesirable refractory fraction. Hence, increasing either the HRT or OLR will affect the H_2 production rate. At a constant OLR with different HRT and substrate concentrations, hydrogen yield was sensitive to HRT but insensitive to the substrate concentration. As a result, as HRT increases the hydrogen content of the biogas as well as the hydrogen yield decreases (Show *et al*., 2007).

Table 2.1. The effect of OLR and substrate on fermentation hydrogen production

Type of reactor	Substrate	Range of OLR (gCOD/L.d)	Optimum OLR (gCOD/L.d)	Maximum H_2 Production		References
				HPR	H_2 yield	
Batch:	Sucrose	10-40	20	-	4.00 mmol H_2/ g COD	Wu *et al.*, 2005
	Sucrose	5-30	20	0.234 mol H_2/L.d	-	Wu and Chang, 2007
	Dairy wastewater	2.4-4.7	3.5	70.7 mol H_2/kg COD_R.d	-	Mohan *et al.*, 2007
	Chemical wastewater	6.3-7.9	6.3	13.44 mol H_2/kg COD_R.d	-	Bhaskar *et al.*, 2008
	Glucose	3-18	9	-	9.53 mmol H_2/ g COD	Liu et al., 2009
	Food waste	20.7-41.4	41.4	0.019 mol H_2/L.d	-	Gomez *et al.*, 2009
	Raw starch	10-25	10	-	9.05 mmol H_2/g COD	Su *et al.*, 2009
	Gelatinized starch	10-25	10	-	9.47 mmol H_2/g COD	Su *et al*., 2009
	Hydrolyzed starch	10-25	25	-	10.4 mmol H_2/g COD	Su *et al.*, 2009
	Ground wheat powder solution	0.87-4.4	1.93	0.018 mol H_2/L.d	-	Ozmihci And Kargi, 2010
	Glucose	5-90	5	-	2.14 mmol H_2/ g COD	Ruggeri *et al.*, 2009
Continuous:	Glucose	1.1-11.2	11.2	0.214 mol H_2/L.d	-	Zhang *et al.*, 2006
	Glucose	2.5-20	10	1.75 mol H_2/kg COD_R.d	-	Show *et al.*, 2007
	Cheese processing wastewater	5-14	14	-	3.12 mmol H_2/g COD	Yang *et al.*, 2007
	Glucose	4-30	22	-	9.27 mmol H_2/ g COD	Shen *et al.*, 2009
	Sucrose	20-160	120	-	9.88 mmol H_2/ g COD	Lin *et al.*, 2009
	Cheese processing wastewater	21-47	35	-	9.00 mmol H_2/g COD	Azbar *et al.*, 2009
	Glucose	6.5-42.8	25.7	-	14.58 mmol H_2/ g COD	Hafez *et al.*, 2010

Moreover, it must be noted that in the case of feeding real wastewater to microbes (Lin *et al*., 2009; Liu *et al*., 2009). From several studies, high substrate concentration showed the metabolic pathway change (Fabiano and Perego, 2002; Oh *et al*., 2003; Liu *et al*., 2009); whereas, metabolic activity is the effectual key for H_2 yield in the fermentative hydrogen production (Mohan *et al*., 2007). Therefore, metabolic activity of the microorganisms must be improved through stepwise growth and adaptation in high substrate concentration (Zhang *et al*., 2006).

Table (2-1) listed various ranges of OLRs as investigated by previous researches and also the obtained optimum OLR values. The maximum HPR attained for each study is also given. A wide range of OLR from 0.87-160 g COD/L.d was investigated utilizing either batch or continuous reactors with various organic substrates such as glucose, sucrose, starch and in a few cases with organics available in real wastewaters.

As shown in Table 2.1, there is no definitive range for optimum OLR in fermentative hydrogen production and occasionally the achieved results are extremely divergent. For instance, Lin and coworkers (2009) found the maximum hydrogen yield at optimum OLR 120 g COD/L.d, while Ozmihci and Kargi (2010) reported 1.93 g COD/L.d as the optimum OLR. This phenomenon could be due to the diverse environmental/operating conditions or ranges of the variables applied in the studies. The applied ranges and obtained results for some of the studies were illustrated in Figure (2.2): Lin *et al*. (2009) reported increased H_2 production to 3.46 mol H_2/g COD.d with the increase in OLR from 20 to 120 g COD/L.d; however, the yield fell to 1.96 mol H_2/g COD.d as higher OLR of 160 g COD/L.d was examined. Similar ascending and descending trend was observed by Show *et al*. (2007) and Liu *et al*. (2009) in the range of 2.5-20 and 3-18 g COD/L.d, respectively. Nevertheless, results achieved by Wu *et al*. (2005) and Wu and Chang (2007) showed negligible variation in hydrogen yield through alteration of OLR since approximately constant values were reported for H_2

production. Contradictory results, which took place occasionally for the same OLR ranges could be due to dissimilarity in other effective factors such as pH, temperature, substrate, reactor design, pre-conditioning of inocula, or types and population of microorganisms (Wang and Wan, 2009). For example, Wu *et al*. (2005) and Wu and Chang (2007) examined similar ranges of 10 to 40 and 5 to 30 g COD/L.d, respectively, in batch experiments with sucrose as the organic source; however their processes differed in the applied pH, preparation of the synthesis wastewater, and reactor design. As a result, trace amount of hydrogen was produced by Wu and Chang (2007), while Wu *et al.* (2005) attained 1.42 mol H_2/g COD.d, and it was apparently due to employing a new synthetic polymer (ethylene-vinyl acetate copolymer) as the bio-carrier which resulted in the improvement of microbial growth and activity.

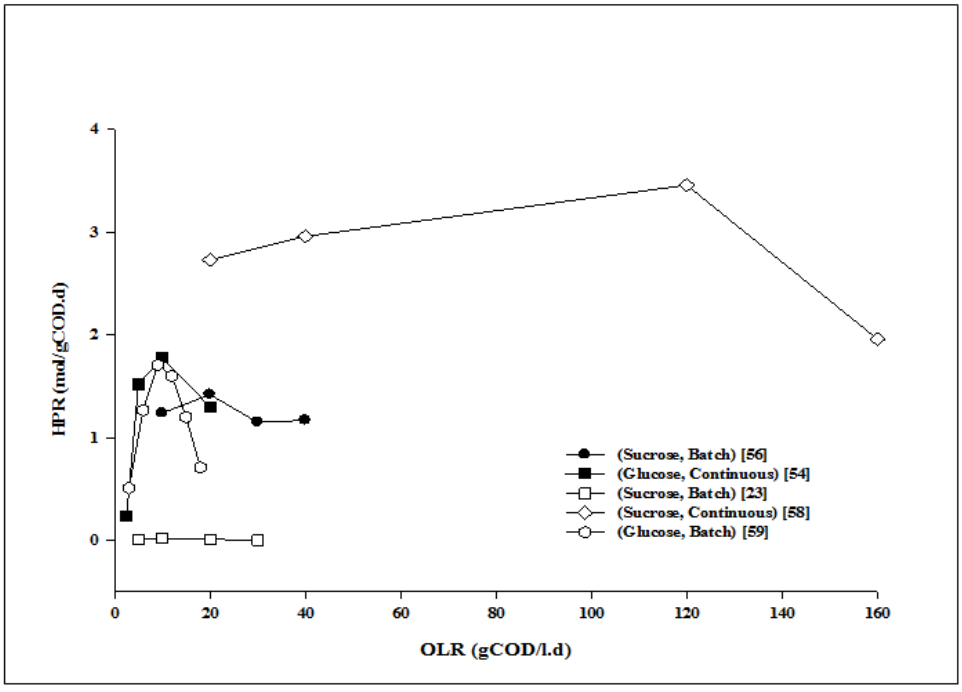

Figure 2.2. Effect of organic loading rate on biohydrogen production

2.2.2. Hydraulic retention time (HRT)

Hydraulic retention time is one of the notable parameters in continuous biological processes, and is in inverse relation with food to microbe ratio (F/M). It

implies the time provided for microorganisms to utilize the fed substrates; therefore, inadequately long or short HRT results in unfavourable metabolic phase of the microbes. The hydrogen production increased to a higher value with the increase in HRT when adequate time was given to microbes for metabolizing the substrates. However, decline in H_2 production rate was seen when HRT was increased exceedingly. It was attributed to a shift of metabolic flux that might occur at a shorter HRT where more substrate is shifted to reaction end products instead of bacterial growth or maintenance, leading to an increased hydrogen yield (Zhang *et al*., 2007; Mu and Yu, 2007; Show *et al*., 2007; Kim *et al*., 2008; Jo *et al*., 2008a). In a normal condition without pH adjustment, the methane production will be inhibited due to the higher acidogenic rate compared to methanogenics, and pH drops below 5.0, which favors hydrogen generation process. If pH was maintained in the range favorable for methanogenic activities, decrease in HRT enhances anaerobic methanogens reaction rate which results in methane production (Yang *et al*., 2007). On the other hand, the hydrogen content of the biogas decreases by the increase in HRT due to the favouring of some other undesirable reactions besides hydrogen production reactions. However, in some cases, the low substrate concentration resulted in the yield increment when HRT was constant (Lin *et al*., 2009; Ntaikou *et al*., 2009).

The nature of the substrates and configuration of the reactor are also crucial factors in the biohydrogen production. The type of substrate present determine the pathways that will lead to hydrogen generation, and design of the reactor will affects the solid retention time (SRT) which in turn is highly interactive with HRT (Kim *et al*., 2008). More H_2 yield is attained when sufficient quantity of the acclimated H_2-producing bacteria with high synergistic relation exist in the system. Hence, the attempts are directed towards high H_2 production rate by achieving the optimum solid retention time (SRT) at a relatively low optimum HRT (Kim *et al*., 2008). The acetate

and butyrate are generated along with hydrogen generation while no hydrogen is produced in the course of the propionate production (Nandi and Sengupta, 1998; Jo *et al*., 2008b). Since the HRT has an influence on bacterial competition, lower HRT values seem to have a positive effect on hydrogen yield (Ntaikou *et al*., 2009).

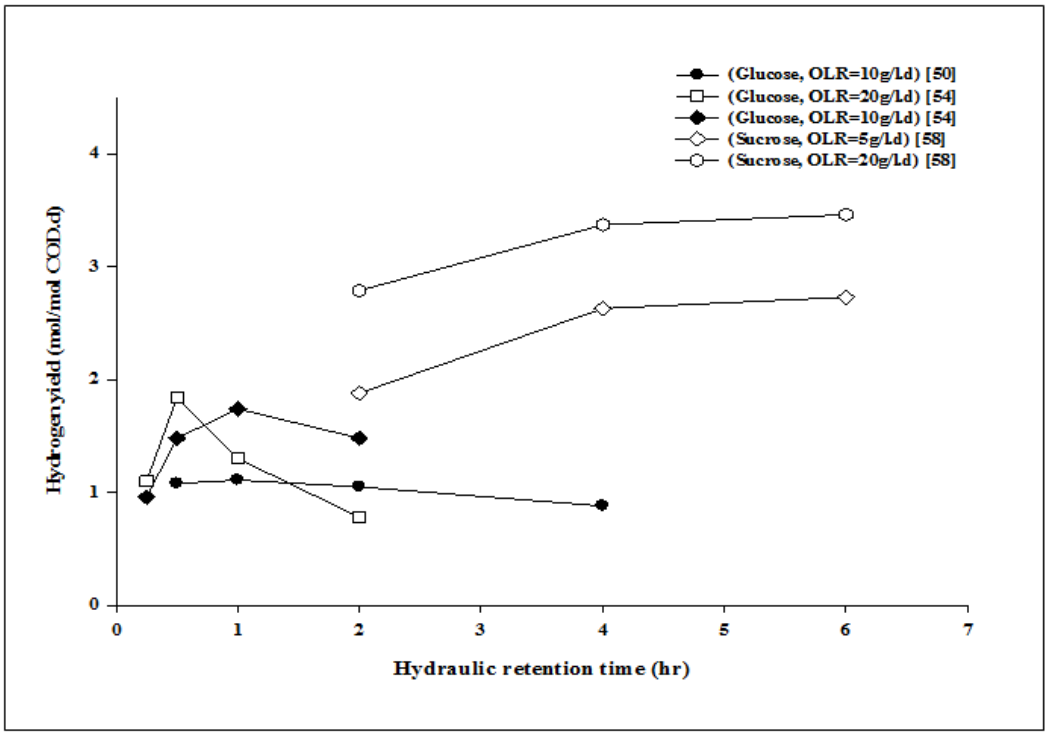

Figure 2.3. Effect of hydraulic retention time (HRT) on biohydrogen production in continuous reactors

Table (2.2) lists down various ranges of HRTs investigated by previous researches and also the obtained optimum HRT values. The maximum hydrogen yield attained for each study is also given. A wide range of HRT from 0.25 to 60 h was investigated utilizing mainly continuous reactors with various organic substrates such as glucose, sucrose, starch and in a few cases with organics available in real wastewaters.

Table 2.2. The effect of HRT and substrate on fermentative hydrogen production

Type of reactor	Substrate	Range of HRT (hr)	Optimum HRT (hr)	Maximum H_2 production		References
				H_2 yield	HPR	
Batch:	Food waste	24-42	36	3.32 mmol H_2/g VSS_{added}	-	Kim *et al.*, 2008
Continuous:	Glucose	0.5-4	1	6.19 mmol H_2/g COD	-	Zhang *et al.*, 2007
	Glucose	3-30	25	7.39 mmol H_2/g COD	-	Yang and Yu, 2007
	Glucose	0.25-2	0.5	0.08 mmol H_2/g VSS	-	Show *et al.*, 2007
	Sucrose	2-6	6	9.88 mmol H_2/g COD	-	Lin *et al.*, 2009
	Glucose	1-24	2	-	7.2 L H_2/L.d	Jo *et al.*, 2008b
	Olive oil mill effluent	7.5-60	14.5	-	200 L H_2/L.d	Ntaikou *et al.*, 2009
	Cheese processing wastewater	1-5	3	22 mmol H_2/g COD	-	Azbar *et al.*, 2009
	Primary sewage biosolids	18-48	24	21.86 L H_2/kg VS	-	Nicolau *et al.*, 2010
	Starch	3-48	6	-	4 L H_2/L.d	Akutsu *et al.*, 2009

Table (2.2) also shows there is no definitive range or optimum HRT in fermentative hydrogen production and sometimes the achieved results are not in consensus with each other. For instance, Kim and coworkers (2008) found the maximum hydrogen yield at optimum HRT 36 h, while Show *et al*. (2007) reported 0.5 h as the optimum HRT. This phenomenon can be due to the diverse environmental/operating conditions or ranges of the variables applied in the different studies. The applied ranges and obtained results for some of the studies were illustrated in Figure (2.3). Show *et al*. (2007) reported increase of H_2 production to 1.74 mol H_2/mol COD.d with the increase in HRT from 0.25 to 1 h using 10 g COD/L.d as OLR; however, the yield fell to 1.48 mol H_2/mol COD.d when a higher HRT at 2 h was applied. They observed similar ascending-descending trend within this range at OLR of 20 g COD/L.d, with maximum HPR of 1.84 mol H_2/mol COD.d when HRT was at 0.5 h. On the other hand, results achieved in OLRs 5 and 20 g COD/L.d by Lin and coworker (2009) showed increase in hydrogen yield *via* shifting of HRT from 2 to 6 h. Nevertheless, results achieved by Zhang *et al*. (2007) showed negligible variation in hydrogen yield through alteration of HRT since approximately constant values were reported for H_2 production.

2.2.3. Temperature

Biological hydrogen production can be affected by the variation in the environmental temperature. Hydrogen producing bacteria are mostly categorized in two main groups: mesophilic and thermophilic bacteria whose favourable ranges of temperature are 30 to 40 °C and 45 to 55 °C, respectively. It is reported that increase of temperature generally improves HPR, and enhancements in HPR were observed through temperature increment for thermophilic bacteria rather than mesophilic bacteria (Liu *et al*., 2003; Chong *et al*., 2009). However, extreme temperature rise may cause a strong

shift in microbial activities, which impacts biohydrogen production adversely (Lin *et al*., 2008a). Nevertheless, a sudden fall in temperature decreases the hydrogen concentration rapidly, although it can be alleviated following the adaptation of the microorganisms to the new culture environment (Huang *et al*., 2004). Studies revealed that after the perturbation of the temperature, the required time to reach a comparable hydrogen production is longer for mesophilics than for the thermophilics (Lin *et al*., 2008b). Moreover, in some cases when the temperature shifted considerably lower than the tolerable ranges, the bacteria needed more ferrous ion to activate the hydrogenase so that it could oxidize reduced ferredoxin to produce more hydrogen (Lee *et al*., 2001; Zhang and Shen, 2006; Chong *et al*., 2009).

As a matter of fact, there is no explicit optimum temperature in biohydrogen production. The optimum temperature for producing hydrogen *via* dark fermentation depends on the type of H_2 producers and also the carbon source used. For example, Wu *et al*. (2005) reported the optimum temperature in the range of 37 to 45°C for the pure cultures of *Clostridium* or *Enterobacter* species; whereas, the optimum temperature for *Thermoanaerobicterium thermosaccharolyticum* PSU-2 was found at 60°C by Sompong *et al*. (2008). Lin and coworkers (2008b) reported 260% increase in maximum HPR when the temperature was varied from 45 to 55 °C, while they achieved only 100% improvement of maximum HPR within the temperature range of 30 to 40 °C.

Table (2.3) compiles various ranges of temperatures investigated in the literature and also the prevailing optimum temperature values. The maximum HPR attained for each study is also given.

Table 2.3. The effect of temperature and substrate on fermentative hydrogen production

Type of reactor	Substrate	Range of temperature (°C)	Optimum temperature (°C)	Maximum H_2 production		References
				H_2 yield	HPR	
Batch:	Sucrose	30-45	40	3.27 mmol H_2/g COD	-	Wu *et al.*, 2005
	Glucose	33-41	41	8.69 mmol H_2/g COD	-	Mu *et al.*, 2006c
	Rice slurry	37-55	37	14.18 mmol H_2/g COD	-	Fang *et al*., 2006
	Sucrose	30-40	35	-	5.88 L H_2/L.d	Wu and Chang, 2007
	Glucose	20-44	37	6.98 mmol H_2/g COD	-	Xing *et al.*, 2008
	Xylose	30-55	40	14.9 L H_2	-	Lin *et al.*, 2008b
	Glucose	25-55	40	0.06 mmol H_2/g COD	-	Wang and Wan, 2008
	Sucrose	40-80	60	13.18 mmol H_2/g COD	-	Sompong *et al.*, 2008
	Starch	37-55	55	1.44 mmol H_2/g starch	-	Lee *et al.*, 2008
	Cattle wastewater	30-55	45	13.52 mmol H_2/g COD_R	-	Tang *et al.*, 2008
	POME	30-55	37	-	6.70 L H_2/L.d	Chong *et al.*, 2009
	Glucose	35-55	55	15.10 mmol H_2/g COD	-	Akutsu *et al.*, 2009
	Glucose	37-55	37	11.35 mmol H_2/g COD	-	Baghchehsaraee *et al.*, 2009
Continuous:	Esterification wastewater	15-25	25	150 ppm H_2	-	Huang *et al.*, 2004
	Sucrose	30-45	40	9.00 mmol H_2/g COD	-	Lee *et al.*, 2006
	Xylose	30-55	50	7.29 mmol H_2/g COD	-	Lin *et al.*, 2008a

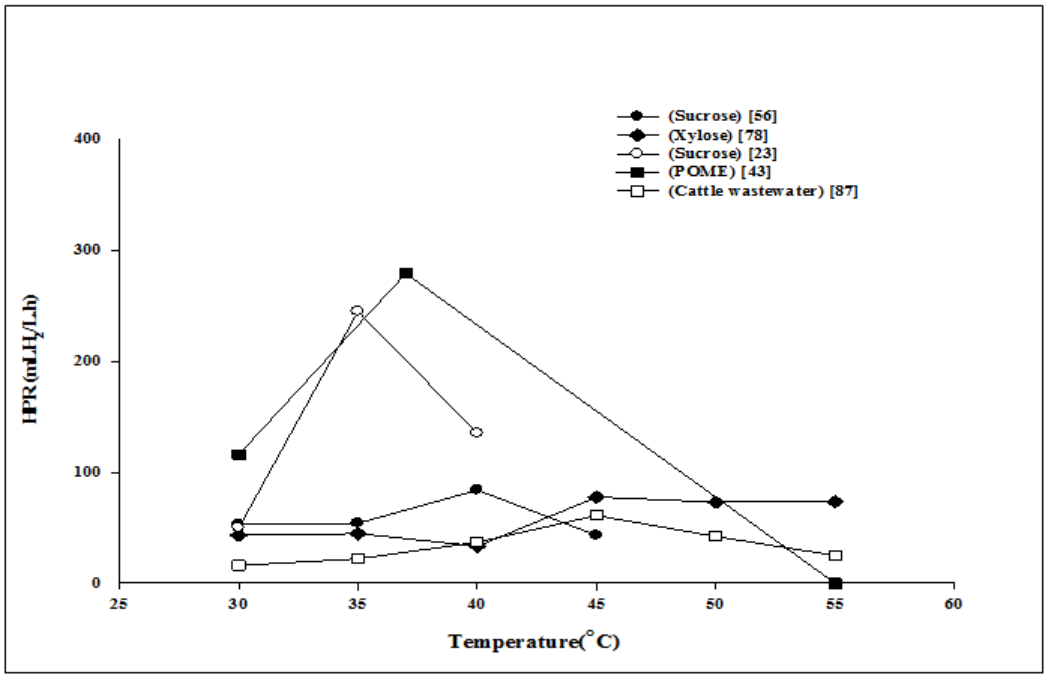

Figure 2.4. Effect of temperature on biohydrogen production in batch reactors

A wide range of temperature from 15 to 80 °C was investigated utilizing mainly batch reactors with various organic substrates such as glucose, sucrose, starch and few cases with organics available in real wastewaters. As shown, there is also no definitive range or optimum temperature in fermentative hydrogen production and sometimes the achieved results disagree with each other. For instance, Sompong and coworkers (2008) found the maximum HPR at optimum temperature of 60 °C, while Huang *et al.* (2004) reported 25 °C as the optimum temperature. The applied temperature ranges and the results obtained therein for some of the studies are presented in Figure (2.4). Wu and Chang (2007) reported an increase in H_2 production to 245 mL H_2/L.h with the increase in temperature from 30 to 35 °C; however, the HPR dropped to 135 mL H_2/L.h at 40 °C. Similar trend was observed by Chong *et al*. (2009) in the range of 30-55 °C. Nevertheless, results achieved by Wu *et al*. (2005), Lin *et al*. (2008b), and Tang *et al*. (2008) showed negligible variation in HPR through alteration of temperature since approximately constant values were reported for H_2 production.

2.2.4. pH

pH is another important environmental factor influencing fermentative hydrogen production, since it directly affects the hydrogenase metabolism (especially acidogens) and their activities. The initial pH of substrate is of special importance in fermentative hydrogen processes as it directly affects the hydrogen yield (Wang and Wan, 2009). That is due to the fact that the structure of the microbial communities' composition depends on the initial pH of the media, and different values of pH favour the growth of different hydrogenase species. For example, Fang and Liu (2000) reported the initial pH of 4 and 5.5 led to H_2 content of 42% and 64%, respectively, ascribed to different pre-dominant hydrogenase species.

Effect of environmental pH was widely investigated and most of the published reports found the maximum hydrogen yield to be in the range of 5.5 to 6.0 (Tang *et al*., 2008; Zhu *et al*., 2009; Chong *et al*., 2009; Wang and Wan, 2009). Some studies reported inhibition of hydrogen production at pH values as low as 5 (Chong *et al*., 2009; Wang and Jin, 2009; Zhu *et al*., 2009); in contrast, other workers found the maximum H_2 production achieved at pH value as low as 4.5 using mixed microflora (Fang *et al*., 2006; Mu *et al*., 2006b; Ren *et al*., 2010). Ren *et al*. (2009) found out that application of pH out of the optimum range decreased the level of adenosine triphosphate (ATP) in the cells, which leads to the curtailment of the hydrogen producing bacteria's growth. In mixed culture, the optimum pH for H_2 production varied widely, and it may be due to the complex nature of the prevailing bacterial populations and substrates. Therefore, discovering an effective initial pH and also ability to control pH of the medium to be within a favourable range will be crucial (Yokoi *et al*., 2001; Soloman *et al*., 2007; Wang and Jin, 2009; Chong *et al*., 2009).

Table 2.4. The effect of pH and substrate on fermentation hydrogen production

Type of reactor	Substrate	Range of pH	Optimum of pH	Maximum H_2 production		References
				H_2 yield	HPR	
Batch:	Sucrose	4.7-6.3	5.5	8.58 mmol H_2/g COD	-	Wang *et al.*, 2005
	Sucrose	4.5-6.5	5.5	0.05 mmol H_2/ g COD	-	Mu *et al.*, 2006a
	Rice slurry	4.0-7.0	4.5	14.18 mmol H_2/g starch	-	Fang *et al.*, 2006
	Sucrose	5.0-7.0	6.0	-	8.83 L H_2/L.d	Tao *et al.*, 2007
	Sucrose	5.5-7.0	6.0	-	5.71 L H_2/L.d	Wu and Chang, 2007
	Cattle wastewater	4.5-7.5	5.5	14.80 mmol H_2/g COD_R	-	Tang *et al.*, 2008
	POME	5.0-8.5	5.5	11.43 mmol H_2/g COD_R	-	Chong *et al.*, 2009
	Fresh water pound sludge	6.5-8.0	7.0	2.71 mol H_2/mol substrate	-	Ren *et al.*, 2009
	Molasses	5.0-8.0	6.5	8.3 L H_2/L	-	Wang and Jin, 2009
	Carbohydrate-rich organic waste	4.9-6.7	4.9	5.87 mmol H_2/g COD	-	Chen *et al.*, 2009
Continuous:	Glucose	4.0-7.0	5.5	10.94 mmol H_2/g COD	-	Fang and Liu, 2002
	Sucrose	3.4-6.3	4.2	8.39 mmol H_2/g COD	-	Mu *et al.*, 2006b
	Sucrose	6.1-9.5	7.0	3.73 mmol H_2/g COD	-	Zhao and Yu, 2008
	Glucose	4.7-5.9	5.0	9.35 mmol H_2/g TVS	-	Zhu *et al.*, 2009
(attached growth)	Molasses	3.7-4.4	4.0	-	9.72 L H_2/L.d	Ren *et al.*, 2010
(suspended growth)	Molasses	4.2-4.9	4.5	-	6.65 L H_2/L.d	Ren *et al.*, 2010
	Glucose	5.5-6.2	5.5	9.90 mmol H_2/g COD	-	Hwang *et al.*, 2009

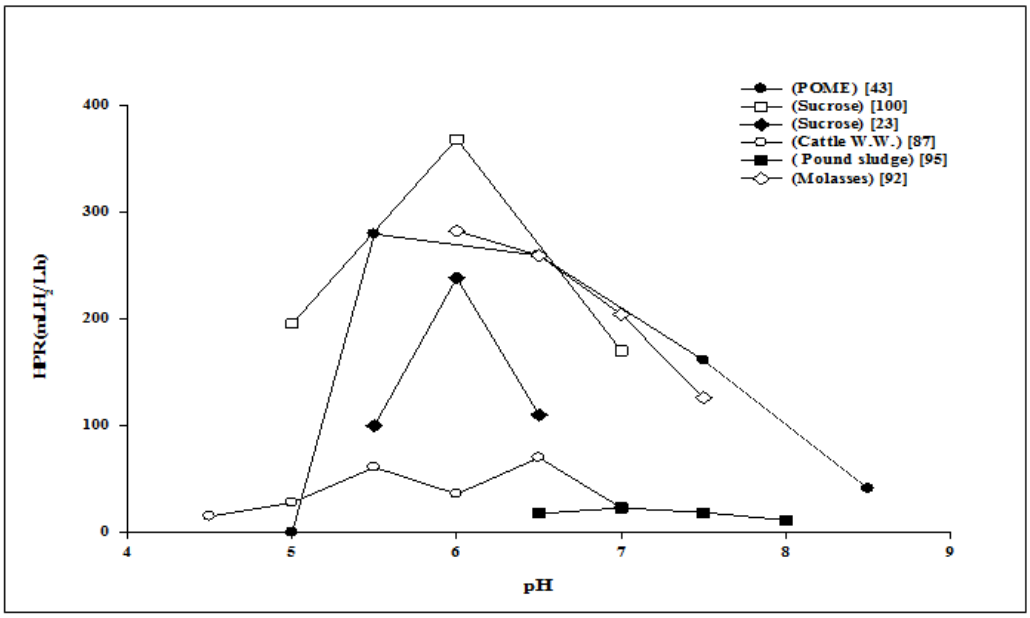

Figure 2.5. Effect of pH on biohydrogen production in batch reactors

Table (2-4) lists various ranges of pH investigated by the previous researches and also the attained optimum pH values. The maximum HPR observed for each study is also given. A wide range of pH from 3.7 to 9.5 was investigated using batch and continuous reactors with different synthetic and real wastewaters as substrate. As shown in Table (2.4), there exists no exact agreement on the optimum pH in fermentative hydrogen production. For instance, Zhao and Yu (2008) and Ren *et al*. (2009) found the maximum hydrogen yield at optimum pH 7.0, while Ran *et al*. (2009) reported pH 4.0 as the optimum pH. The possible reason for the observed disparities is the variance among these studies in the terms of substrate, inocula and pH range applied. The employed ranges and obtained results for some of the studies were illustrated in Figure (2.5). Tao *et al*. (2007) reported an increase of H_2 production to 368 mL H_2/L.h with the increase in pH from 5.0 to 6.0; however, the yield fell to 170 mL H_2/L.h as a higher pH of 7.0 was used. Similar trend was observed by Wu and Chang (2007) and Chong *et al*. (2009) in the range of pH 5.5 to 6.5 and 5.0 to 8.5, respectively. The results reported by Wang and Jin (2009) showed the decline of HPR from 282 to 126 mL H_2/L.h with the increase in pH from 6.0 to 7.5. Nevertheless, results achieved by Tang *et al*. (2008) and Ren *et al*. (2009) showed insignificant

difference in hydrogen yield through alteration of pH since approximately constant values were reported for H_2 production. Such inconsistent results for the same pH ranges could be due to contrasting effect of applied factors such as OLR, temperature, substrate, reactor design, preconditioning of inocula, or types and population of microorganisms (Wang and Wan, 2009). For example, Tao *et al*. (2007) and Wu and Chang (2007) examined similar ranges of pH 5.0 to 7.0 and 5.5 to 6.5, respectively in batch experiments with sucrose as the organic source; however their processes differed in the applied OLR, preparation of the sludge as inocula, and pre-treatment of sludge. As a result, maximum amount of HPR produced by Wu and Chang (2007) was 238 mL H_2/L.h, while Tao *et al*. (2007) attained 368 mL H_2/L.h, and it was probably due to employing heat-shock method for preparation of the inocula, which resulted in the enhancement of microbial growth and activities.

2.3. Reactor type

2.3.1. Complete-Mix Process

In a complete-mix anaerobic digester, the hydraulic and solids retention times are equal (HRT=SRT). Typical organic loading rate and hydraulic retention time for the complete-mix process are 1-5 g COD/l.d and 15-30 days, respectively (Metcalf & Eddy, 2003). This process is more suitable for wastes with high concentrations of solids, where thickening of the effluent solids is difficult. The complete mixed reactor (CMR) was extensively applied for continuous fermentative hydrogen generation.

2.3.2. Anaerobic Sequencing Batch Reactor

The anaerobic sequencing batch reactor (ASBR) is a suspended growth process with reaction and solids-liquid separation in the same vessel. The operation of ASBRs

consists of four steps: (1) feed (2) react (3) settle and (4) decant/effluent withdrawal. The critical feature of the ASBR process is the settling velocity of the sludge during the settling period before decanting the effluent. After sufficient operating time, a dense granulated sludge will develop to improve liquid-solids separation rates. At HRT values of 6 to 24 h, the SRT ranged from 50 to 200 days (Metcalf & Eddy, 2003).

2.3.3. Up-flow Anaerobic Sludge Blanket (UASB) Reactor

The up-flow anaerobic sludge blanket (UASB) system is the most commonly used high rate anaerobic treatment process. The UASB reactor as a high rate anaerobic system is considered suitable for the treatment of wastewater with high organic content due to its high biomass retention ability and rich microbial diversity (Schmidt and Ahring, 1996; Buzzini and Pires, 2002; Rao and Bapat, 2006). The waste is pumped into the reactor at the bottom, where upon contact with the sludge bed, it is degraded to H_2 and CO_2 (Figure 2.6). Gas formation and evolution will provide sufficient mixing in the bed (Droste, 1997). This reactor represents positive features, like allowing high OLR, short HRT and has a low energy demand (Metcalf and Eddy, 2003). Granulated sludge is the defining characteristic of UASB reactors as compared to the other anaerobic suspended growth systems. The growth of granulated sludge is affected by the wastewater characteristics (Thaveesri *et al.*, 1994). Other factors affecting the growth of granular sludge are pH, nutrients availability and up-flow velocity (Annachhatre, 1996).

Recommended organic loading at mesophilic condition for soluble feed with COD removal of 85-95 % is 18-25 g COD/l.d. The area served by inlet feed pipes (m^2) has been determined to be greater than 2 m^2 for granular sludge and COD loading larger than 4 g COD/l.d (Lettinga and Hulshoff Pol, 1991). Significant factors for the UASB reactor design are the influent distribution system, the gas-solids separator, and the

outlet design. Guideline for the gas solids separator (GSS) design is summarized as follows (Malina and Pohland, 1992).

- The slope of the settler bottom = 45-60°
- The surface area of the apertures between the gas collector = <15-20 %
- The height of gas collector = 0.2-0.3 reactor height
- A liquid-gas interface should be maintained in the gas collector to facilitate the release and collection of gas bubbles and to control scum layer formation.
- Generally scum layer baffles should be installed in front of the effluent weirs.

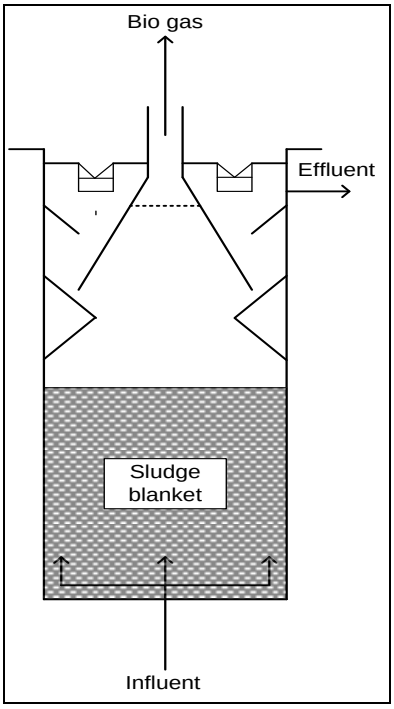

Figure 2.6. Design of a UASB reactor (Metcalf & Eddy, 2003)

Long start-up period is the main problem related to the UASB reactor, which is required for the growth of the microbial granules (Liu and Tay, 2004). Despite of the benefits of the granulated sludge, treatment of wastewaters with flocculated sludge UASB reactors has also been reported (Gooden *et al*., 2001). Particulate fractions of solids content of wastewater have adverse impact on UASB reactors' performance. They can cause a decline in microbial activities that leads to wash out of alive biomass

(Torkian *et al.,* 2003). The ratio of suspended solids to soluble COD is therefore important in evaluating the applicability of the process. As the ratio in the wastewater increases, the formation of a compact granular sludge reduces (Mahmoud *et al.,* 2003).

In order to overcome this limitation, an integration of granular sludge system and a fixed film reactor in a single reactor has been suggested by Speece (1996). This allows sludge retention to be virtually independent of HRT. This was a good strategy to retain sludge in the UASB reactor. The media used in the UASB reactor led to a longer solids retention time and better gas/liquid/solid separation (Zinatizadeh *et al.,* 2007).

The upflow anaerobic sludge blanket fixed film (UASB-FF) bioreactor is a combination of a granulated sludge part (UASB) and an attached sludge part in a single reactor. The UASB-FF bioreactor has been examined treating many different industrial wastewaters, like slaughterhouse, distillery spent wash, starchy, fiberboard manufacturing and whey wastewater (Borja *et al.,* 1998; Shivayogimath and Ramanujam, 1999; Fernandez *et al.,* 2001 McHugh *et al.,* 2006).

Biological granulation is a self-immobilization of cells that ends in the granule formation (Liu *et al.,* 2004). Recently, many researches have been carried out to enhance the start-up period through rapid granulation by employing chemical agents (Show *et al.,* 2004; Jeong *et al.,* 2005).

2.3.4. Up-flow Fixed Film Reactor

Up-flow fixed film reactors are often called ‘biofilters’. Wastewater is entered from the bottom of the reactor and discharged from the top. Bacteria are attached to media surfaces throughout volume of the reactor. Up-flow reactors keep some solids in suspension in the pores and treatment derives from both suspended and fixed film growth (Droste, 1997). The most common packing materials are corrugated plastic cross-flow or tubular modules and plastic pall rings.

2.3.5. Fluidized Bed Reactor

The fluidized-bed reactor process is similar to the up-flow expanded-bed reactor in physical design. The packing size is between 0.4 mm and 0.5 mm sand or activated carbon. The up-flow liquid velocities in the fluidized-bed reactor must be about 30 m/h for 100 % bed expansion. A higher hydraulic application rate is recommended to select for bacteria with higher tendencies to easily attach to the media under the highly vigorous mixing conditions. The process is best suitable for soluble wastewaters due to its inability to capture solids (Malina and Pohland, 1992; Tay and Zhang, 2000). Process COD loading value of 10 to 20 g COD/l.d are feasible for anaerobic fluidized-bed reactor with more than 90 % COD removal, depending on the wastewater characteristics.

2.4. Pretreatment Processes

Pre-treatment of sludge is normally applied for the preparation of the seed required for anaerobic system to enhance the growth of hydrogenesis bacteria and their activities; simultaneously this enriches this bacterial population number to enhance H_2 generation pursuits (Kim *et al.*, 2003; Zhu and Beland, 2006; Mohan *et al.*, 2007). There are three main steps for the preparation of hydrogen producing bacteria which include (i) the selection of material containing bacterial population of interest; (ii) enrichment of these hydrogen producing bacteria and (iii) acclimatization of the bacteria to specific substrates (Zhu and Beland, 2006). The pre-treatment approaches for enriching hydrogen-producing bacteria that can put significant influence both on the start-up period and efficiency of the hydrogen-producing reactors include load-shock, heat-shock, acid, base, 2-bromoethanesulfonate acid (BESA), aeration, freezing and thawing, chloroform, and iodopropane (Hawkes *et al.*, 2002; Mohan *et al.*, 2008; Wang and Wan, 2008; Sompong *et al.*, 2009). Several research works have been performed to compare

the impact of various pre-treatment approaches on the enrichment of hydrogen producing bacteria in anaerobic hydrogen production processes using different inoculants. There exists certain degree of variations on a suitable pre-treatment method to enrich hydrogen-producing bacteria. From the literature, the use of heat-shock pre-treatment technique resulted in the highest hydrogen production rate (HPR) (Mu *et al.*, 2007; Wang and Wan, 2008). Sompong and co-workers (2009) reported that the successful application of the load-shock treatment method enriching thermophilic hydrogen-producing inocula and resulted in a maximum hydrogen production yield of 1.96 mol H_2/mol hexose with a HPR of 11.2 mmol H_2/L.h. Acid pre-treatment method also showed the highest HPR (Cheong and Hansen, 2007). The BESA pretreatment method also showed high hydrogen yield (0.0317 mmol/g COD) (Mohan *et al.*, 2008). The most common used technique is the heat-shock treatment with temperature in the range of 80 to 121°C depending on the employed bacterial source for an exposure time between 15 to 120 minutes (Lay *et al.*, 1999; Ginkel and Sung, 2001; Logan *et al.*, 2002; Lay *et al.*, 2003; Chang and Lin, 2004; Han and Shin, 2004). However, applying heat-shock treatment showed a reduction in hydrogen production after one month of operation. Thus, to avoid the aforementioned problem, regular repetition of sludge treatment was required (Duangmanee *et al.*, 2007; Sompong *et al.*, 2009).

The different approaches for seeds preparation were based on the physiological discrepancies between hydrogen producing bacteria and hydrogen consuming bacteria. For example, *Clostridium* and *Enterobacter*, which are facultative and capable of forming protective spores, were acclimatized under restrictive environments for hydrogen consuming bacteria such as aerobic condition, extreme acidic or alkaline circumstances, as well as high temperature. However, methanogenic bacteria are obligate anaerobic and have no ability to form spore (Zhu and Beland, 2006).

2.5. Process Modeling and Optimization by Design of Experiments (DoE)

Design of experiments (DoE) has been very useful in the study of complex processes (e.g. anaerobic digestion process) and to determine the optimum process operating conditions with minimum effort and time. Mass transfer coefficient and kinetic are the most important factors that are used to design up-flow bioreactors (UASB). These factors usually were determined *via* steady state models. The model is fundamentally able to forecast the parameters careful in mass balance relations but is incapable to estimate other interrelated effluent responses such as H_2 yield, HPR, SHPR, pH, and etc. (Zinatizadeh *et al.,* 2007). To solve this problem usually process modeling and optimization was conducted applying response surface methodology (RSM) (Baş and Boyaci, 2007). RSM is a collection of mathematical and statistical techniques useful for designing experiments, building models, evaluating relative significance of several independent variables, and determining optimum conditions for desirable responses (Mu *et al.,* 2009).

Previously, the effects of independent factors in chemical and biochemical processes were evaluated and optimized applying RSM such as: optimization of biohydrogen production by *Clostridium butyricum* EB6 from palm oil mill effluent (Chong *et al.,* 2009), optimization of thermophilic fermentative hydrogen production from palm oil mill effluent by *Thermoanaerobacterium*-rich sludge (Sompong *et al.,* 2008). The application of RSM and the central composite design have also been applied to determine optimum conditions for hydrogen production from glucose by an anaerobic culture (Mu *et al.,* 2009), optimization of hydrogen production in a granule-based UASB reactor (Zhao *et al.,* 2008).

The optimum operating conditions is obtained applying RSM that is used along with the Design of Experiments. In this study, the Central Composite design (CCD) due to its suitability to fit quadratic surface was applied to optimize the biological

hydrogen production process. CCD is often applied under RSM design. The design includes of 2^k factorial points augmented by $2k$ (the number of variables) axial points and a center point. The levels of each variable vary from a low to high value and which are numerically expressed or coded as -1 and 1 with intermediate value of 0. Three types of central composite designs for two factors are shown in Figure 2.7. It can be seen that the rotatable design (the original form of CCD) explores the largest process space and the inscribed designs are rotatable designs, but the faced-centered design is not.

In the design, the design points describe a circle circumscribed about the factorial square. Some of points occur outside the range of the factors (Figure 2.6). These points are called axial points. The axial points are at some distance (α) from the center. It is based on the number of factors, k in the design, where α is equal to $\sqrt{k}$. These designs have circular, spherical (for three variables), hyper spherical (for four or more variables) and require five levels for each factor.

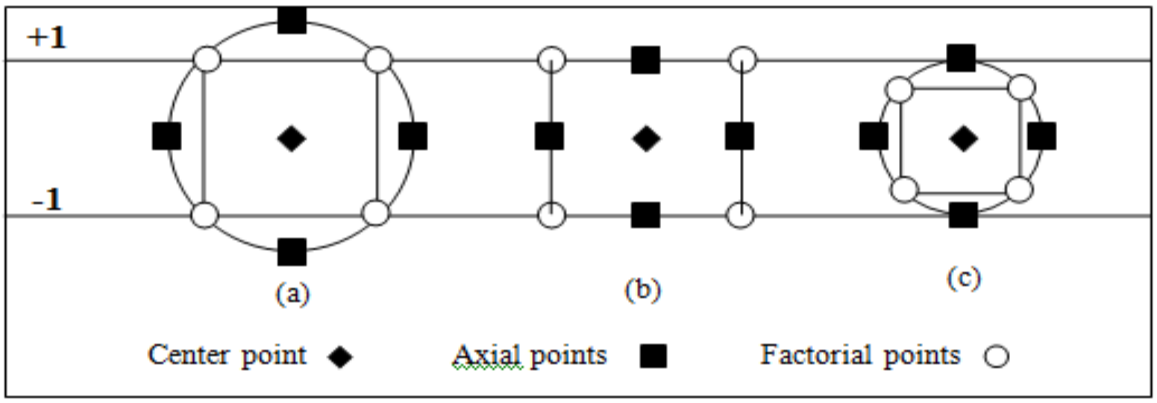

Figure 2.7. The main types of central composite designs for two variables; (a) Rotatable, (b) Face-centered, (c) Inscribed (Montgomery, 1991)

The inscribed design is proposed for conditions in which the range of the factor is actually limits. The factorial points is limited between -1 and +1 and the axial points is limited between – α and + α. The design as well needs five levels of each factor. In the face-centered design, the axial points occur at the center of each face of the factorial space, rather than outside the faces as in the case of a spherical region, so α= ±1. This

diversity needs to 3 levels of each factor. Increasing an existing factorial with suitable axial points can also create this design. In the present study, a central composite face-centered design (CCFD) was applied to design the experiments. Figure (2.8) represents the central composite faced-center design with two variables. The coefficients of the polynomial model were obtained using Eq. 2.5 (Khuri and Cornell, 1996).

$$Y = \beta_0 + \beta_i X_i + \beta_j X_j + \beta_{ii} X_i^{\,2} + \beta_{jj} X_j^{\,2} + \beta_{ij} X_i X_j + \ldots \qquad (2.5)$$

where, ß is the regression coefficient, *i* is the linear coefficient and *j* is quadratic coefficient.

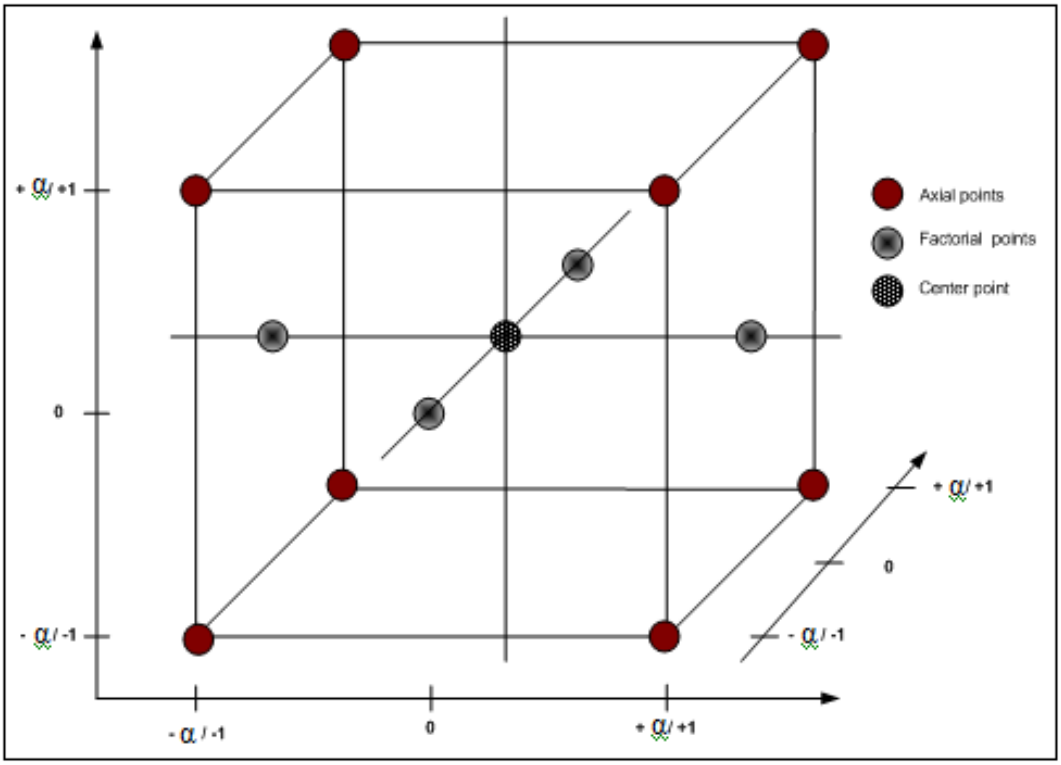

Figure 2.8. Central composite faced-centered design with three variables

Based on *P* value with *95*% confidence level the terms of model may be selected or rejected. The results are analyzed applying analysis of variance (ANOVA) by Design Expert software (Stat-Ease, Version 6.0.8, Inc., Minneapolis, MN). The effects and simultaneous interaction of the variables on the responses are investigated with respect to the three dimensional plots and their respective contour plots obtained. The optimum region is also recognized based on the main responses in the overlay plot.

2.6. Kinetic Modeling

Two interrelated principles must be considered for biological treatment of wastes. Firstly, microorganisms that are metabolically active in catalyzing the pollutant-removing reactions. The rate of pollutant removal depends on the concentration of the catalyst, or the active biomass. Secondly, the active biomass is grown and sustained through the utilization of its energy- and electron generating substrates, which are its electron donor and electron acceptor. The growth rate of active biomass is proportional to the utilization rate of the substrates. The relationship between the active biomass (the catalyst) and the substrates is the most fundamental factor needed for understanding and exploiting the system for pollution control (Rittman and McCarty, 2001).

Bacterial growth kinetics is represented by the relationship between biomass growth and substrate utilization rate by Monod equation (Baily and Ollis, 1985).

$$\mu = \frac{1}{X} \cdot \frac{dX}{dt} = \frac{\mu_m S}{K_s + S} = Y \frac{kS}{K_s + S} - k_d \qquad (2.6)$$

where, μ is specific growth rate (d^{-1}), X is biomass concentration (mg VSS/l), t is time (day), S is concentration of the rate-limiting substrate (mg/l), μ_m is maximum specific growth rate (day^{-1}) and K_s is half-velocity constant (mg/l), Y is biomass yield (mg biomass produced/mg COD removed), and K_d is decay constant (d^{-1}). When the substrate is being used at its maximum rate, the bacteria also grow at their maximum rate. The maximum specific growth rate of the bacteria is thus related to the maximum specific substrate utilization rate as follows:

$$\mu_m = kY_X \quad \text{or} \quad k = \frac{\mu_m}{Y_X} \qquad (2.7)$$

$$Y_X = \frac{\frac{dX}{dt}}{\frac{dS}{dt}} \qquad (2.8)$$

where, k is maximum specific substrate utilization rate (day^{-1}) and Y_X is active biomass (X) yield over substrate (S). By combining Equations (2.7) and (2.8) the substrate utilization rate will become:

$$r_{su} = -\frac{\mu_m XS}{Y_X (K_S + S)} \qquad (2.9)$$

where r_{su} is substrate consumption rate (g/l.d). It is important to note that kinetic expressions used to model substrate utilization and biomass growth rate, are all empirical (based on experimentally determined coefficient values).

The cumulative hydrogen production curves versus time from the experiments were used to determine the hydrogen production potential (P), maximum hydrogen production rate (R), and lag phase time (λ) using the modified Gompertz equation (Van Ginkel et al., 2001; Lay, 2001; Chen et al., 2006).

$$\mathrm{H(t)} = \mathrm{P}\exp\left\{-\exp\left[\frac{\mathrm{R.e}}{\mathrm{P}}(\lambda - \mathrm{t}) + 1\right]\right\} \qquad (2.10)$$

where H(t) is cumulative hydrogen production (mL) at time t; λ is time of lag phase (h); P is hydrogen production potential (mL); R is hydrogen production rate (mL/h); and e = 2.71828.

From other biokinetic studies, the specific growth rates (μ) of hydrogen-producing bacteria growing on sucrose, non-fat dried milk and food waste were found to be 0.10 h^{-1}, 0.176 h^{-1} and 0.215 h^{-1}, respectively (Shihwu Sung *et al.*, 2004). These values were considerably higher than that shown by hydrogen-oxidizing bacteria (0.055 h^{-1}) (Rittmann and McCarty, 2001; Shihwu Sung *et al.*, 2004). Therefore, a fermentative

hydrogen production reactor could potentially be operated at much shorter HRT than the conventional methanogenic reactor.

CHAPTER 3

MATERIALS AND METHODS

3.1. Chemical substances

Table 3.1 lists the chemicals used in this study. The chemicals were used as acquired from the chemical suppliers without further purification.

Table 3.1. List of chemical substances

Name of chemical	Supplier	Purpose of use
$K_2Cr_2O_7$	R&M, UK	COD test
$AgNO_3$	R&M, UK	
$HgSO_4$	R&M, UK	
Potassium hydrogen phthalate	R&M, UK	
KH_2PO_4	R&M, UK	BOD test
NH_4Cl	R&M, UK	
K_2HPO_4	R&M, UK	
Na_2HPO_4. $7H_2O$	R&M, UK	
$MgSO_4$. $7H_2O$	R&M, UK	
$CaCl_2$	R&M, UK	
$FeCl_3.6H_2O$	R&M, UK	
KI	R&M, UK	
NaN_3	R&M, UK	
NaOH	R&M, UK	TKN and BOD test and pH adjustment
H_2SO_4	R&M, UK	Alk linity test, COD, TKN and BOD test
$NaHCO_3$	R&M, UK	Supplying bicarbonate alkalinity
$Na_2S_2O_3.5H_2O$	R&M, UK	TKN and BOD test
n-Hexane	R&M, UK	Oil and grease test
HgO	R&M, UK	TKN test
HCl	R&M, UK	pH adjustment
Filter paper Whatman GF/C (934AH)	Fisher Co.	TSS and VSS test
Reinforced clostridial agar	Merck, Germany	Fast development of biofilm in the fixed film reactor

3.2. Overall experimental flowchart

Figure 3.1 shows the flowchart of the experimental works carried out in this study.

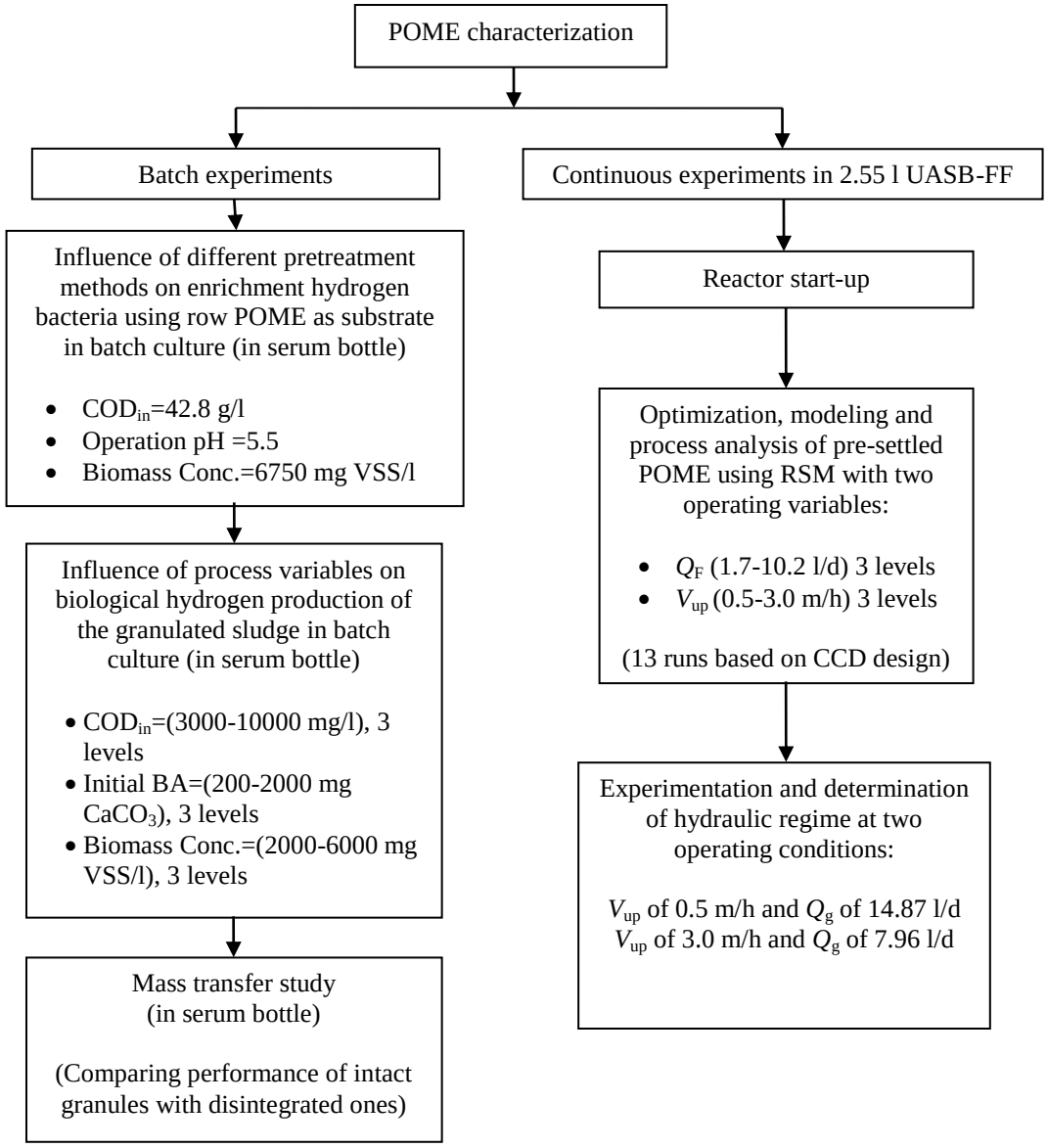

Figure 3.1. Flowchart of overall experimental activities involved in this study (BA: bicarbonate alkalinity)

3.3. Definition of process parameters studied

The following relationships are the parameters that were determined as the process responses in this study.

$$Y_H = \frac{Q_{H_2}}{Q_F \times COD_{in}} \quad (3.1)$$

$$HPR = \left(\frac{Q_{H_2}}{Q_F \times (COD_{in} - COD_{eff})}\right) / HRT \quad (3.2)$$

$$SHPR = \frac{Q_{H_2}}{V \times MLVSS} \quad (3.3)$$

$$SRT = \frac{(V).(VSS)}{(Q_F).(VSS_{eff})} \quad (3.4)$$

$$\frac{F}{M} = \frac{(Q_F).(COD_{in})}{(V).(VSS)} \quad (3.5)$$

$$\text{Hydrogen production rate per volume of reactor} = \frac{Q_{H_2}}{(V)} \quad (3.6)$$

$$\text{Hydrogen production rate per volume of feed} = \frac{Q_{H_2}}{(Q_F)} \quad (3.7)$$

where Y_H hydrogen yield (l H_2/g COD), Q_F is feed flow rate (l/d), Q_{H2} is hydrogen production rate (l H_2/d), COD_{in} is influent COD concentration (mg/l), COD_{eff} is effluent COD concentration (mg/l), *SRT* is solid retention time (d), *VSS* is the biomass concentration in the reactor (mg/l), *V* is the volume of the reactor (liter), *HPR* is hydrogen production rate (l H_2/g $COD_{removed}$.d), *SHPR* is specific hydrogen production rate (l H_2/g VSS.d), *HRT* is hydraulic retention time (d), *F/M* is food to microorganism ratio (g COD_{in}/g VSS.d).

3.4. UASB-FF bioreactor set-up

The schematic diagram of the UASB-FF bioreactor (total volume 3.5 l, working volume 2.55 l, liquid height 80 cm) rig set-up used in this study is shown in Figure 3.2. The bioreactor was fabricated with an internal diameter of 55 mm at the bottom and middle parts and 75 mm at top part. The bioreactor comprised of three sections. The lowest section of the UASB reactor's column with the height of 60 cm (granular sludge

portion) accommodated 67.84% of the total working volume. The middle section with the height of 15 cm (fixed film reactor) accommodated 14.51% of working volume. The top section of the bioreactor accommodated 17.65% of the working volume consisting a gas-solid separator and outlet zone for fermented POME. The middle part of the column was packed with 70 Pall rings (diameter and height 16 mm; specific surface area 341 m^2/m^3) (Fig. 3.3). The void space ratio of the packed-bed reactor was 90.91%. The sampling ports (S1-S5) were designed at appropriate intervals along the height of the reactor (Figure 3.2 and Plate 3.1).

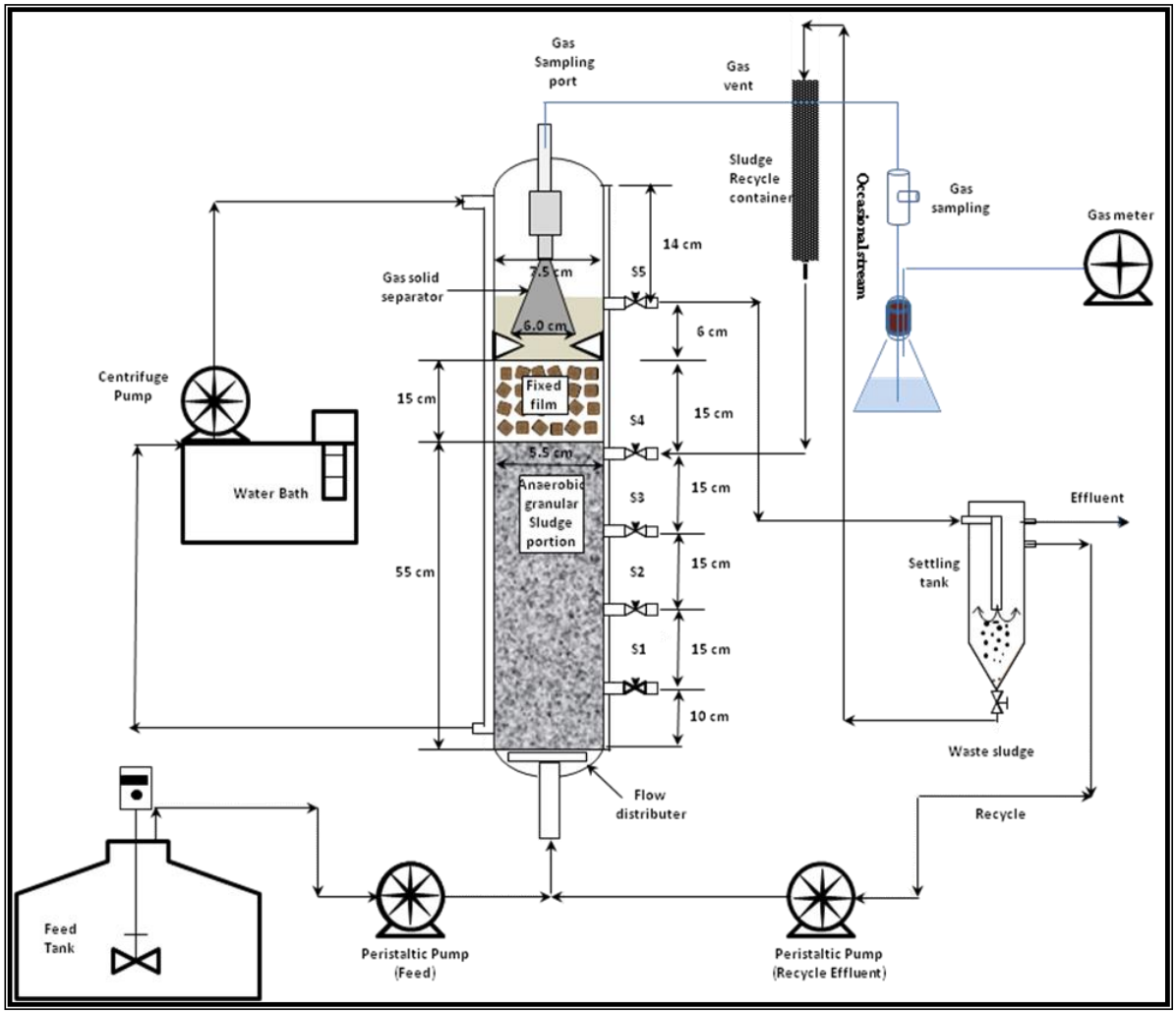

Figure 3.2. Schematic diagram of the experimental set-up

The gas-liquid-solid separator at the top part is for the separation of the washed out solids and the biogas from the liquid phase. To measure the biogas volume generated, a gas meter counter was connected to an inverted funnel and cylinder shaped

gas separator. To sample the biogas for the determination of its composition, a gas sampling port with tubing connector was provided. Before connecting the tubing to the gas meter, a water seal was used to separate gas meter unit from the reactor, providing proper condition for biogas sampling.

Figure 3.3. The Pall rings applied into the middle part of the UASB-FF bioreactor

To ensure isothermal operation of the UASB-FF reactor at the selected temperature, water was circulated through the bioreactor jacket from a thermostated water bath equipped with a centrifugal pump (Lab. Companion, model: CW-05G, Korea). The feeding of substrate (POME) was carried out continuously into the bottom inlet of the reactor using a peristaltic pump (EYELA, model: MP-1000, Japan, 0.24-34.8 l/d) and the effluent went out from the top of the column (S5). A distributor of influent liquid was mounted at the base of the reactor to assist in distributing the feed uniformly into the reactor column.

A cylindrical settling tank was installed in order to settle the washed out suspended solids (SS) from the reactor and also to provide an effluent with low SS for recycling into the reactor. The volume of the settling tank is 880 ml. The effluent was continuously recycled using a peristaltic pump (EYELA, Japan). For recycling the washed out granular sludge (settled at the bottom of the settling tank) into the reactor, a column was fitted to the setup and connected to sampling port #4 (S4) in order to transfer the granular sludge into the anaerobic lower part of the reactor without disintegration. In order to ensure a homogenous substrate supply, a magnetic stirrer was

used to agitate the feed reservoir.

Plate 3.1. Laboratory-scale experimental set-up used in this study

3.5. Pretreatment on anaerobic mixed microflora

3.5.1. Experimental

In this study, experiments were conducted to assess the influence of different pretreatment methods on anaerobic sludge in order to increase H_2 production efficiency using POME as substrate. The sludge was sieved using mesh with grid size of 2.0 mm to remove coarse matters and prior to washing with tap water. Subsequently, it was treated to disable primarily H_2 consuming bacteria and enrich hydrogenesis by one of the following methods: chemical pretreatment, acid hydrochloric pretreatment, heat-shock pretreatment, alkaline (base) pretreatment, freezing and thawing pretreatment.

The chemical pretreatment was conducted by adding 0.1% (v/v) of chloroform into the sludge for 24 h at room temperature (Hu and Chen, 2007). The acid pretreatment was conducted by adjusting the pH of the sludge to 3.0 by adding concentrated HCl (6N) and kept for 24 h, and subsequently re-adjusted the pH to 5.5 by NaOH solution (2N) (Chen *et al.*, 2002; Sompong *et al.*, 2009; Lee *et al.*, 2009). The heat shock pretreatment was conducted by heating the sludge to 100ºC for 1 h in the water bath (Ginkel and Sung, 2001; Mohan *et al.*, 2008). The base pretreatment was conducted by adjusting the pH of the sludge to 12 by adding NaOH (6 N) and kept for 24 h and subsequently re-adjusted the pH to 5.5 by HCl solution (1 N) (Cai *et al.*, 2004; Sompong *et al.*, 2009). Freezing and thawing pretreatment was conducted by freezing the sludge to -10ºC for 24 h and then thawing it in a water bath at 30ºC until it reached room temperature (Cheong and Hansen, 2006). A control experiment using the non-treated sludge was also conducted.

3.5.2. Experimental set-up

The serum bottle was used as a batch reactor in this study. Six 500 ml serum bottles were used for each run at 10% v/v sludge. The sludge samples in different serum bottles

were subjected to the aforementioned pretreatments. After the pretreatments, POME was added into each bottle to obtain a final working volume of 200 ml. The run was conducted at 35 ± 2ºC and an agitation rate of 120 rpm. The pH of the mixture was also adjusted to 5.5 ± 0.3 before initiating the batch test. In order to obtain an anaerobic condition for the bacteria, the entire serum bottle volume (headspace plus liquid) was sparged with nitrogen for 15 min at a flow rate of 10 ml/s. The batch runs lasted for 72 h and all experiments were performed in three replicates.

3.6. Studies of UASB-FF bioreactor performance

3.6.1. Bioreactor start-up

3.6.1(a) Wastewater preparation

The reactor was fed with a pre-settled palm oil mill effluent (POME). POME samples were taken from SIME Darby Plantation Palm Oil Industry Sdn. Bhd., Nilai, Malaysia. The samples were transferred to the laboratory immediately and stored in a cold room (4^oC) before use. Various dilutions of POME were made using tap water. The pH and alkalinity of the feed was adjusted to 5.5 and 1400-1600 mg $CaCO_3$/l using NaOH solution (3N) and $NaHCO_3$, respectively. Supplementary nutrients such as nitrogen (NH_4Cl) and phosphorous (KH_2PO_4) were added to give a ratio of COD: N: P of 550:7.4:1 (Sompong *et al.*, 2008).

3.6.1(b) Seed sludge preparation

The inoculum for seeding of the reactor was a sludge taken from digested sludge from palm oil mill industry (SIME Darby Plantation Sdn. Bhd., Nilai, Malaysia). The sludge was initially passed through a screen to remove debris and solid particles and then heated at 100°C for 1 h to enrich hydrogen producing microbes and to inhibit methanogens which are unable to form heat-resistant capsule (Mohammadi *et al.*, 2011).

The initial volatile suspended solids (VSS) concentration of the seed was measured at 4600 mg/l. In order to test microbial activities of the seed sludge, 40 ml POME (4680 mg COD/l) was added to 10 ml of sludge sample in a serum bottle and the gas produced was analyzed after 24 h.

3.6.1(c) Bioreactor operation

Initially, to make the packing surface sticky for fast development of biofilm in the packed bed section, the pall rings were immersed in a 2 % (w/v) agar solution for a few minutes. The reactor was inoculated with 850 ml heat pretreated sludge. For the first five days, the bioreactor was fed in closed-loop, batch mode for acclimatization of the microorganism with the POME strength (COD 4680 mg/l and HRT 24 h). The effluent was continuously recycled into the reactor until the next feeding cycle. The average VSS concentration within the reactor was increased to 5650 mg/l after a five-day closed-loop, fed-batch mode.

Subsequently, the bioreactor was fed in continuous mode with an initial organic loading rate (OLR) of 9.36 g COD/l.d and a HRT of 12 h. The HRT was maintained constant for the rest of the start-up period. The influent COD concentration was increased stepwise to 25880 mg/l (OLR= 51.8 g COD/l.d) from day 8 to day 22. In order to improve hydrogen production performance and maintain an up-flow velocity of 1.0 m/h (Metcalf and Eddy, 2003), fresh feed was mixed with recycled effluent at a ratio of 1:10.4. The high recycle ratio helped to eliminate high organic overloading and provide suitable alkalinity by mixing the recycled effluent with high alkalinity and the fresh feed with the low COD concentration. The temperature was maintained at 38°C using thermostated water bath with water circulation system. The pH of the reactor was adjusted to 5.5 by using NaOH (1N) and HCl (1N). Hydrogen production, COD reduction, TSS and VSS concentration were monitored periodically.

3.6.2. Optimization, modeling and process analysis of dark fermentative hydrogen production from pre-settled POME

3.6.2(a) Experimental design and mathematical model

Dark fermentative hydrogen production in up-flow reactors depends on a multitude of variables. The main factors that affected the process were feed flow rate, up-flow velocity (V_{up}), COD concentration, alkalinity, pH and MLVSS concentration. In this study among aforementioned factors, Q_F and V_{up} are the most critical operating and independent factors, and were chosen due to the following reasons:

a) The main purpose of this research was to study the performance of the bioreactor in biological hydrogen production from the pre-settled POME with a relatively constant COD concentration 28-30 g/l. In order to investigate the effect of organic loading rate on hydrogen production, feed flow rate was selected as a key operating variable.

b) According to the previous studies, it was found that during fermentative hydrogen production processes, bicarbonate alkalinity was generated. Hence, to provide the required alkalinity hydrogenesis, the recirculation of effluent is an alternative instead of external addition of alkalinity to feed. It also avoids of considerable concentration gradient as a function of bioreactor height in high strength substrate (Leitão *et al.,* 2006). Therefore, V_{up} is an important variable that reflects the rate of alkalinity recycle from effluent to influent and the dilution coefficient of the influent feed. V_{up} is calculated by following equation:

$$V_{up} = \frac{Q_F + Q_R}{A} \qquad (3.10)$$

where Q_F and Q_R are feed flow rate (l/d) and recycle flow rate (l/d), respectively, and A is reactor surface area (m^2). V_{up} also affects the settling velocity and sludge volume index (SVI) of the granulated sludge (Liu and Tay, 2004). Therefore, in this study the

two factors i.e. Q_F and V_{up} were chosen as the independent variables for the purpose of modeling.

According to Table 3.2, the range of Q_F and V_{up} investigated for biological hydrogen production from POME were 1.7-10.2 l/d and 0.5-3.0 m/h, respectively. In this study, the influent COD concentration of pre-settled POME was maintained at 15000 mg/l in all experiments. Therefore, Q_F was determined to be in the range of 1.7 to 10.2 l/d (corresponding to HRT of 36 to 6 h) in order to find the optimum conditions for increasing the effluent quality and process stability. This would cover an OLR range of 10 to 60 g COD/l.d. Selection of the range of the OLR studied was based on the results obtained from previous studies by other researchers.

Metcalf and Eddy (2003) has suggested that the suitable up-flow velocity to be used should be in the range of 0.5 to 3 m/h. The attainment of steady state condition for each experiment is expected after several turnovers.

Table 3.2. Experimental range of the independent variables

Variables	Range		
	-1	0	1
feed flow rate	1.7	5.95	10.20
up-flow velocity	0.5	1.75	3.0

In the present study, hydrogen production from POME in a UASB-FF bioreactor was evaluated and optimized employing RSM with a central composite design. The main and interactive effects of feed flow rate (Q_F) and up-flow velocity (V_{up}) on the process responses were explained. Table 3.3 shows the experimental conditions for fermentative hydrogen production from POME based on CCD design.

In order to perform a comprehensive analysis of the fermentative hydrogen production process, 11 dependent parameters viz. H_2 percentage in biogas, hydrogen yield (Y_H), hydrogen production rate (HPR), specific hydrogen production rate (SHPR),

COD removal efficiency, effluent pH, effluent bicarbonate alkalinity (BA), effluent total volatile fatty acid (TVFA), effluent total suspended solids (TSS), sludge height in the UASB portion and food to microorganism ratio (F/M) as response were evaluated. The number of experiments is eliminated systematic errors with an estimate of the experimental error and minimizes by statistical method of factorial DoE (Zinatizadeh *et al.,* 2007).

Table 3.3. Experimental conditions for fermentative hydrogen production from POME based on CCD design

Run No.	**Variables**	
	Feed flow rate (l/d)	**Up-flow velocity (m/h)**
1	(-1)1.7	(-1)0.50
2	(0)5.95	(-1)0.50
3	(0)5.95	(0)1.75
4	(0)5.95	(0)1.75
5	(-1)1.7	(0)1.75
6	(0)5.95	(0)1.75
7	(1)10.2	(-1)0.30
8	(-1)1.7	(1)3.00
9	(1)10.2	(0)1.75
10	(0)5.95	(0)1.75
11	(0)5.95	(0)1.75
12	(1)10.2	(1)3.00
13	(0)5.95	(1)3.00

The data were analyzed using ANOVA in the Design Expert software (Stat-Ease Inc., version 6.0.5). The design of experiments was also used to identify important factors that affect the process, and the optimal operational conditions were determined by response surface methodology (RSM). The obtained results were presented as two- and three-dimensional contour plots to study the effect of variables interaction on the

responses. The overlay plot was used to identify and navigate quickly to the optimum region. Table 3.3 depicts the experimental conditions in this study.

3.6.2(b) Bioreactor operation

The bioreactor was operated with pre-settled POME as the feed and operational conditions are as presented in Table 3.3. The fermentative hydrogen production data from POME was used in the modeling by RSM.

3.7. Biological hydrogen production using granulated sludge in batch experiments

3.7.1. Influence of process variables on biological hydrogen production of the granulated sludge

The effects of three important process variables (COD concentration, initial bicarbonate alkalinity and biomass concentration) on biological hydrogen production from POME in batch culture were investigated. The experiments were designed as central composite face-centered design (CCFD) using DoE (version 6.0.5).

Results obtained from the previous experiments showed that bicarbonate alkalinity (BA) was produced during POME anaerobic digestion process. Since one of the aims in this study was to determine the optimum initial BA which could maintain the pH at favorable range for hydrogenesis activity, therefore the range of BA was chosen from a minimum amount of 200 to 2000 mg $CaCO_3$/l.

A wide range of food to microorganism (F/M) ratio from about 0.25 to 2.5 g COD/g VSS.d was considered and examined as a criterion for determining the range of COD and biomass concentration in this study. The ranges of the variables are presented in Table 3.4. The experimental conditions are presented in Table 3.5.

Table 3.4. Experimental range of the independent variables

Variables	Unit	Range		
		-1	**0**	**1**
COD concentration	mg/l	3000	6500	10000
MLVSS concentration	mg/l	2000	4000	6000
Initial bicarbonate alkalinity	mg $CaCO_3$/l	200	1100	2000

Table 3.5. Experimental conditions applying CCD in this study

Run	Designed values of variables by DOE		
	COD_{in} (mg/l)	**MLVSS conc. (mg VSS/l)**	**Initial bicarbonate alkalinity (mg $CaCO_3$/l)**
1	(+1) 10000	(-1) 2000	(+1) 2000
2	(0) 6500	(+1) 6000	(0) 1100
3	(0) 6500	(0) 4000	(0) 1100
4	(-1) 3000	(-1) 2000	(+1) 2000
5	(+1) 10000	(-1) 2000	(-1) 200
6	(0) 6500	(0) 4000	(+1) 2000
7	(+1) 10000	(+1) 6000	(-1) 200
8	(0) 6500	(-1) 2000	(0) 1100
9	(0) 6500	(0) 4000	(-1) 200
10	(-1) 3000	(+1) 6000	(+1) 2000
11	(-1) 3000	(-1) 2000	(-1) 200
12	(0) 6500	(0) 4000	(0) 1100
13	(-1) 3000	(0) 4000	(0) 1100
14	(0) 6500	(0) 4000	(0) 1100
15	(-1) 3000	(+1) 6000	(-1) 200
16	(+1) 10000	(+1) 6000	(+1) 2000
17	(0) 6500	(0) 4000	(0) 1100
18	(0) 6500	(0) 4000	(0) 1100
19	(+1) 10000	(0) 4000	(0) 1100
20	(0) 6500	(0) 4000	(0) 1100

Experiments were performed in 163-ml serum bottles with 50 ml medium (experimental conditions as shown in Table 3.5) and sealed with butyl rubber stoppers and aluminum seals as shown in Plate 3.2. The biomass was obtained from the UASB-FF bioreactor operated at steady-state in our laboratory for biological hydrogen

production from POME. The pH was adjusted to 5.5. The medium was distributed anaerobically under O_2-free nitrogen gas into the serum bottles.

The gas phase was purged using nitrogen gas. The serum bottles were placed in a shaking incubator (DAIHAN LABTECH Co., Singapore) (120 rpm) at 38°C. At intervals of 8 h, the composition of gas and liquid (H_2 percentage, volume of biogas produced, alkalinity and COD) were measured. The results after two days of fermentation were used to analyze the process using ANOVA (Design Expert Software). Three process parameters (hydrogen yield, specific hydrogen production rate and COD removal efficiency) were studied as the process responses. Three-dimensional plots were used to visualize the effects of the studied variables. The simultaneous interactions of the variables on the responses were also studied from these three-dimensional plots.

Plate 3.2. Serum bottles used for batch experiments

3.7.2. Mass transfer evaluation on POME-grown microbial granules

Experiments were performed in 163-ml serum bottles with 50 ml medium (containing 3500 mg VSS/l biomass and 5500 mg/l COD) as described in section 3.7.1.

The granular sludge was obtained from the UASB-FF bioreactor operating at steady-state. The pH was adjusted to 5.5. $NaHCO_3$ (2000 mg/l $CaCO_3$) is added to provide the initial bicarbonate alkalinity. The medium was distributed anaerobically under O_2-free nitrogen gas into 10 serum bottles.

The serum bottles were subsequently placed in a shaking incubator (DAIHAN LABTECH Co., Singapore) at 38 °C and 120 rpm. At 12 h intervals, the composition of gas and liquid (H_2 percentage, volume of biogas produced, and COD, respectively) in the serum bottles containing disintegrated and intact sludge were measured.

3.8. Analytical techniques

3.8.1. Basic water quality parameters measurement

The parameters viz. biochemical oxygen demand (BOD), chemical oxygen demand (COD), total suspended solids (TSS), volatile suspended solids (VSS), alkalinity, total Kjeldahl nitrogen (TKN), oil and grease, and pH were analyzed using procedures outlined in the APHA Standard Methods (1999).

A titrimetric method with closed reflux method (5220C) was developed for COD measurement. A semi-micro Kjeldahl method was used for TKN measurement. The pH was measured by using the pH meter model pH600 from EUTECH (Singapore). Oil and grease was measured by partition gravimetric method. In this method, oil & grease content of the sample was initially extracted using *n*-hexane as solvent. Hexane was then evaporated in a rotary evaporator. The residual is reported as oil and grease. The SVI was measured according to the Standard Methods (APHA, 1999).

3.8.2. Biogas Analysis

A gas-tight syringe (Hamilton CO., USA) was used to take gas samples from the gas sampling port. The biogas composition was determined using a gas chromatograph

(Perkin Elmer, Auto system GC), equipped with thermal conductivity detector (TCD) and data acquisition system with Total Chrom® software. H_2 content was also analyzed by GC-TCD fitted with a 1.5 m stainless steel column (SS350A) packed with a molecular sieve (80/100 mesh). The temperature values of the injection port, oven and detector were 80, 200, and 200°C, respectively. Argon was used as a carrier gas at a flow rate of 30 ml/min. The gas sample (1 ml) was injected in replicates. A sample of the report generated by this workstation is attached in Appendix A.

3.8.3. Volatile Fatty Acids Measurement

The liquid samples for VFAs determination were analyzed by a gas hromatograph (Perkin Elmer, Auto system GC) equipped with a flame ionization detector (FID). A 2 m × 2 mm stainless steel, 80/120 mesh Carbopack B-DA/4 % Carbowax 20 M (Supelco) column was used. The oven temperature was maintained at 175°C while the injector and detector temperatures were 200 and 220°C, respectively. The carrier gas (helium) flow rate was set at 40 ml/min.

3.9. Hydrodynamic studies of UASB-FF Bioreactor

In order to carry out the analysis of the hydrodynamic process within the UASB-FF, the reactor was filled with water till the top level of the outlet. Then, pulses of an inert substance is introduced into the reactor inflow and subsequently measured at the outflow. To study the flow pattern in the reactor, a technique involving analysis of tracer-response profiles was used. In this tracer study, Rhodamine B as a tracer is introduced into the influent end of the reactor and collected the tracer-output profile in the fluid leaving the reactor. Rhodamine B was used as a tracer because this substance will not be absorbed on or reacts with the exposed reactor surface, and can be detected at very low concentration using a spectrophotometric method. In each run, the influent

of water into the reactor was adjusted and fed by peristaltic pump. Subsequently, 2.5 ml of 0.01 M Rhodamine B was immediately fed into the inlet of the reactor. Effluent samples were collected immediately and then at every 5 minutes, or at even shorter time intervals if required. The collected samples were subjected to spectrophotometric reading at 554 nm. The operation was continued until no tracer was detected for at least two or three consecutive samples.

Up-flow velocity (V_{up}) and biogas production rate (Q_g) are two important hydraulic factors and can impact significantly on the hydraulic regime of the UASB-FF bioreactor. In this study, V_{up} and Q_g were selected as the most critical factors on the hydraulic regime the UASB-FF bioreactor. The region of exploration for hydraulic regime UASB-FF bioreactor was decided as the area enclosed by V_{up} (0.5 and 3.0 m/h) and Q_g (14.87 and 7.96 l/d). Selection of the values of the Q_g was based on the results obtained from the earlier studies.

3.10. Scanning Electron Microscopy (SEM)

Scanning electron microscopy (SEM) was used to examine the physical features of the granules. A specimen was bombarded with scanning beam of electrons and then slowly moving "secondary electrons" were collected, amplified and displayed on a cathode ray tube. The electron beam and the cathode ray tube scan synchronously so that an image of the specimen surface is formed. Specimen preparation includes fixation with 5% glutaraldehyde and 1% osmium tetroxide, followed by dehydration with 50 to 100 % ethanol and drying, finally making the specimen conductive to electricity. The sample was examined using a Leo Supra 50 VP Field emission SEM (UK) equipped with Oxford INCA 400 energy dispersive X – ray microanalysis system.

CHAPTER 4

RESULTS AND DISCUSSION

The results obtained throughout this research will be presented and discussed in this chapter in the following order.

- POME characterization;
- Effects of different pretreatment methods on anaerobic mixed microflora;
- The start-up of up-flow anaerobic sludge blanket fixed film (UASB-FF) bioreactor;
- Modeling and optimization of biological hydrogen production from POME in the UASB-FF bioreactor;
- Kinetic evaluation of fermentative hydrogen production from POME in the UASB-FF bioreactor;
- Biological hydrogen production of the granulated and disintegrated sludge in batch experiments;
- Hydrodynamic study of the UASB-FF bioreactor;
- The effect of the fixed film part on bioreactor performance.

4.1. Palm oil mill effluent characterization

The average values of the basic water quality parameters for POME are summarized in Table 4.1. The raw POME is a brown slurry colloidal suspension containing 95–96 % water, high organic matter content between 45000 and 55000 mg COD/l, about 2% suspended solids concentration and 0.4–0.5% oil. The values of parameters are averages of three measurements.

Table 4.1. Characteristics of raw POME

Parameters	Amount	Standard of deviation
BOD_5 (mg/l)	22500	±2150
TCOD (mg/l)	49800	±4250
SCOD (mg/l)	21950	±2320
SS (mg/l)	18800	±1240
TKN (mg/l)	430	±32
TP (mg/l)	84	±7.5
Oil & Grease (mg/l)	4250	±62
pH	4.2	±0.2

4.2. Effects of different pretreatment methods on anaerobic mixed microflora

4.2.1. Effect of different pretreatments on H_2 production

The effects of various pretreatment methods on the enrichment of H_2 evolving bacterial population and their H_2 production efficiency using POME as substrate were studied. Figure 4.1 showed the variation of H_2 production yield from the serum bottles inoculated with sludge subjected to different pretreatments and from the serum bottles without any pretreatment (control) during 72 h cultivation time. Experimental results demonstrated the need for inoculum pretreatment for improved H_2 generation by the microbial population as compared to the control experiment. Heat shock pretreatment was shown to be the most effective in enhancing the biological H_2 production up to 48 h cultivation, which appeared to coincide with the leveling of the COD reduction efficiency (see next section).

The H_2 yield from this method was 0.41 mmol H_2/g COD. H_2 yield from control experiment was the lowest i.e. 0.12 mmol H_2/g COD. The relatively low pH between 5.5 and 6.0 for the entire duration of the batch process could have inhibited the growth of H_2 consuming bacteria (Tang *et al.,* 2008; Wang and Wan, 2009; Zhu *et al.,* 2009; Chong *et al.,* 2009). H_2 yield following the heat shock treatment was 3.4 times higher

than that obtained in the control experiment. When the seed sludge was treated under harsh conditions, *Clostridium* or *Enterobacter* would have a better chance to survive than some homoacetogens. Therefore, appropriate pretreatment of the seed sludge can suppress as much homoacetogens as possible while still preserving the activity of the hydrogen-producing bacteria. The digested sludge pretreated by heat-shock could obtain the maximal hydrogen production. This is mainly because heat-shock was able to suppress homoacetogens effectively.

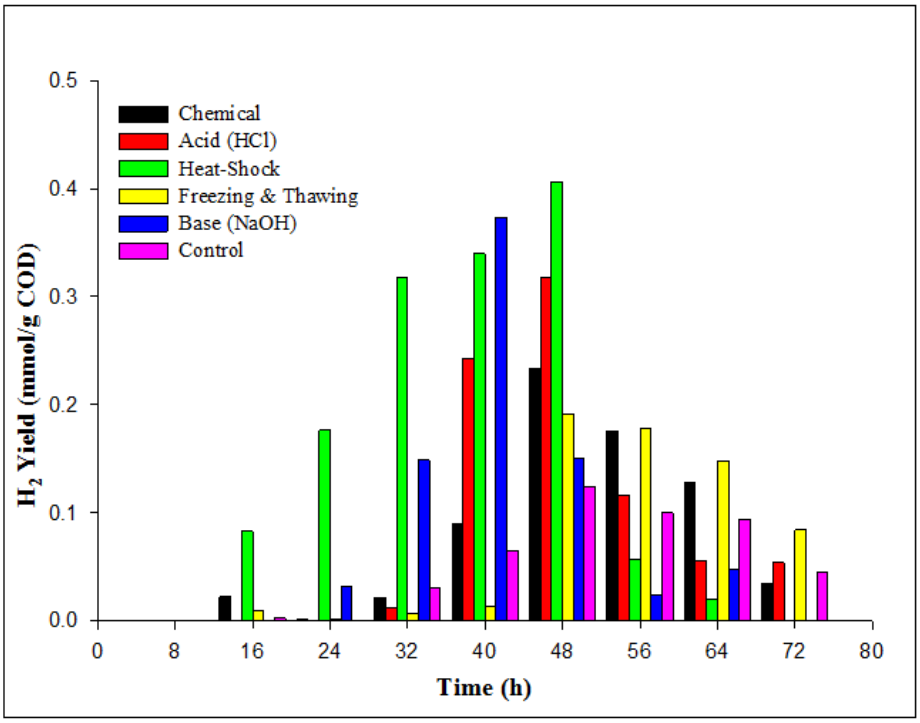

Figure 4.1. Hydrogen yield as a function of pretreatment methods and time (maximum standard deviation for the measurements made was ±0.01 mmol/g COD)

Among the pretreatment methods applied, the freezing and thawing method produced the lowest H_2 yield (0.19 mmol/g COD), which was approximately 58% higher than the control. Although, H_2 production was possible without any pretreatment (control), the application of different types of pretreatment resulted in a significant increase in H_2 yield. The time profiles of the H_2 production following the different pretreatments showed common maxima at 48 h cultivation. Thus, it is suggested that the

harvesting of the pretreated sludge for the subsequent H_2 production process should be no later than 48 h.

The cumulative H_2 production profiles following different pretreatment methods are shown in Figure 4.2. The highest cumulative H_2 production (8.89 mmol) was observed from the heat shock pretreated sludge. The acid and base pretreatments showed similar influence on the cumulative H_2 production but their H_2 yields were lower than heat-shock treated sludge. The freezing and thawing pretreatment method produced only 4 mmol H_2 and had the least influence on H_2 production among the different pretreatments.

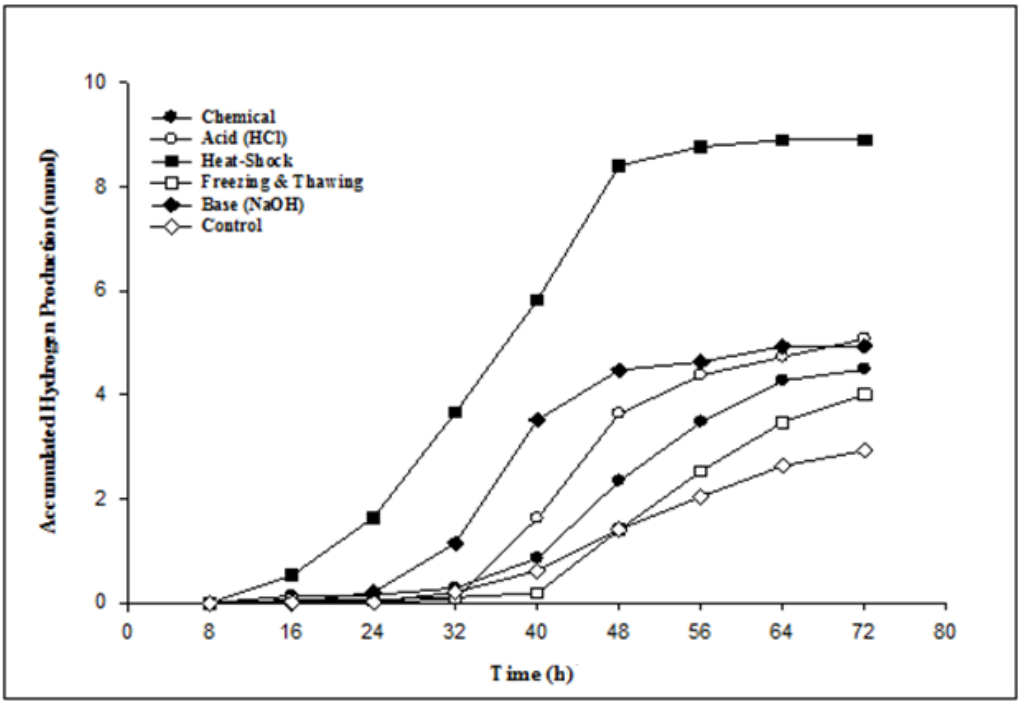

Figure 4.2. Cumulative H_2 production as a function of pretreatment methods and time (maximum standard deviation for the measurements made was ±0.12 mmol)

The lag time before significant increase in H_2 production was observed to vary between 8 (minimum) to 40 (maximum) h for heat shock and freezing & thawing pretreatment methods, respectively. The rest of the pretreatments and control exhibited lag time for H_2 production in between this range. Cultures that were subjected to treatments using heat shock and base leveled off in their H_2 production at 48 h whereas the rest were still showing increase albeit slower in their H_2 evolution.

4.2.2. Effect of different pretreatments on COD removal efficiency

It was observed that the COD removal corresponded well with H_2 production in this study. The time profile of COD removal efficiency during the H_2 generation process is shown in Figure 4.3. Progressive COD removal was observed for all the cultures after 48 h during which the H_2 production rate started to level off.

Among the studied pretreatment methods, heat shock pretreatment demonstrated maximum efficiency for COD removal (86%) with respect to H_2 yield (0.41 mmol H_2/g COD). In the freezing and thawing, and base pretreatment methods similar COD removal efficiency of about 59% was achieved; the H_2 yields however, were calculated at 0.19 and 0.37 mmol H_2/g COD, respectively. Chemical and acid pretreatment methods also resulted in approximately 51% in COD removal efficiency whereas H_2 yields from these methods were 0.23 and 0.32 mmol H_2/g COD, respectively. Control experiment achieved 66% COD removal with the lowest H_2 yield at 0.12 mmol H_2/g COD. Among all the pretreatment methods studied, heat shock method showed superior effect over the other methods with respect to H_2 yield and COD removal efficiency.

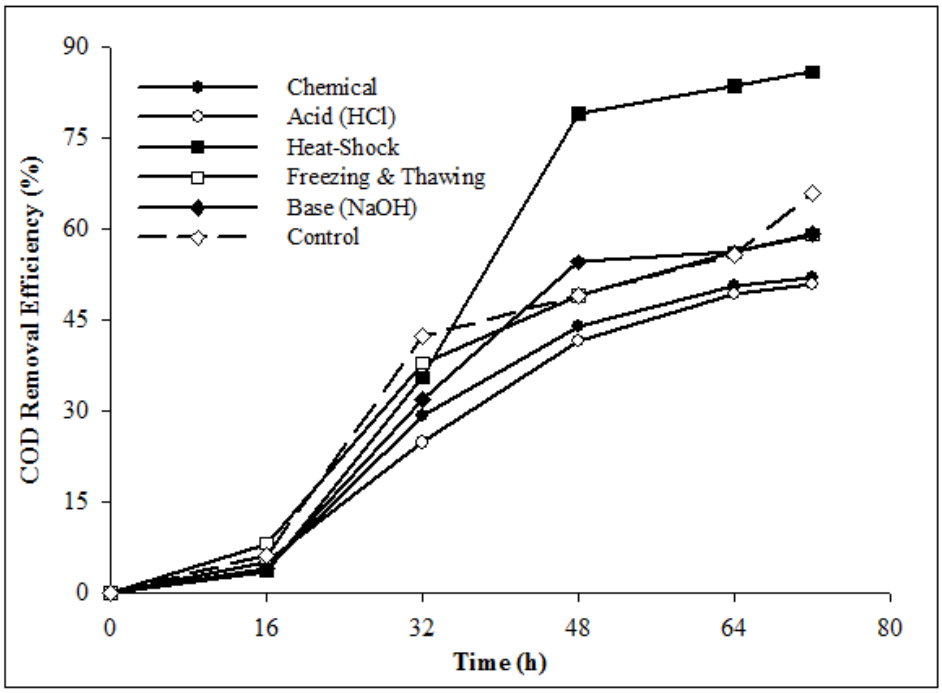

Figure 4.3. COD removal efficiency as a function of pretreatment methods and time (maximum standard deviation for the measurements made was ±1.82%)

4.3. The start-up of an up-flow anaerobic sludge blanket fixed film (UASB-FF) reactor

The UASB-FF reactor was initially inoculated with heat pretreated seed sludge as inoculum. After five days of closed-loop fed-batch operation, the reactor was continuously fed at HRT of 12 h using fresh pre-settled POME. The UASB-FF reactor start-up process was analyzed in terms of hydrogen production, COD removal, and sludge development as follows:

4.3.1. Hydrogen production

The biogas was found to contain 42-58% hydrogen and 42-58% CO_2 (Figure 4.4). No methane production was detected during the experiments demonstrating that the heat-shock pretreatment of sludge successfully inactivated the hydrogen consuming population. The hydrogen production attained at the end of start-up period was 4.61 l H_2/d. The hydrogen content of the biogas increased as the OLR was increased, due to increase in the reaction rate and the hydrogen evolved. The result showed that, even at high biogas production (8.15 lit /d of biogas), the H_2 level in the biogas was consistently elevated at 56.6 %.

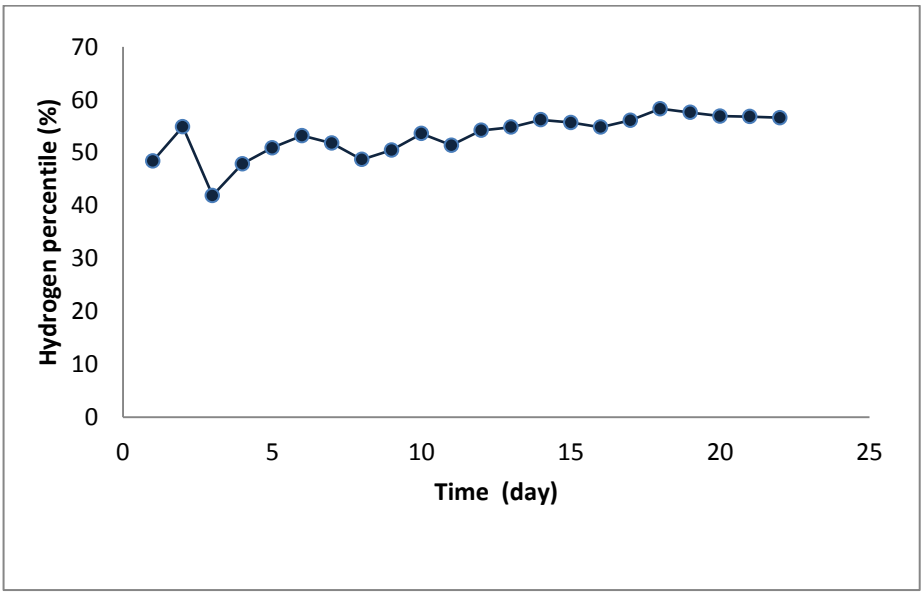

Figure 4.4. Hydrogen fraction in biogas during start-up period

4.3.2. COD removal

Figure 4.5 shows the performance of the UASB-FF reactor during the start-up period (22 days). The reactor was fed with the POME as substrate at a constant COD concentration of 4680 mg/l (HRT 24 h) in the first five days. The results showed that the COD removal efficiency was increased from 25.8% to 38.4% on the fifth day. The reactor was then fed with the COD concentration of 4680 mg/l and HRT 12 h, and subsequently, the COD concentration was increased stepwise to 25880 mg/l during the rest of start-up period. The COD removal efficiency decreased when the influent COD concentration was increased from 4680 to 6470 mg/l and 10350 to 14650 mg/l. This was attributed to the relative decrease in HRT for an increase in OLR, which resulted in organic shocks to the microorganisms. Naturally, the microorganisms need acclimatization time in order to adapt well to the new condition before they regained their pre-shock treatment efficiency. The COD removal efficiency was 42.5 % at an influent COD concentration of 25880 mg/l corresponding to OLR of 51.8 g COD/l.d at the end of the experimental run.

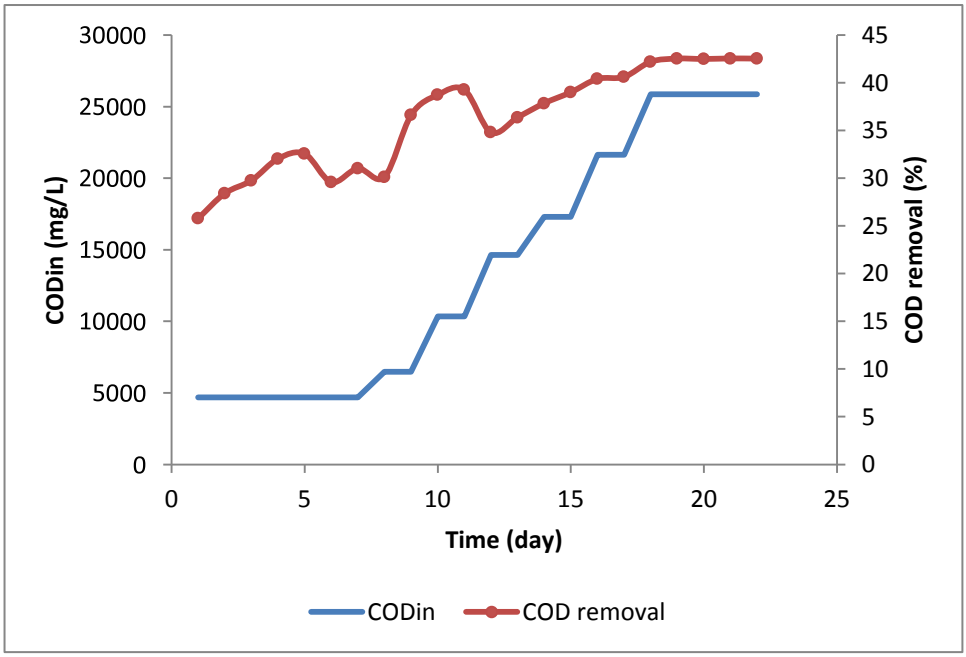

Figure 4.5. COD removal efficiency during start-up period

In this study, the granulated sludge washout phenomenon was negligible during of the UASB-FF bioreactor operation. Also, granulation time in the UASB-FF bioreactor was observed to occur at shorter interval (22 days) whereas it generally requires a longer time in the bioreactor (>60 days) (Lettinga, 1995; Schmidt and Ahring, 1996). The growth of microbial agglomerates was likely promoted by the internal recirculation of the dispersed bacterial population.

4.3.3. Sludge bed growth

Figure 4.6 depicts considerable growth in the height of granule sludge bed within the UASB-FF bioreactor during the start-up period. Measurement of the height of sludge bed after stopping the feed and settling the sludge in the reactor for 1 h evidenced the satisfactory sludge growth. At the beginning of the experiment, the height of the sludge bed was 160 mm. The initial increase of the height of the granulated bed due to bacterial growth was relatively slow, but after 10 days, the rate showed an accelerated increase (Figure 4.6). This was attributed to the existence of the fixed film section above the sludge blanket acting as a buffer zone against complete washout alongside the provision of the internal sludge recirculation. The increase in sludge bed height with increase in OLR was also due to increase of gas bubbles entrapped within granular bed. The height of sludge bed was increased to 174 mm when the OLR increased from 4.68 to 51.8 g COD/l.d. The specific hydrogen production rate was 0.514 lit H_2 /g VSS.d at the end of the start-up period.

Suspended and colloidal components of wastewater in the form of fat, protein and cellulose have adverse impact on UASB reactors' performance. They can cause deterioration of microbial activities that leads to wash out of active biomass (Torkian *et al.,* 2003). The fraction of particulate versus soluble COD is therefore important in determining the applicability of the process. As the fraction of solids in the wastewater

increases, the ability to form a dense granulated sludge decreases (Mahmoud *et al.*, 2003).

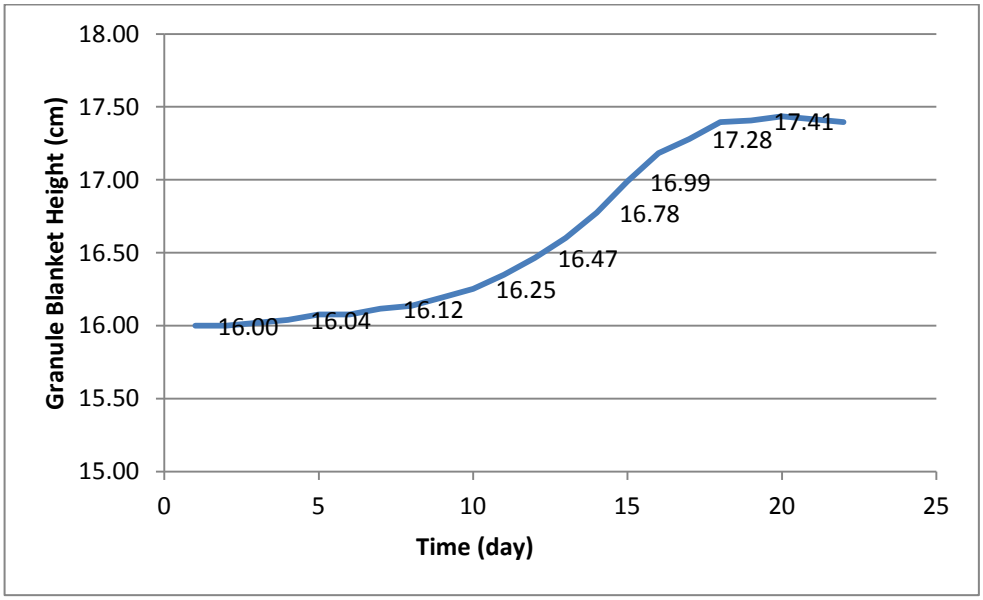

Figure 4.6. Growth of sludge blanket height in UASB-FF bioreactor during the start-up period

The obtained data for COD removal efficiency and hydrogen production in the start-up duration indicated that in the UASB-FF bioreactor, sludge flocculation was satisfactorily achieved and attained good stability at high organic loading. The primary reason for the speeded start-up process was the use of hydrogenesis-enriched pretreated sludge for the inoculation of the bioreactor and the retaining of the majority of flocculated and dispersed sludge in the UASB portion by the fixed bed portion.

The development of hydrogenesis sludge granules was improved by the proportional inoculum seeding to feeding of POME into the bioreactor. The prompt development of bio-granules also was attributed to biomass recirculation and the existence of a fixed film at the upper section of the UASB that resulted improved interaction among the bacterial consortium. The visual sequence of sludge granulation in the UASB-FF reactor during the start-up is shown in Plate 4.1. The granules average diameter increased to >1 mm at the end of the start-up period. The reactor operating conditions have been shown to affect the development of microbial granules (Liu *et al.*,

2003), where in this case, rapid microbial granulation in UASB-FF reactor was thought to be promoted by cell precipitation from the fixed film part, gas bubble generation from sludge blanket and high TSS concentration of POME.

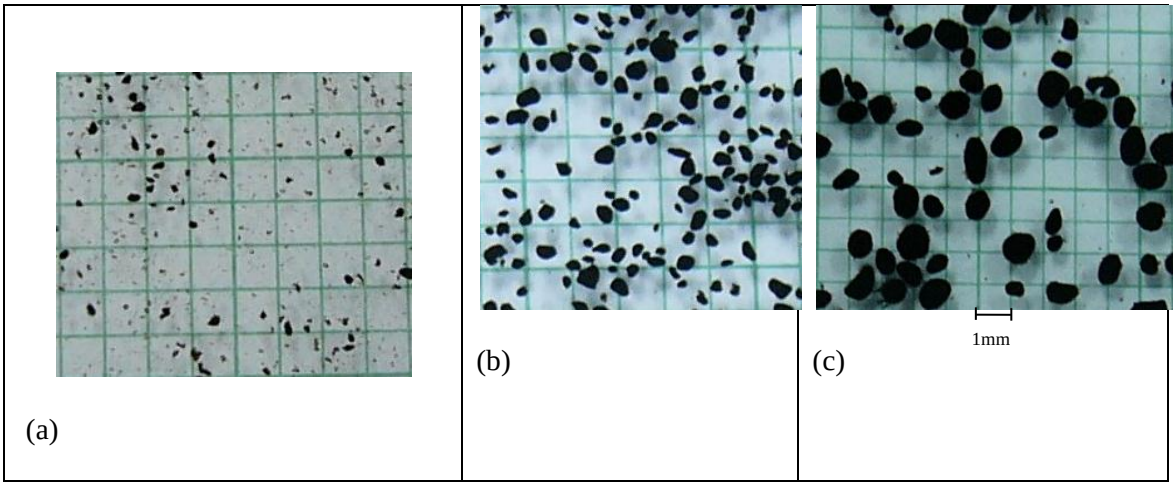

Plate 4.1. Sequence of bio-granule formation in the UASB-FF reactor (a) after 10 days, (b) after 20 days, (c) after 30 days

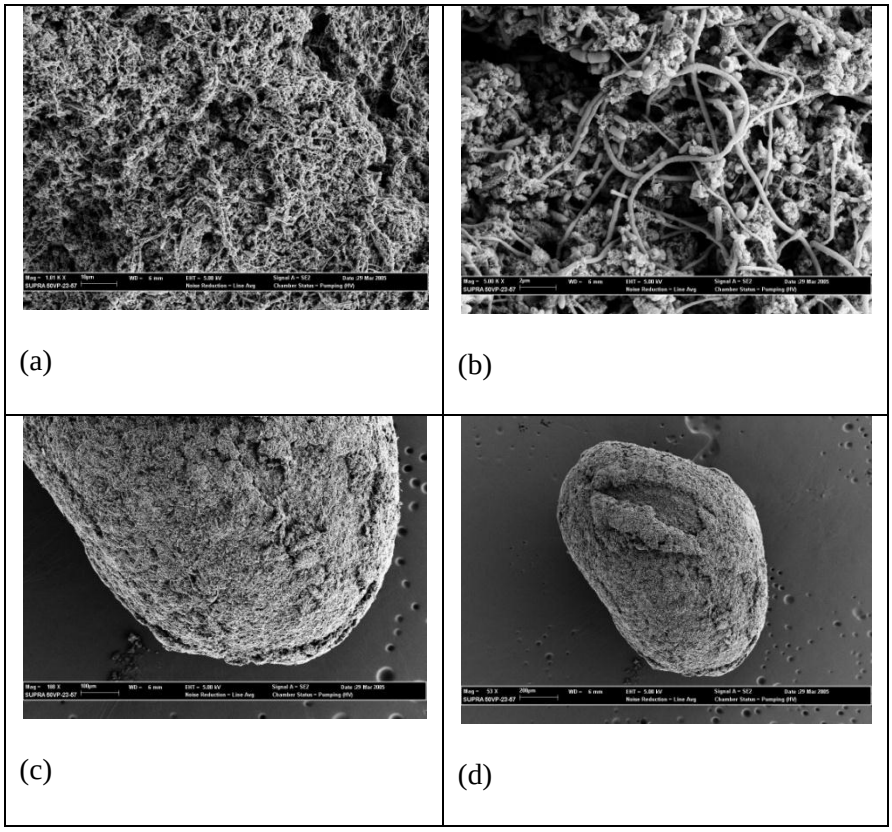

Plat 4.2. SEM images of (a, b) the fine structure of the hydrogen-producing mesophilic granules (*Clostridia butyricum and Escherichia coli*) and (c, d) a full-grown compact granule

Plate 4.2a and b showed the fine structure of hydrogen-producing mesophilic granules obtained by scanning electron microscopy (SEM). Plate 4.2c and d showed a compact granule arising from cellular multiplication of the entrapped bacteria, and became spherically dense due to the hydrodynamic shear force caused by the up-flow liquid and biogas generated.

4.4. Optimization, modeling and process analysis

In this study, 11 dependent variables (either measured directly or calculated) as responses have been used to perform a comprehensive analysis of the biological hydrogen production process. These parameters were H_2 percentage in biogas, hydrogen yield (Y_H), hydrogen production rate (HPR), specific hydrogen production rate (SHPR), COD removal, effluent pH, effluent bicarbonate alkalinity (BA), effluent total volatile fatty acid (TVFA), effluent total suspended solids (TSS), food to microorganism ratio (F/M), and the height of sludge blanket bed in the UASB zone.

Table 4.2. Characteristics of pre-settled POME

Parameter	values	Standard of deviation
BOD_5	19400	±215
COD	28800	±260
Soluble COD	17140	±165
TSS	850	±21
Oil and grease	1480	±13.8
TKN	382	±3.5
TP	84	±1.5
Al	23.4	±0.18
Co	0.11	±0.01
Cr	0.21	±0.02
Cu	0.53	±0.04
Fe	89.15	±0.75
Mg	413.6	±5.3
Mn	3.97	±0.06
Pb	0.18	±0.02
Zn	3.19	±0.06
pH	4.2	±0.15

*All in mg/l except pH

The characteristics of pre-settled POME used in this study are as shown in Table 4.2. Table 4.3 shows the experimental results obtained. The values of parameters are averages of three measurements.

4.4.1. Statistical analysis

In Table 4.4, the ANOVA results for all responses were summarized. In this study, polynomial models of different degrees were used for data fitting as various responses were investigated. The regression equations obtained were presented in Table 4.4. The data obtained from the experimental results to quantify the curvature effects were fitted to higher degree polynomial equations i.e. two factor interaction (2FI), quadratic and so on. For TVFA response was applied $\log_{10}$ function.

According to the statistical analysis, the models were greatly significant with *P* values lower than 0.003 that showed the model terms of independent variables were significant at the 99% confidence level. The correlation coefficient (R^2) for each response was also calculated that showed high significant regression at 95% confidence level.

The lack-of-fit *F*-tests were used to test the models adequacy (Montgomery, 1991). The lack of fit results were not statistically significant as the *P* values were greater than 0.05. Adequate precision is a measure of the range in predicted response relative to its associated error and its desired value is 4 or more (Mason *et al.,* 2003). The reliability of the experiments and good precision were found with low values of the CV (less than 18.59 %).

Table 4. 3. Experimental results of central composite design

Run no.	Variables		Response										
	Q_F (l/d)	V_{up} (m/h)	COD removal (%)	H_2 percentage (%)	H_2 yield (l H_2 /g COD)	HPR (l H_2 /g COD_{rem}.d)	SHPR (l H_2/g VSS.d)	pH -	TVFA (mg acetic acid/l)	BA (mg $CaCO_3$/l)	TSS (mg/l)	F/M ($gCOD_{in}$ /g VSS.d)	Sludge height (%)
1	1.7	0.5	67.7	53.19	0.310	0.306	0.151	5.70	3654	3110	508	0.487	45.2
2	5.95	0.5	59.0	43.35	0.060	0.238	0.102	5.38	2864	3960	318	1.689	46.1
3	5.95	1.75	59.6	52.49	0.068	0.264	0.117	5.47	2855	4230	566	1.729	56.3
4	5.95	1.75	59.2	52.54	0.066	0.260	0.115	5.45	2965	3860	558	1.740	56.4
5	1.7	1.75	66.0	70.22	0.247	0.249	0.121	5.63	2924	3350	490	0.492	53.6
6	5.95	1.75	60.2	54.23	0.065	0.251	0.112	5.50	2774	4270	556	1.726	56.4
7	10.2	0.5	43.5	21.06	0.011	0.099	0.032	4.78	2705	2040	148	2.941	50.5
8	1.7	3.0	65.3	60.16	0.202	0.206	0.100	5.42	3988	3710	575	0.495	57.6
9	10.2	1.75	56.1	52.87	0.031	0.223	0.093	5.50	2475	3290	457	2.985	62.8
10	5.95	1.75	61.3	52.86	0.065	0.246	0.112	5.57	2850	4230	555	1.728	56.8
11	5.95	1.75	59.2	52.76	0.059	0.233	0.102	5.47	2877	4130	547	1.733	56.1
12	10.2	3.0	58.7	57.55	0.030	0.204	0.090	5.39	3779	2920	572	3.000	63.3
13	5.95	3.0	60.6	46.73	0.054	0.208	0.094	5.27	3972	4220	544	1.746	61.9

Table 4.4. ANOVA results for the equations of the Design Expert 6.0.8 for with the studied responses as predictor variables

Response	Transformation	Modified Equations with Significant Terms	Probability	R^2	Adj. R^2	Adeq. precision	SD	CV	PRESS	Probability for lack of fit
H_2 fraction	-	$53.27 – 8.5A + 7.63B + 6.26A^2 – 10.24B^2 + 7.13AB$	0.003	0.8896	0.8107	12.905	4.79	9.31	1298.89	0.059
Hydrogen yield	-	$0.062 – 0.11A – 0.016B +0.076A^2 + 0.032AB$	<0.0001	0.991	0.9865	43.64	0.011	11.1	$4.66x10^{-3}$	0.1625
HPR	-	$0.25 – 0.039A – 0.037B^2 + 0.051AB$	0.0004	0.8588	0.8117	15.558	0.021	9.12	0.01	0.0929
SHPR	-	$0.11 – 0.026A – 0.015B^2 + 0.27AB$	<0.0001	0.9192	0.8923	22.026	$8.744x10^{-3}$	8.46	$1.95x10^{-3}$	0.1362
COD removal	-	$59.66 – 6.78A + 2.4B + 4.4AB$	<0.0001	0.9286	0.9048	22.141	1.82	3.05	110.65	0.1101
Effluent pH	-	$5.53 – 0.18A– 0.21B^2 + 0.22AB$	0.0005	0.8483	0.7977	14.06	0.1	1.9	0.33	0.156
TVFA	Base 10 log	$3.45 -0.027A + 0.054B + 0.09B^2 + 0.027AB$	<0.0001	0.9551	0.9326	17.262	0.018	0.52	0.01	0.0723
Effluent BA	-	$2201.76 – 113.67A – 955.67A^2 – 694.66B^2$	<0.0001	0.9061	0.8748	11.881	267.66	18.59	$1.668x10^{+6}$	0.1071
F/M	-	$1.73 + 1.24A + 0.02B$	<0.0001	0.9996	0.9996	286.764	0.018	1.06	$6.17x10^{-3}$	0.612
Effluent TSS	-	$529.43 - 66A + 119.5B – 85.26B^2 + 89.25AB$	0.0006	0.8949	0.8424	13.869	49.53	10.11	74335.65	0.0579
Sludge height	-	$56.81 + 3.37A + 6.83B – 2.71B^2$	<0.0001	0.96	0.9466	28.01	1.31	2.36	35.38	0.0691

A: Q_F; B: V_{up}; SD: standard deviation; CV: coefficient of variation; PRESS: prediction error sum of squares

4.4.2. Effects of Q_F and V_{up} on biogas composition, hydrogen yield, HPR, and SHPR

To evaluate the bioreactor performance, hydrogen production was monitored in terms of H_2 content in the biogas, H_2 yield, HPR and SHPR as responses. Figure 4.7 depicts the three dimensional plots the variations of H_2 content in the biogas, H_2 yield, HPR and SHPR as functions of variables (Q_F and V_{up}). According to Table 4.4, a reduced quadratic model described the variation in these responses as a function of variables being studied. The response surface plot for hydrogen content in the biogas is shown in the Figure 4.7a. According to the model presented in Table 4.4 and the Figure 4.7a, positive effect of increase in B and AB terms on hydrogen content at V_{up} values less than 1.75 m/h was attributed to the increase in pH caused by recycled alkalinity; while the negative effect of the increase in B^2 on hydrogen percentage dominated at V_{up} values greater than 1.75 m/h. The hydrogen percentage was found to increase with an increase in V_{up} at Q_F higher than 8 l/d which indicated the influencing effect of V_{up} on the improvement of the hydrogen content in biogas from the system. The contour plot of hydrogen yield (Figure 4.7b) showed that an increase in the response was yielded by a decrease in the variables. The highest value of yield was 0.310 l H_2/g COD at Q_F and V_{up} of 1.7 l/d (HRT=1.5d) and 0.5 m/h (Q_R=15.77), respectively while the model predicted 0.301 l H_2/g COD in this condition.

The contour plots of HPR and SHPR (Figure 4.7c, d) depicted the HPR and SHPR as a function of V_{up} and Q_F. Figure 4.7c, d shows that in the lowest V_{up} (0.5 m/h) HPR and SHPR decrease with increasing Q_F, while in the highest V_{up} (3 m/h), increasing Q_F did not affect significantly HPR and SHPR. This was interpreted as an indication of the beginning of an instable condition due to very high Q_F relative to Q_R ratio and inappropriate F/M. It was also found that HPR and SHPR values at the reactor destabilization condition (the highest feed flow rate) was satisfactorily high because of

higher F/M ratio as SHPR is calculated by the value of produced hydrogen and the value of biomass concentration within the bioreactor (Table 4.3). As a conclusion, the interactive effects of the studied variables on hydrogen production (responses) were well demonstrated by the models.

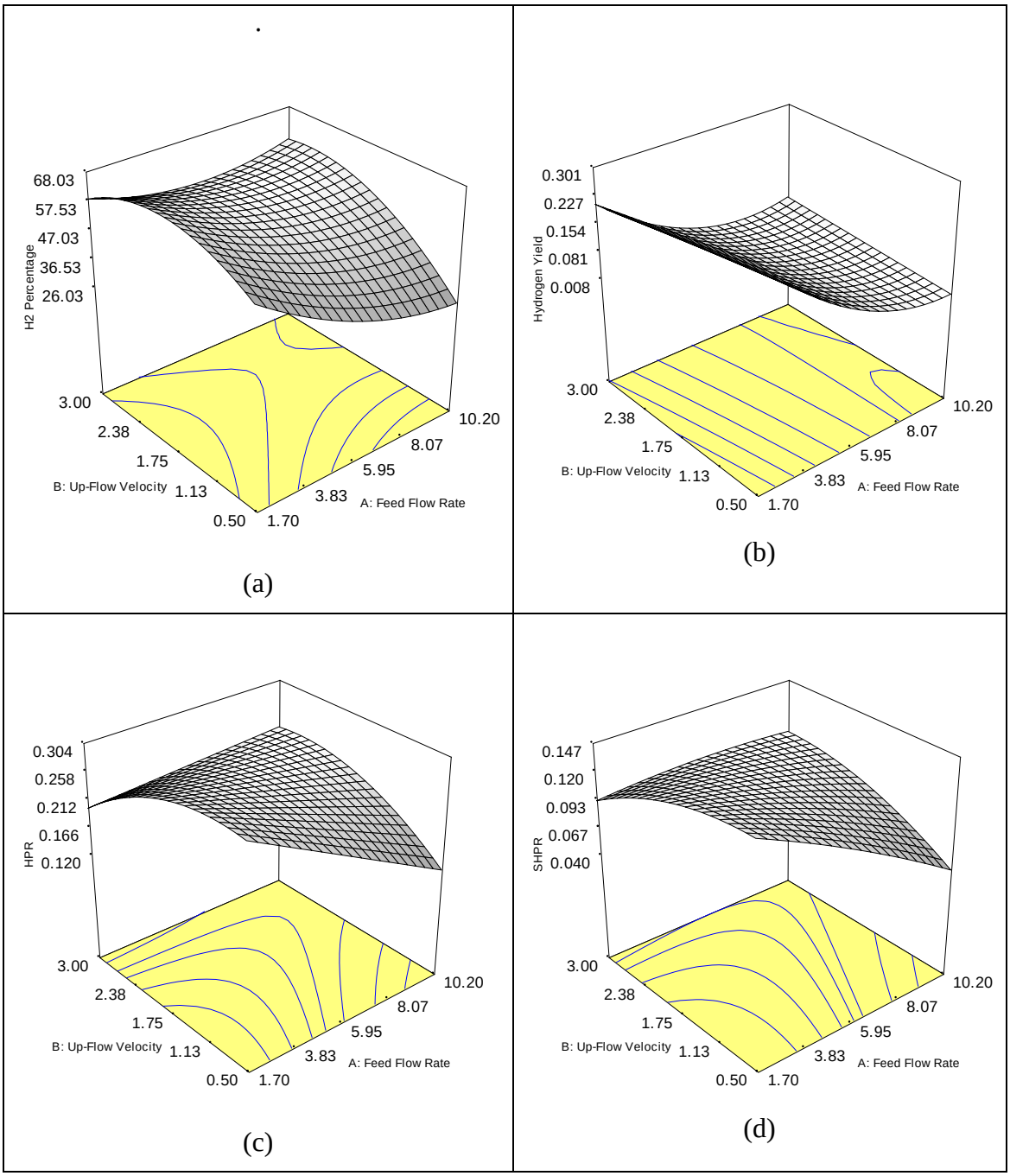

Figure 4.7. Three-dimensional contour plots for (a) hydrogen percentage, (b) hydrogen yield, (c) HPR, and (d) SHPR

4.4.3. Effects of Q_F and V_{up} on COD removal

The COD removal efficiency was also monitored to evaluate the reactor performance. Figure 4.8 shows three-dimensional plots for the variations of COD removal efficiency as a function of Q_F and V_{up}. The COD concentration of the feed flow was constant throughout the experiments. The different influence of V_{up} on COD removal efficiency was observed at constant feed flow rates Q_F. The COD removal efficiency at feed flow rates lower than 3.6 l/d decreased slightly as V_{up} increased while at Q_Fs higher than 3.6 l/d the COD removal efficiency decreased significantly with increasing V_{up} that was attributed to high OLR with short HRT. The lowest COD removal efficiency was 43.5% at the OLR of 60 g COD /l.d (the highest Q_F). It was attributed to an incomplete fermentation process and significant production of acids (the system's pH was lowest at this point). The COD removal efficiency decreased considerably as the feed flow rate increased. The negative effect of Q_F on COD removal efficiency was removed with increasing the up-flow velocity. The change in COD removal for lower limit of V_{up} (0.5 m/h) was 22.36%, while the corresponding value for the upper limit of V_{up} (3.0 m/h) was 4.76%.

The improvement of substrate diffusion rate into the granules due to higher flow velocity may determine the trend of COD removal efficiency at low Q_F (Beyenal and Lewandowski, 1999; Zinatizadeh *et al.,* 2007). Meanwhile, trend at high OLR demonstrated that at this condition, the effect of substrate concentration on the diffusion rate was stronger than that of V_{up}.

It is concluded that to eliminate the negative effects of organic shock produced by high feed flow rate, proper value of V_{up} for each OLR is required. The trend of COD variations as a function of the studied variables could be described well by a first order polynomial model with a good correlation coefficient of $R^2 = 0.93$ (Table 4.4).

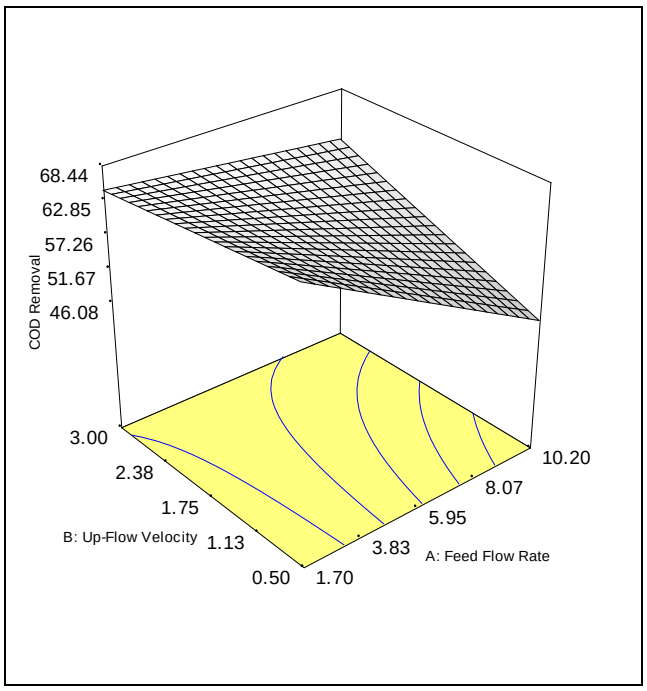

Figure 4.8. Three-dimensional contour plot of the model for COD removal

4.4.4. Effects of Q_F and V_{up} on pH, bicarbonate alkalinity and total volatile fatty acids

Figure 4.9 depicted three-dimensional contour plots for pH, BA and TVFA obtained from the models offered in Table 4.4. There was a relatively strong interaction between the variables (P values <0.0005) as evidenced by the graphs' curvatures.

In Figure 4.9a, increasing V_{up} at various feed flow rates resulted in dynamic changes in the pH. An increase in V_{up} caused a decrease in pH at low Q_F which could be due to low rate of alkalinity production and higher CO_2 dissolution while at high feed flow rates, the increase in pH was attributed to alkalinity build-up following intensified metabolic activities. Similar observation was made during effluent recycle.

Bicarbonate alkalinity is an important control parameter in fermentative hydrogen production process. For normally operated digesters, the bicarbonate alkalinity is almost the same as the total alkalinity due to the low concentration of volatile acids (Rittmann and McCarty, 2001). However, according to equation (4.1) BA and consequently pH will be in imbalanced condition due to increasing VFA.

$$HCO_3^- + CH_3COOH \rightarrow CH_3COO^- + H_2O + CO_2 \quad (4.1)$$

In this condition, VFAs are measured as alkalinity and the total alkalinity will not change considerably. The following equation was applied to calculate the bicarbonate alkalinity (Rittmann and McCarty, 2001).

$$BA = TA - 0.708TVFA \quad (4.2)$$

where, TA is total alkalinity (mg $CaCO_3$/l) and TVFA is total volatile fatty acids (mg/l acetic acid).

The significant effects of the variables interaction on bicarbonate alkalinity are shown in Figure 4.9b. According to the figure, the highest value of bicarbonate alkalinity was obtained at the middle level of the variables and was reduced as Q_F and V_{up} moved away from the central region simultaneously. It is suggested that the bicarbonate alkalinity was generated from dark fermentation hydrogen production reactions from POME, allowing some extent of pH control, except in the overloading conditions (Q_F 10.2 l/d, V_{up} 0.5 m/h).

The values of the effluent volatile fatty acids measured at steady state condition of each run are summarized in Table 4.5. The main aqueous products in this study were butyrate, acetate and ethanol. Propionate concentration was relatively low during most runs. The effect of Q_F and V_{up} on the yield of VFAs and ethanol was evaluated using RSM central composite design. To fit the data, a logarithmic function with base 10 was applied due to the high ratio between the maximum and minimum effluent TVFA value (1.61). The high regression coefficient (0.9551) suggests that the regression equation of TVFA yield was appropriate for modeling the experimental results. Figure 4.9c shows the three-dimensional contour plots for the TVFA as a function of the studied variables. Both Q_F and V_{up} had a significant individual influence on the yield of TVFA. The minimum TVFA yield was estimated from model to be 2454 mg/l when V_{up} and Q_F were 1.13 m/h and 10.2 l/d, respectively. Figure 4.9c illustrates that the TVFA increased

significantly as the V_{up} increased at fixed Q_Fs. At V_{up} higher than 1.45 m/h, the TVFA yield increased logarithmically with increasing V_{up}. In addition, the model was significant ($P < 0.0001$), which indicated a satisfactory explanation of the dynamics of the effluent TVFA by the model. The minimum and maximum levels of butyrate were 471 and 1500 mg/l corresponding with the lowest and highest H_2 yields 0.011 and 0.31 l H_2/gCOD, respectively.

The effluent VFA at overloading (Q_F 10.2 l/d, HRT 6 h) where the destabilization of the reactor was observed, was 1210, 471,630 and 510 mg/l of acetic, butyric, propionic acids and ethanol, respectively.

Table 4.5. The amounts of the effluent VFAs at various trials

Run no.	Acetate mg/l	Butyrate mg/l	Propionate mg/l	Ethanol mg/l	TVFA (mg Acetic acid/l)
1	1370	1500	570	615	3654
2	1080	1340	160	570	2864
3	1215	1155	210	525	2855
4	1260	1175	230	552	2965
5	653	1468	340	765	2924
6	1151	1149	208	516	2774
7	1210	471	630	510	2705
8	1320	1650	435	915	3988
9	850	1085	145	590	2475
10	1218	1153	214	517	2850
11	1226	1174	215	520	2877
12	1720	865	570	774	3779
13	1154	1376	835	925	3972

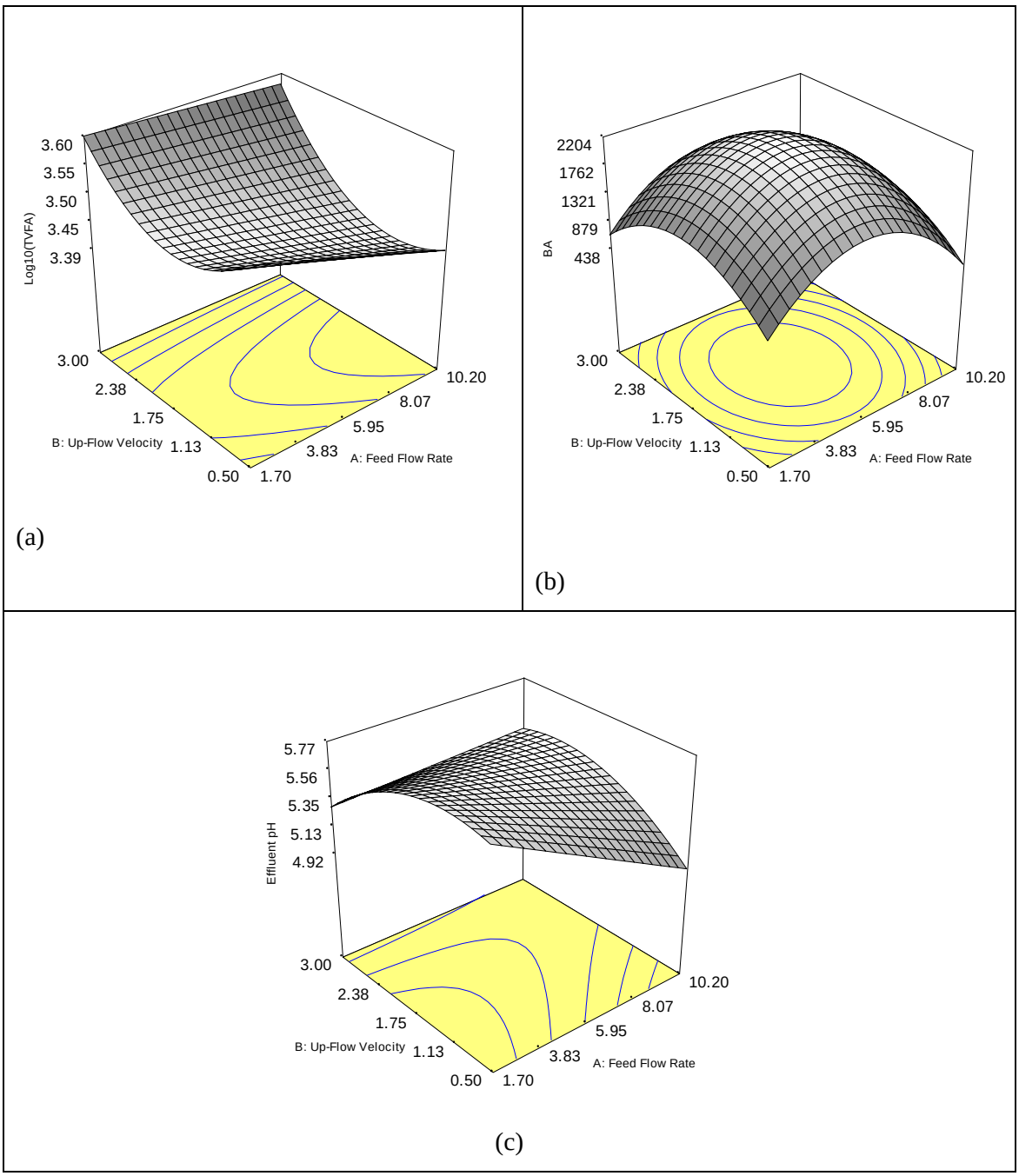

Figure 4.9. Three-dimensional contour plots of the two-factor interaction models for (a) TVFA, (b) bicarbonate alkalinity, (c) pH in the effluent

4.4.5. Effects of Q_F and V_{up} on the operating parameters

In order to investigate the process behavior of the sludge in the present bioreactor, the height of sludge blanket within the UASB portion, effluent TSS, VSS and SRT have been measured and calculated as operating parameters. The effects of variables on operating parameters were shown in Figure 4.10. It was resulted that with

simultaneous increase in feed flow rate and up-flow velocity, the height of sludge blanket in the UASB portion also increased. The highest sludge height was found to be 64.3% of the height of UASB portion when the Q_F and V_{up} were 10.2 l/d and 3.0 m/h, respectively. With respect to low TSS concentration content of the influent and similarly for the ratio of VSS to TSS in the reactor and effluent (about 0.75), the VSS content of effluent represented biomass washout from the reactor. It was suggested that the most important factor governing the washout phenomenon was the gas generation rate and the up-flow velocity.

The three-dimensional contour plots of the model for TSS as a function of the studied variables are shown in Figure 4.10b. The maximum effluent TSS occurred when Q_F and V_{up} were 8.0 l/d and 3.0 m/h, respectively.

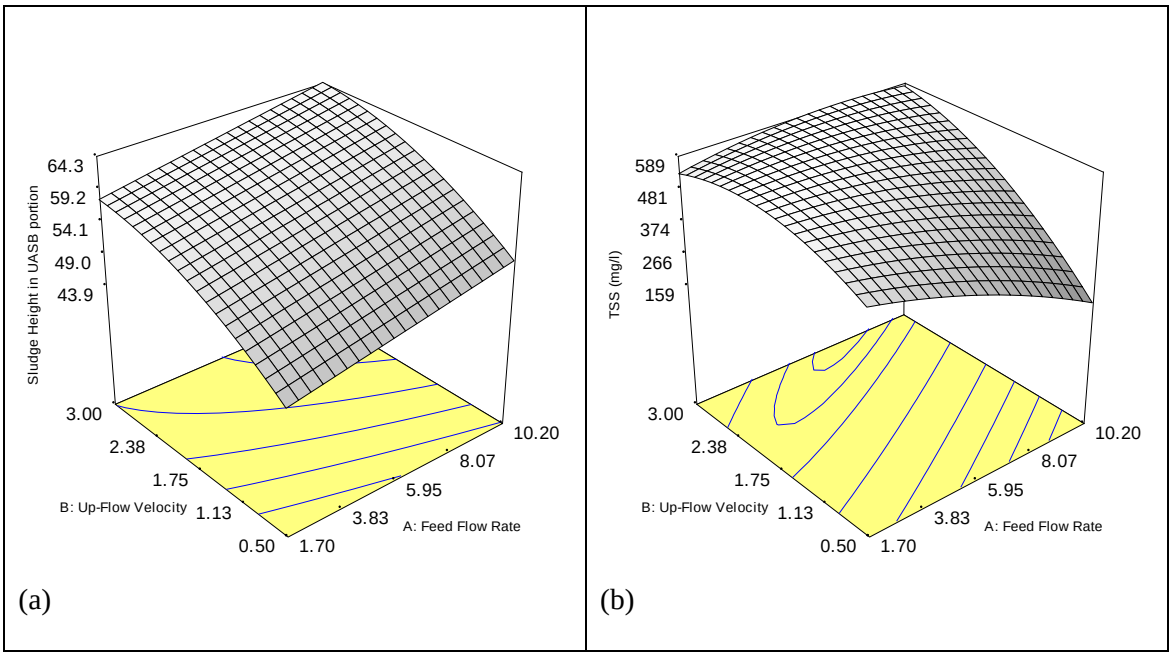

Figure 4.10. Three-dimensional contour plots of the two-factor interaction model for (a) sludge height and (b) effluent TSS

The up-flow velocity had more influence on SRT variations in this study. The sludge age decreased as the variables increased, and it was attributed to the increase in up-flow velocity and gas bubble generation causing hydrodynamic instability thus high turbulence within the reactor.

4.4.6. Effects of Q_F and V_{up} on food to microorganism ratio

An important parameter to control the process in this study is food to microorganism (F/M) ratio. Figure 4.11 depicts the three-dimensional contour plot of the F/M ratio as a function of the studied variables. It is shown that increasing Q_F resulted to the increase in the F/M ratio while V_{up} had little effect on F/M ratio as it was mostly supplied by the effluent recycling. A dramatic increase in the F/M ratio due to high OLR was attributed to the slow microbial growth rate in the anaerobic system. The optimum value of F/M ratio (1.7 g COD/g VSS.d) was achieved at Q_F lower than 5.95 l/d.

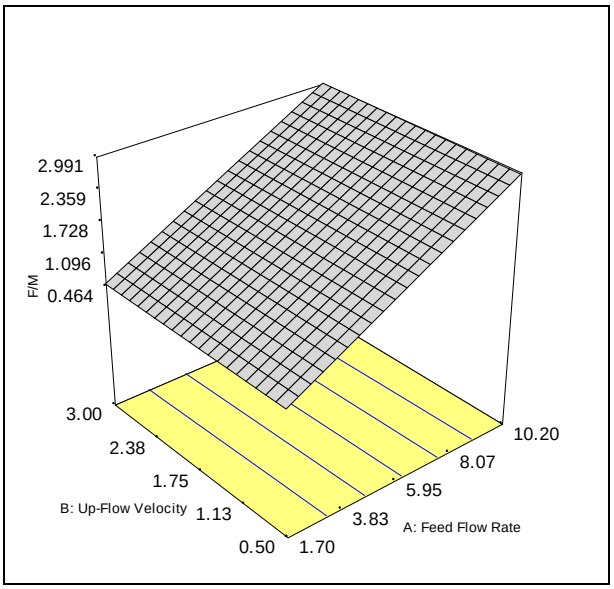

Figure 4.11. Response surface plot for F/M ratio

4.4.7. Process Optimization

To determine the optimum region for the studied variables, the responses that were used to check the bioreactor performance in this study were modeled. H_2 percentage, H_2 yield, SHPR, and COD removal as responses were each optimized as a function of the studied variables viz. Q_F and V_{up}. Figure 4.12 illustrated the optimum region (shaded in yellow) identified based on the four responses. These parameters were

chosen due to their considerable importance for a reliable representation and optimization of the fermentative hydrogen production process.

To confirm the reliability of the models' predictions, two points within the optimum region were chosen for implementation in verification experiments. They were as follows: one point at the maximum feed flow rate (Q_F 3.71 l/d with the corresponding V_{up} 1.48 m/h) and one point at maximum up-flow velocity (V_{up} 2.31 m/h with the corresponding Q_F 2.03 l/d) from within the optimum region. Experiments were carried out to verify the experimental results with the predicted values. Table 4.6 presents the experimental conditions and results. It is shown that the verification experimental results agreed reasonably well to those corresponding values predicted by the model at the optimum conditions. This strongly evidenced that the optimization of the hydrogen production in the UASB-FF bioreactor using RSM central composite design analysis was successful.

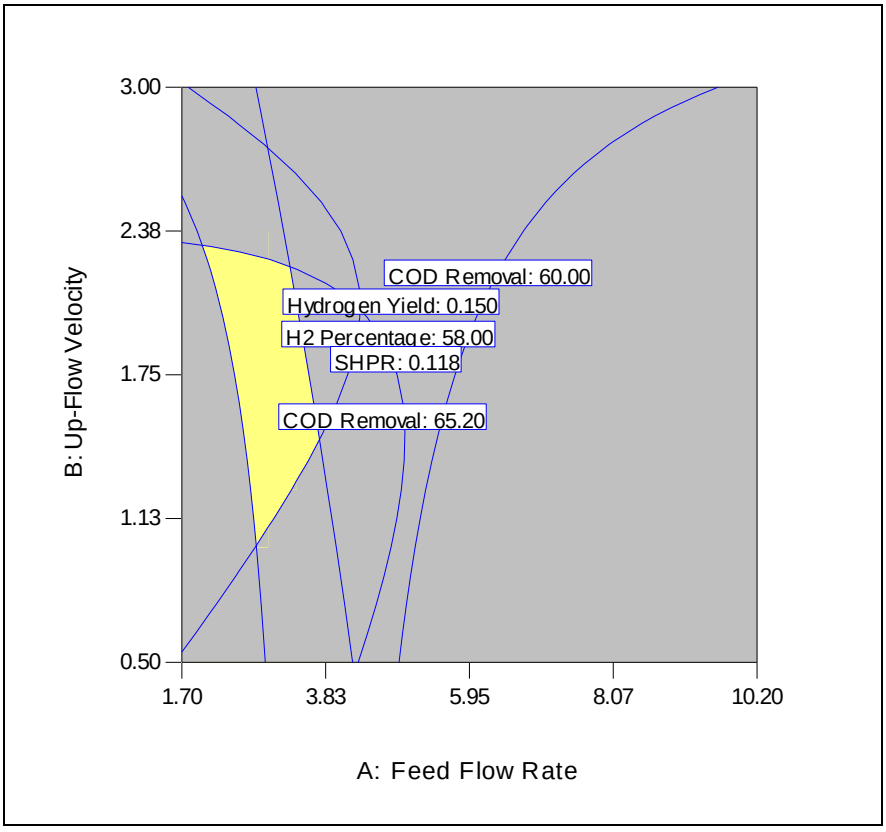

Figure 4.12. Overlay plot for optimal region

Table 4.6. Verification experiments at optimum conditions

Run	Conditions		Responses								
			H_2 Percentage (%)	**H_2 yield (l H_2/g COD)**	**HPR (l H_2/g COD_{rem}.d)**	**SHPR (l H_2/g VSS.d)**	**COD removal (%)**	**Eff. pH**	**Eff. BA (mg $CaCO_3$/l)**	**Eff. TVFA (mg acetic acid/l)**	**Eff. TSS (mg/l)**
1	Q_F = 3.71 l/d V_{up} = 1.48 m/h	Experimental Values	53.3	0.144	0.259	0.121	60.6	5.55	1820	3145	550
		Predicted values	52.8	0.151	0.272	0.127	63.2	5.64	1964	2910	575
		Standard deviation	±0.25	±0.004	±0.007	±0.003	±1.3	±0.05	±72.0	±117.5	±12.5
2	Q_F = 2.03 l/d V_{up} = 2.31 m/h	Experimental Values	62.2	0.209	0.251	0.111	61.2	5.53	1315	3380	845
		Predicted values	64.9	0.213	0.255	0.118	65.2	5.57	1355	3265	810
		Standard deviation	±1.35	±0.002	±0.002	±0.004	±2.0	±0.02	±20.0	±57.5	±17.5

Eff. =Effluent

4.4.8. Kinetic evaluation of biohydrogen production from POME in the UASB-FF bioreactor

The fermentation of organic substrate is a relatively complex process, by which the organic compounds are converted to liquid organics and biogas (i.e. H_2 and CO_2). The hydrolysis conversion rate and the soluble substrate utilization rate for fermentation are two important rate-limiting steps in anaerobic biohydrogen production processes. POME includes some volatile acids, hydrolyzable substrate and simple compounds that are used for metabolism by the fermentative bacteria. Therefore, the fermentative hydrogen production process from POME must be considered in the kinetic terms. The fermentative process is commonly modeled as a first order reaction with respect to substrate concentration (Droste, 1997). In fermentation processes the main part of hydrolyzable substrate are hydrolyzed in specified HRT and subsequently utilized by acidogenesis and hydrogenesis bacterias. The equation (4.2) below is used in the substrate mass balances:

$$\frac{ds}{dt} = r_{su} = -\frac{k.S.X}{K_S+S} \qquad (4.2)$$

where r_{su} is rate of substrate concentration change due to utilization (mg/l.d), k is maximum specific substrate utilization rate (mg COD/mg VSS.d), X is biomass concentration (mg VSS/l), S is substrate concentration (mg COD/l), and K_s is half-velocity substrate constant (mg/l).

The Monod equation is an appropriate model to describe and calculate the microbial growth parameters of fermentative anaerobic reactions.

$$\frac{1}{\mu} = \frac{K_S}{\mu_{max}} * \frac{1}{S} + \frac{1}{\mu_{max}} \qquad (4.3)$$

The kinetic parameters were calculated according to equation (4.3) and the Lineweaver-Burk plot (Figure (4.13)). According to Figure 4.13, slope equals to $\frac{\mathbf{K_S}}{\boldsymbol{\mu_{max}}}$ and intercept equals to $\frac{\mathbf{1}}{\boldsymbol{\mu_{max}}}$.

The maximum specific growth rate (μ_{max}) of hydrogenesis in this study was calculated to be 0.371 d^{-1} at 38 °C. The half-velocity constant (K_s) was 10.9 g/L when POME concentration was 15.0 g/L.

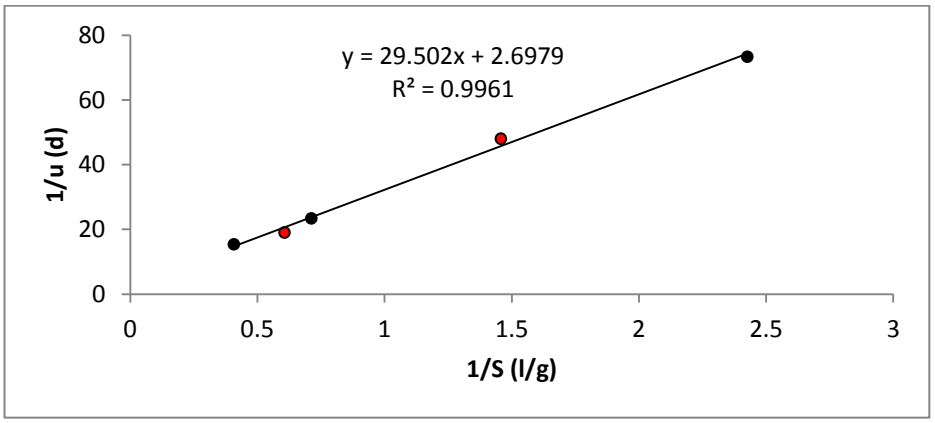

Figure 4.13. Line weaver-Burk plot for reciprocals of specific growth rate versus COD concentration (the black color is based on data obtained experimentally and red color is based on Monod equation calculation)

The maximum specific growth rate of the bacteria is related to the maximum specific substrate utilization rate *k* according to equation (4.4).

$$\mu_{max} = kY \quad (4.4)$$

and

$$k = \frac{\mu_{max}}{Y} \quad (4.5)$$

where *Y* is the biomass yield (g $VSS_{produced}$/g $COD_{removed}$).

Figure 4.14 demonstrated the relationship between specific substrate utilization rate (g COD/g VSS.d) and inverse SRT at different HRT with influent COD concentration of 15000 mg/l. According to Figure 4.14, slope equals to *Y* and intercept equals to K_d where K_d is endogenous decay coefficient (g VSS/g VSS.d). In this study, the kinetic parameters *Y*, K_d, and *k* were obtained 0.093 g/g, 0.0046 d^{-1}, and 3.99 g COD/g VSS.d, respectively.

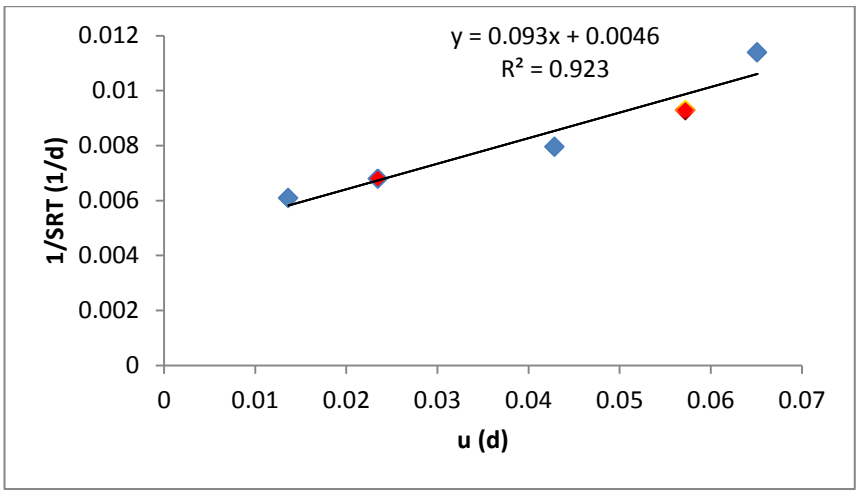

Figure 4.14. The reciprocal of SRT versus specific substrate utilization rate (the blue color is based on data obtained experimentally and red color is based on Monod equation calculation)

Table 4.7 illustrates kinetic coefficients obtained for influent COD concentration of 15000 mg/l used in this study as compared to those reported by Chen *et al.* (2001).

Table 4.7. Kinetic parameters for biohydrogen production from POME in different reactors and operating conditions

Type of reactor	Substrate	S_0 (g/l)	Y g/g	K_s (g/l)	μ_m (d^{-1})	Coefficient basis	Reference
UASB-FF	POME	15.0	0.093	10.9	0.371	COD	This study
CSTR	Sucrose		0.1	0.068	0.172	COD	Chen, (2001)

The value of Y (0.093 g/g) obtained in the present study was the identical to that calculated by Chen *et al.* (2001) for sucrose fermentation in a CSTR. This value is within the reasonable range of anaerobic processes. High K_s value (10.9 g COD/l) showed that the most of the bacteria have low affinity for POME as substrate, due to the reactor being operated at high OLR. The maximum specific microbial growth rate (μ_{max}) is related to the concentration of active biomass in the reactor. This relatively high μ_{max} (0.371 d^{-1}) was indicative of the high proportion of active biomass concentration within the reactor (> 20 g/l). The biomass and partially degraded influent

VSS made up the total VSS value in the reactor, therefore, it is not an unreasonable expectation that the real μ_{max} value was actually higher.

4.5. Effects of process variables on biological hydrogen production of the granulated sludge

Effects of three important variables viz. initial COD concentration (COD_{in}), biomass concentration and initial bicarbonate alkalinity (BA) on the biological activity of the granulated sludge were also investigated in batch culture. In order to evaluate the granular sludge under various process conditions, three responses were selected and the experimental results after two days are presented in Table 4.8. The ANOVA values for response surface models are shown in Table 4.9. Detail explanations for each response are presented in the next section.

Table 4.8. Experimental results of central composite design

Run	Variables			Responses		
	COD_{in} (mg/l)	**MLVSS (mg/l)**	**Alkalinity (mg $CaCO_3$/l)**	**H_2 yield (mmol H_2/g COD_{rem})**	**SHPR (mmol H_2/g VSS.d)**	**COD removal (%)**
1	10000	2000	2000	39.09	41.92	42.9
2	6500	6000	1100	62.13	17.77	52.8
3	6500	4000	1100	72.82	33.96	57.4
4	3000	2000	2000	118.46	40.42	45.5
5	10000	2000	200	48.76	53.39	43.8
6	6500	4000	2000	58.92	25.95	54.2
7	10000	6000	200	27.67	9.18	39.8
8	6500	2000	1100	62.92	55.42	54.2
9	6500	4000	200	69.18	28.89	51.4
10	3000	6000	2000	116.88	14.11	48.3
11	3000	2000	200	115.70	43.56	50.2
12	6500	4000	1100	69.39	34.22	60.7
13	3000	4000	1100	124.48	25.30	54.2
14	6500	4000	1100	78.57	36.64	57.4
15	3000	6000	200	107.72	12.36	45.9
16	10000	6000	2000	52.84	24.39	55.4
17	6500	4000	1100	66.53	33.08	61.2
18	6500	4000	1100	62.35	30.19	59.6
19	10000	4000	1100	58.86	37.08	50.4
20	6500	4000	1100	69.12	32.85	58.5

Table 4.9. ANOVA for response surface models applied

Response	Model type	ANOVA					
		Source	**Sum of square**	**DF**	**Mean square**	***F* value**	**Prob>*F***
Hydrogen Yield,	Reduced quadratic	Model	14171.68	4	3542.92	97.18	< 0.0001
		A	12677.87	1	12677.87	347.75	< 0.0001
		A^2	1259.60	1	1259.60	34.55	< 0.0001
(mmol H_2/g COD_{rem})		B^2	307.64	1	307.64	8.44	0.0109
		BC	212.18	1	212.18	5.82	0.0291
		Residual	546.85	15	36.46		
		Std. Dev.=6.04		*C.V.*=8.15		*PRESS*=996.61	
		R^2=0.9628		Adj. R^2=0.9529		Adeq. Precision=28.542	
SHPR,	Reduced quadratic	Model	2798.18	5	559.64	53.57	< 0.0001
		A	91.32	1	91.32	8.74	0.0104
(mmol H_2 /g VSS.d)		B	2462.07	1	2462.07	235.68	< 0.0001
		B^2	30.53	1	30.53	2.92	0.1094
		C^2	118.54	1	118.54	11.35	0.0046
		BC	124.66	1	124.66	11.93	0.0039
		Residual	146.25	14	10.45		
		Std. Dev.=3.23		*C.V.*=10.25		*PRESS*=368.97	
		R^2=0.9503		Adj. R^2=0.9326		Adeq. Precision=25.601	
COD removal,	Reduced quadratic	Model	693.56	8	86.70	19.35	< 0.0001
		A	13.92	1	13.92	3.11	0.1057
(%)		C	23.10	1	23.10	5.16	0.0443
		A^2	58.19	1	58.19	12.98	0.0041
		B^2	31.79	1	31.79	7.09	0.0221
		C^2	46.23	1	46.23	10.32	0.0083
		AB	12.50	1	12.50	2.79	0.1231
		AC	36.12	1	36.12	8.06	0.0161
		BC	69.62	1	69.62	15.54	0.0023
		Residual	49.30	11	4.48		
		Std. Dev.=2.12		*C.V.*=4.06		*PRESS*=262.24	
		R^2=0.9336		Adj. R^2=0.8854		Adeq. Precision=13.116	

A: COD_{in}; B: MLVSS; C: initial bicarbonate alkalinity.

4.5.1. Hydrogen yield

Results of ANOVA in Table 4.8 showed that the model of hydrogen yield was significant. The model was reduced to squared and quadratic regressors after the elimination of non-significant model terms. The R^2 value of the model was 0.9624 and was higher than as that of the model for COD removal. The main and second-order effects of the variables (A, A^2 and B^2) and two-level interactions of MLVSS and initial bicarbonate alkalinity (BC) were significant model terms. The regression equation of the reduced quadratic model for the response is as follows:

$$\text{Hydrogen yield} = 34.55 - 17.8A + 9.8A^2 - 4.78B^2 + 2.58BC \quad (4.6)$$

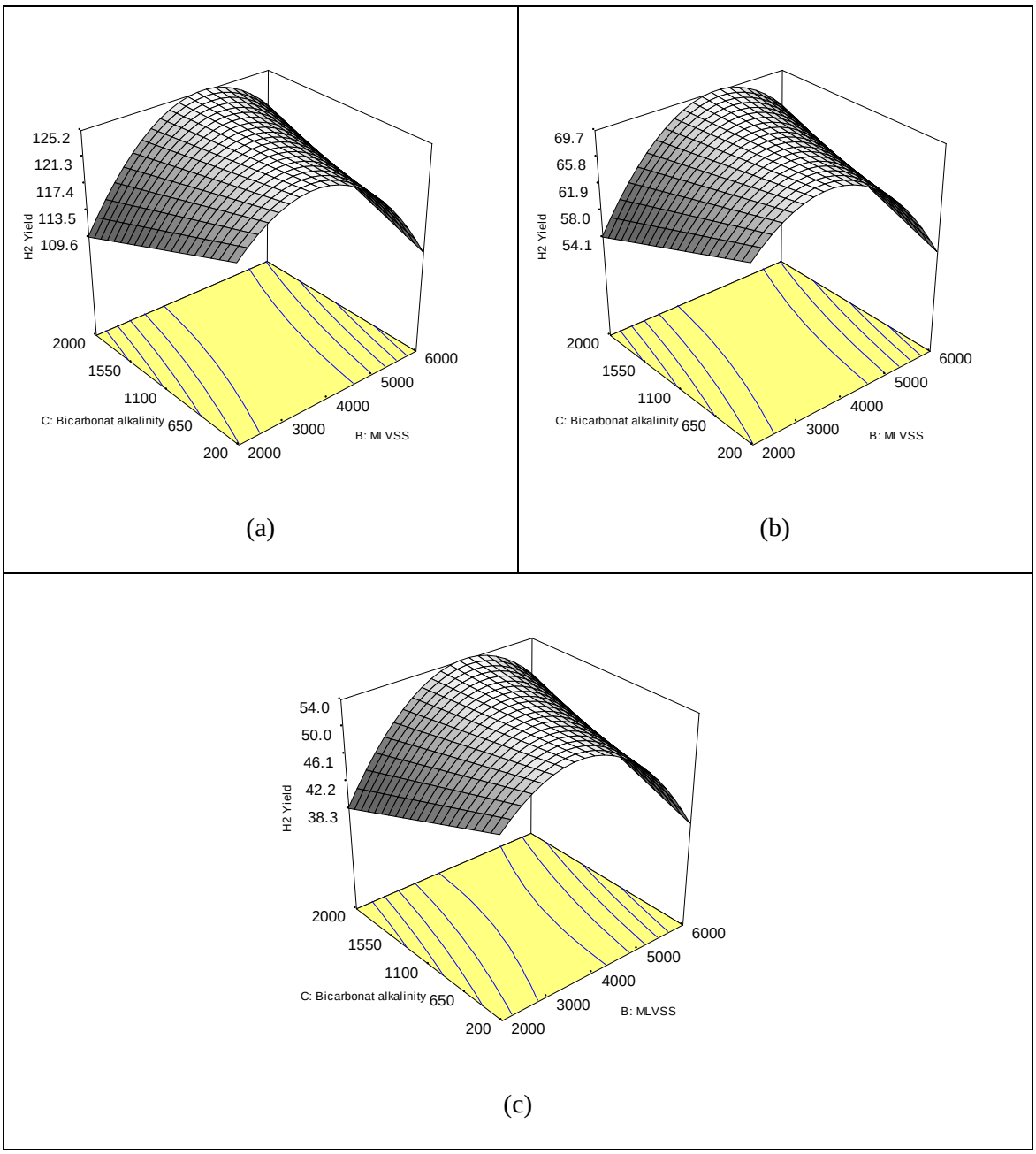

Figure 4.15. Three-dimensional contour plots of the model for hydrogen yield (mmol H_2/g $COD_{removed}$) as a function of variables of initial BA and MLVSS at COD concentration of 3000 mg/l (a), 6500 mg/l (b) and 10000 mg/l (c)

Figure 4.15 shows three-dimensional contour plots of the model for variation in hydrogen yield, as a function of MLVSS (B) and initial BA (C) with three different substrate concentrations (3000, 6500 and 10000 mg COD/l). It can be seen from the response surface plots (Figure 4.15) that the hydrogen yield increased upon increasing of the MLVSS at any initial BA until the MLVSS concentrations reached to a level of

3450 mg/l (for initial BA 200 mg $CaCO_3$/l), 4000 mg/l (for initial BA 1100 mg $CaCO_3$/l), and 4550 mg/l (for initial BA 2000 mg $CaCO_3$/l). Further increase in MLVSS concentrations beyond these resulted in the decrease in the hydrogen yield for all the substrate concentration tested. The interaction showed that the MLVSS and initial BA could affect significantly the hydrogen yield. According to Figures 4.15, the maximum hydrogen yields were achieved at biomass concentrations of 3460 mg/l and 4510 mg/l and initial bicarbonate alkalinity of 205 mg $CaCO_3$/l and 1995 mg $CaCO_3$/l, respectively. Afterwards, the hydrogen yield decreased as COD concentration increased. The maximum amount of hydrogen yield was achieved at 124.5 mmol H_2/g COD removed for COD concentration of 3000 mg/l.

4.5.2. Specific hydrogen production rate (SHPR)

Table 4.9 shows the ANOVA results obtained for SHPR. The variation of the SHPR as a function of the studied variables (COD_{in}, MLVSS and initial bicarbonate alkalinity) was described with a reduced quadratic model. The R^2 value of the model for SHPR was 0.95. The main and second-order effects of the variables (A, B, B^2 and C^2) and two-level interactions of MLVSS and initial bicarbonate alkalinity (BC) were significant model terms. Other model terms, which were insignificant, were eliminated to simplify the model. The regression equation of the reduced quadratic model for the response is as follows:

$$\text{SHPR, mmol } H_2\text{/g VSS.d} = 16.52 + 1.51A - 8.74B + 1.54B^2 - 3.04C^2 + 1.97BC \quad (4.7)$$

Figure 4.16 showed the three-dimensional contour plots of the model for variation in SHPR as a function of MLVSS (B) and initial bicarbonate alkalinity (C) at three various COD concentration values within the design space. It is shown that by decreasing the

MLVSS at the middle of initial BA, more favorable environment for fermentative reaction was provided. Low amounts of SHPR at high MLVSS concentrations were mainly due to high concentration of VSS from one side and low amount of COD_{in} from another side as SHPR is expressed as mmol H_2/g VSS.d. It can be observed in Figure 4.16a, b and c, at the same MLVSS and bicarbonate alkalinity, greater SHPR was obtained from the condition with high substrate concentration (shown in Figure 4.16c).

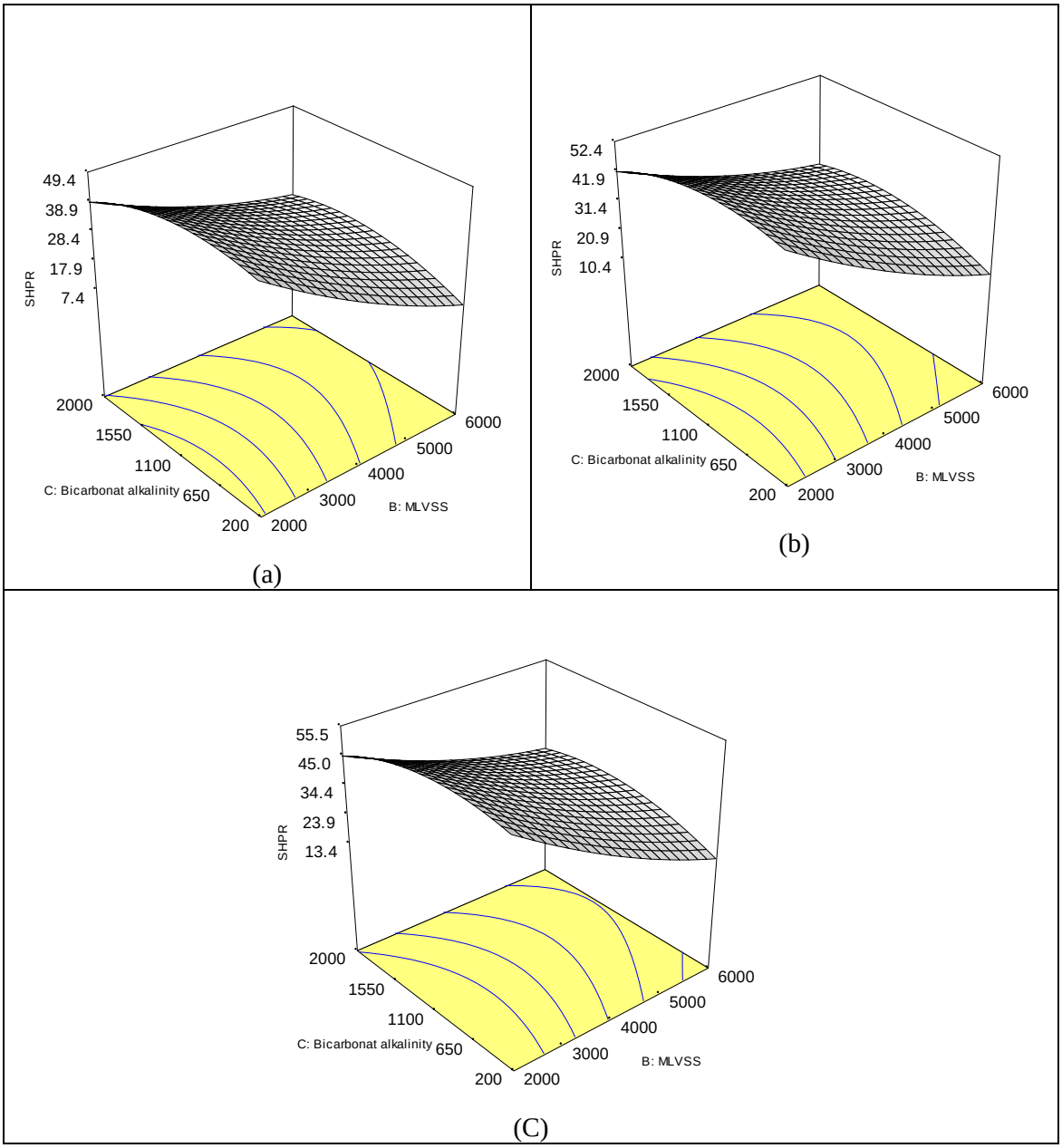

Figure 4.16. Three-dimensional contour plots of the model for SHPR (mmol H_2 /g VSS.d) as a function of initial BA and MLVSS at COD concentration of 3000 mg/l (a), 6500 mg/l (b) and 10000 mg/l (c)

Maximum SHPR was modeled to be 55.43 mmol H_2 /g VSS.d under MLVSS, initial BA and COD_{in} concentration of 2000 mg VSS/l, 830 mg $CaCO_3$/l and 10000 mg COD/l, respectively. In contrast, minimum SHPR (8.05 mmol H_2 /g VSS.d) was obtained under the lowest initial BA (200 mg $CaCO_3$/l) and the highest MLVSS (6000 mg/l) with COD_{in} of 3000 mg/l. It is concluded that high specific hydrogenesis activity could be achieved at intermediate initial bicarbonate alkalinity value and high food to biomass concentration ratio.

4.5.3. COD removal efficiency

Table 4.9 shows the ANOVA results obtained for COD removal efficiency. The variation of the COD removal as a function of the studied variables (COD_{in}, MLVSS and initial bicarbonate alkalinity) was described using a reduced quadratic ($P < 0.0001$). The R^2 value of the model for COD removal was 0.9336. The main effects, second-order effects and the two-level interactions of COD_{in}, MLVSS, and initial BA (A, C, A^2, B^2, C^2, AB, AC, and BC) are significant model terms. Only factor B was not a significant model term and it was eliminated to simplify the model.

The determination coefficient (R^2 = 0.9336) showed that only an insignificant 6.64% of the total variation was not explained by the model (as R^2 is a ratio of sum of square regression to total sum of square). The high value for adjusted R^2 (0.8854) also corroborated the significance of the model. The reasonable precision and reliability of the experiments was proved by a low variation coefficient value (4.06) (Kuehl, 2000). The regression equation of the reduced quadratic model for the response is as follows:

$$\text{COD removal, \%} = 58.24 - 1.18A + 1.52C - 4.6A2 - 3.4B2 - 4.1C2 + 1.25AB + 2.12AB + 2.95BC \quad (4.8)$$

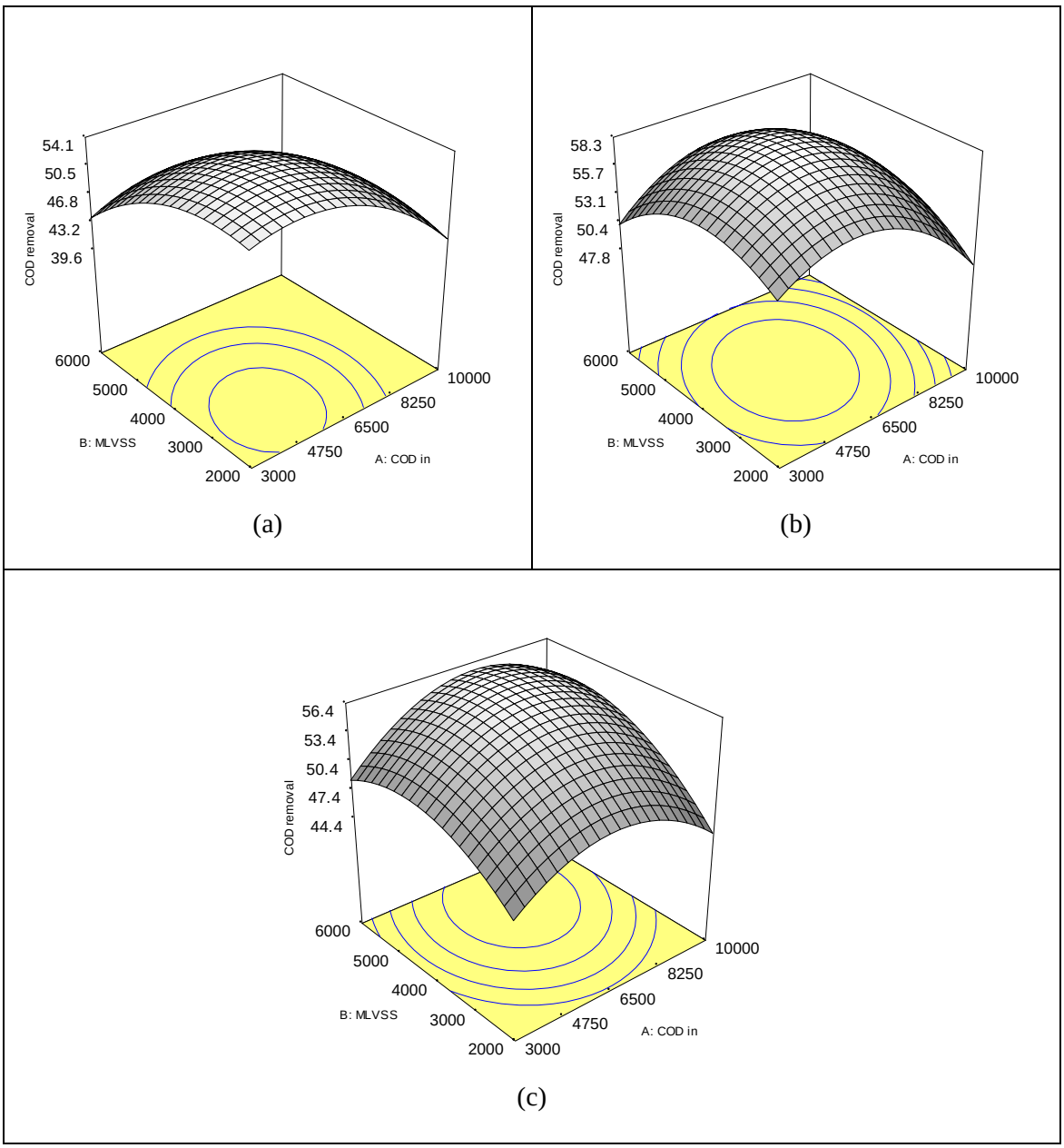

Figure 4.17. Three-dimensional contour plots of the model for COD removal as a function of COD_{in} and MLVSS at initial BA of 200 mg $CaCO_3$/l (a), 1100 mg $CaCO_3$/l (b), 2000 mg $CaCO_3$/l (c)

Figure 4.17 shows three-dimensional contour plots of the model for variation in COD removal efficiency as a function of COD_{in} (A) and MLVSS (B) with the different values of initial bicarbonate alkalinity of 200 mg $CaCO_3$/l (a), 1100 mg $CaCO_3$/l (b) and 2000 mg $CaCO_3$/l (c). The maximum COD removal efficiency (>58.3 %) was obtained at COD_{in}, MLVSS and initial BA of 6024 mg/l, 3956 mg/l and 1100 mg $CaCO_3$/l, respectively. The minimum COD removal efficiency (39.6 %) was

obtained at COD_{in} of 10000 mg/l, MLVSS of 6000 mg/l and initial BA of 200 mg $CaCO_3$/l.

The drop in pH below 5.0 observed earlier in the UASB-FF was attributed to the high production of VFAs at the beginning of the process and insufficient bicarbonate alkalinity to buffer the process. The results obtained from this part of the study can be used to project the required amount of initial BA for effective buffering action in the UASB-FF based on the influent CODin (at the bottom of the reactor) as well as the recycle ratio. As a conclusion, the hydrogen yield of 124.5 mmol H_2/g $COD_{removed}$ was occurred at the CODin, MLVSS and initial BA of 3000 mg/l, 4000 mg/l and 1100 mg CaCO3/l, respectively in batch experiment.

4.5.4. Kinetic analysis of hydrogen production

The cumulative hydrogen production and COD concentration curves were obtained from the experiments with COD_{in}, MLVSS and initial BA of 6500 mg/l, 4000 mg/l and 1100 mg $CaCO_3$/L, respectively (Run# 14) and are presented in Fig. 4.18. This run was chosen because it was generated the maximum hydrogen production (P) and hydrogen production rate (R_{max}). During the experiment, no methane production was detected based on the analysis of the collected biogas. All cumulative hydrogen production was well correlated to the modified Gompertz equation with R^2 more than 0.99. The kinetic parameters for total accumulated hydrogen production (ml) were P: 329.8 ml, R_{max}: 83.5 ml H_2/h and λ: 5.45 h.

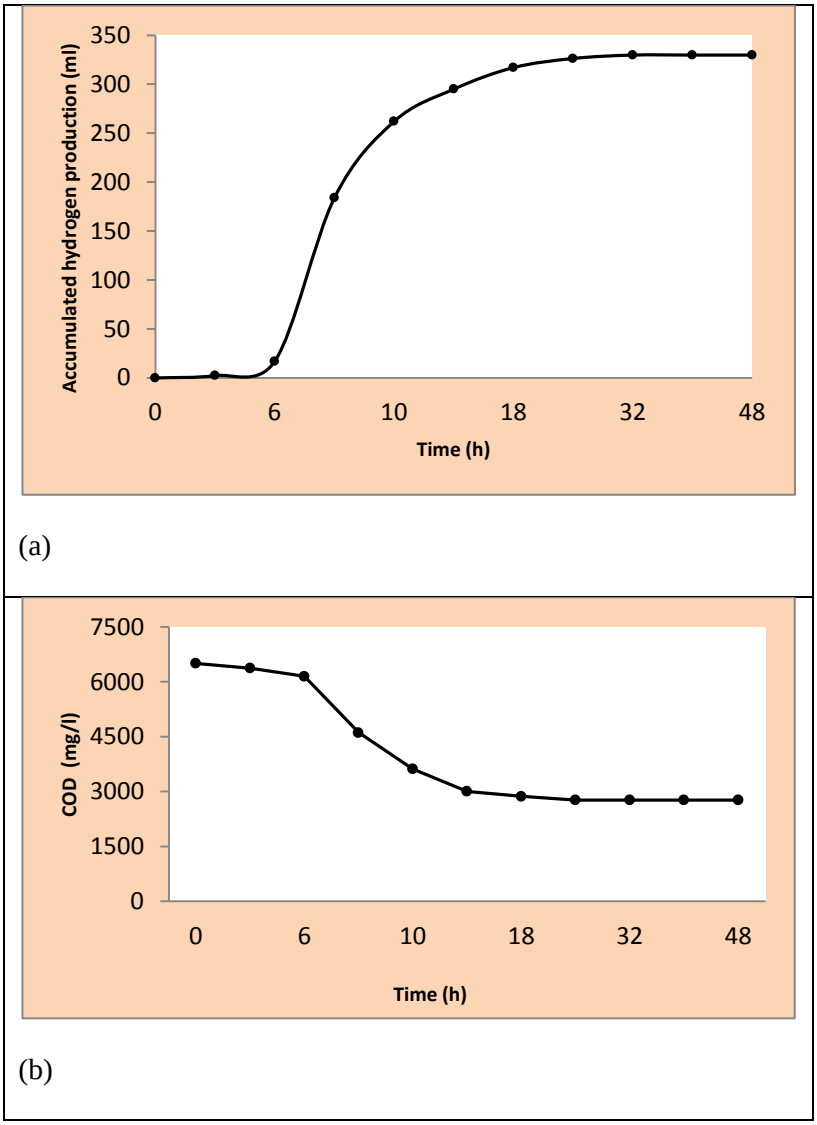

Fig. 4.17. Cumulative hydrogen production from POME at the COD_{in}, MLVSS and initial BA of 6500 mg/l, 4000 mg/l and 1100 mg $CaCO_3$/L, respectively (Run #14) in a batch experiment; (a) Profile of hydrogen production (ml), (b) Profile of COD concentration

4.6. Mass-transfer Evaluation on POME-grown Microbial Granules

In order to examine the mass transfer resistance in the granulated sludge, the effect of the granular structure of the microbial aggregates on the specific hydrogenesis activity was studied. Different factors may affect the mass transfer process in a fermentative hydrogen production by granulated sludge such as granule size and morphology, the specific hydrogenesis activity of the biomass, substrate concentration, the degree of mixing, and so on (Dolfing, 1986).

The fermentative hydrogen production from POME in disintegrated and intact granules at a mesophilic condition (38°C) was compared in terms of SHPR. The effectiveness factor (η) is computed by the ratio of the SHPR of disintegrated versus intact granules, that dependent on the total mass transfer resistance of the granules (Schmidt and Ahring, 1991). Figure 4.19 shows cumulative H_2 production as a function of time for intact (1.5-2.0 mm) and disintegrated (pinpoint, less than 0.1 mm) granules. After 40 h, a slightly higher cumulative hydrogen was obtained with intact granules i.e. 15.29 mmol H_2/l as compared to 14.44 mmol H_2/l for disintegrated granules. The SHPR was determined to be 2.62 and 2.25 mmol H_2/g VSS.d, respectively for intact and disintegrated granules.

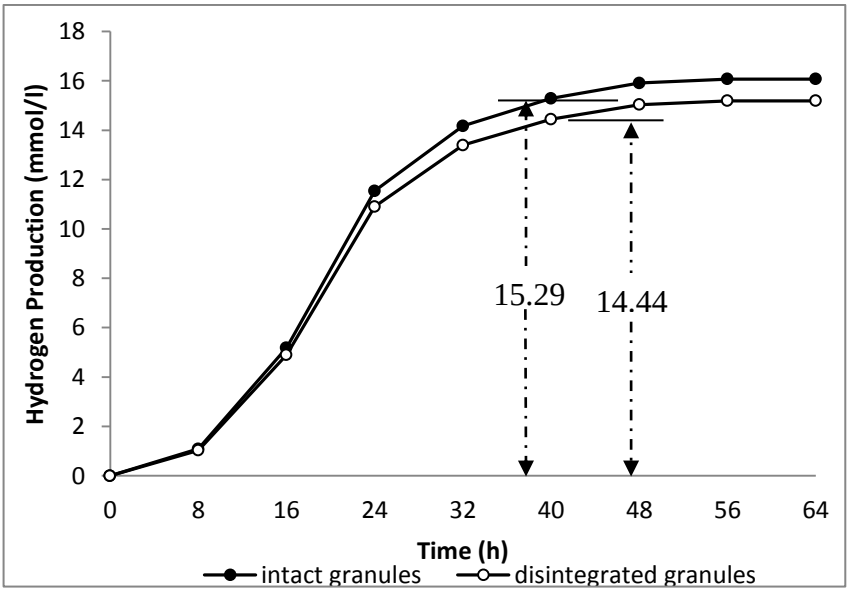

Figure 4.19. Cumulative H_2 production versus time

The value of η was calculated to be 0.94, indicating comparable specific hydrogenesis activity of disintegrated and intact granules. It shows that there is likely no significant mass transfer resistance due to internal (substrate diffusion from the surface to the center of the granules) and/or external (substrate transportation from bulk solution to the surface of the granules) factors. However, the value did indicate a slightly higher

specific hydrogenesis activity of intact granules, which might be due to its higher substrate utilization rate. This is attributed to concentrated microbial communities within the aggregates. Another possible explanation is that substrate convection might be a significant mechanism for substrate mass transport inside the granules (Yang and Lewandowski, 1995). Convective mass transport in the biofilm (or in the pores of the film/aggregate) can be created by intensifying the hydraulic turbulence in the bulk of the liquid by increasing the superficial liquid velocity in the reactor (Lettinga, 1995). As a conclusion, substrate mass transfer into granules was not a limiting factor in POME anaerobic fermentation by the microbial granules.

4.7. Experimentation and determination of hydraulic regime

To obtain the maximum absorption of Rhodamine B (2×10^{-4}M), the absorption spectrum was measured in water, in the range of 400–630 nm (Fig. 4.20). The maximum absorption was observed at 554 nm (at room temperature). This maximum absorption was used in all color tracing experiments.

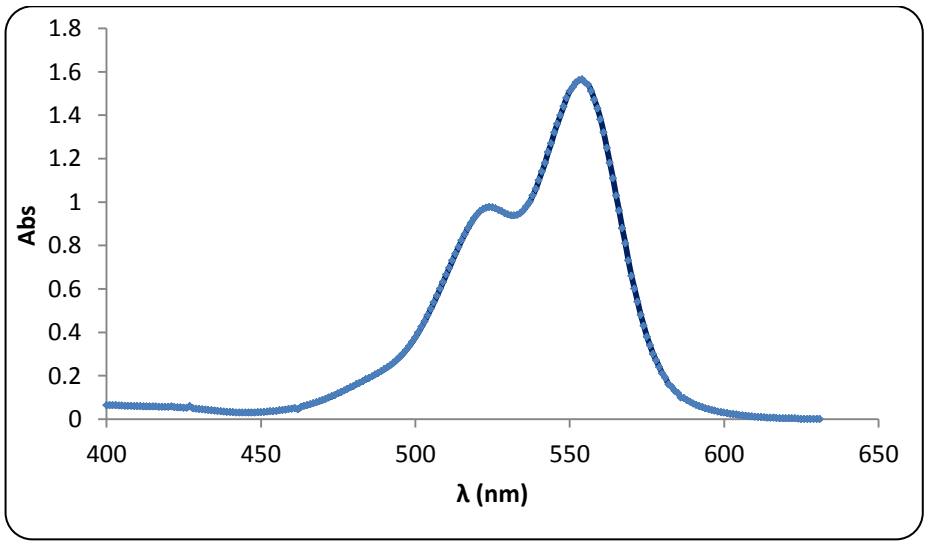

Fig. 4.20. Absorption spectra of 2×10^{-4} M Rhodamine B

Fig. 4.21 shows the calibration plot obtained for Rhodamine B at λ_{max} 554 nm. Eleven standard concentrations of Rhodamine B were measured for their respective absorbances.

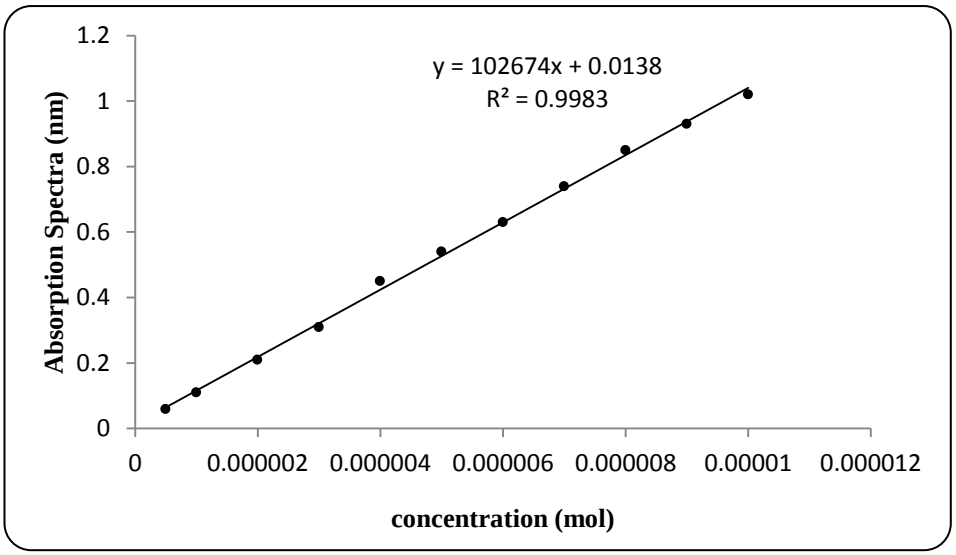

Fig. 4.21. Calibration graph for determination of Rhodamine B

Linear calibration graph was obtained in the range of 0.5–10 µM. Applying least square method to the calibration plot provided confidence limit for the slope and intercept using a significant test at 0.05-probability level. The regression equations are represented by:

$$Y = 102674X + 0.0138 \quad (4.9)$$

where X is the average reference assay and Y is the average of the absorbance. This linear equation showed correlation coefficient values of 0.9983 for Rhodamine B (Fig. 4.21). This equation can be utilized for determining Rhodamine B amount in output of the reactor. The lowest Rhodamine B concentration detected at the outlet was 0.5 µM.

4.7.1. Hydraulic performance analysis

The hydraulic performance of the UASB-FF bioreactor is analyzed by studying water flow patterns or hydraulic residence time distributions (RTD) obtained from the tracer experiments. Fig.4.22a-b presents the modeled and experimental data curves of tracer concentration time distribution at different V_{up} (0.5 and 3.0 m/h) and Q_g (14.87

and 7.96 l/d). The ideal flow concentrations were calculated based on the equation (4.10):

$$C, Ideal, (mmol) = C_0 \times Exp(-\frac{t}{\tau}) \qquad (4.10)$$

where, C is the ideal flow concentration (mM), C_0 is the initial flow concentration of the tracer (mM), t is sampling time (min), and τ is theoretical retention time (min).

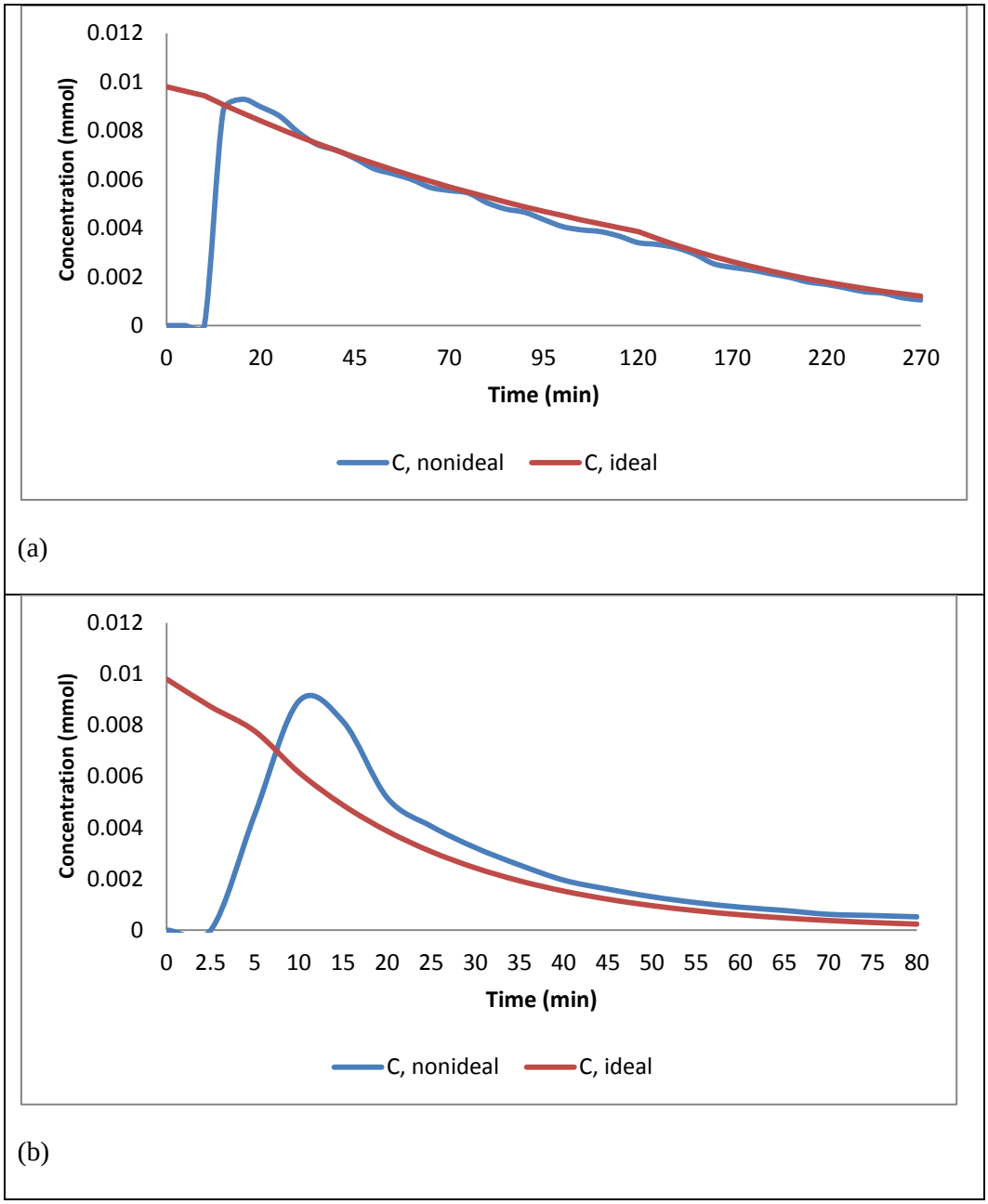

Fig.4.22- Mathematical and empirical curves of tracer concentration time distribution for (a) V_{up}=0.5 m/h and Q_g=14.87l/d, (b) V_{up}=3.0 m/h and Q_g=7.96 l/d

It is clear from the figure that the increase in V_{up} resulted in pronounced deviation from ideal flow pattern. It can be seen that the deviation obtained at V_{up} of 0.5 m/h and Q_g of 14.87 l/d was less than the deviation obtained at V_{up} of 3.0 m/h and Q_g of 7.96 l/d. As depicted in Fig.4.22b, high volume of the tracer arrives at the outlet before complete mixing with the bulk of the liquid in the reactor. It could be due to the short cut phenomenon occurred originated from the reactor geometry, inlet and outlet design and inadequate mixing (see next section). If the concentration versus time tracer response curve is defined by a series of discrete time step measurements, the theoretical mean residence time is typically approximated as:

$$\bar{t}_{\Delta c} \approx \frac{\sum t_i C_i \Delta t_i}{\sum C_i \Delta t_i} \qquad (4.11)$$

where, $\bar{t}_{\Delta c}$ is the mean detention time based on discrete time step measurements, (min), t_i is the time at *i*th measurement, (min), C_i is the concentration at *i*th measurement, (mmol/l), and Δt_i is the time increment about C_i, (min).

4.7.2. Statistical analysis

4.7.2 (a) Deviation from ideal retention time (Δτ)

Deviations from the ideal retention time **(Δτ)** can be caused by a number of factors viz. channeling and/or recycling of fluid, short-circuiting, creation of stagnant regions in the vessel, and etc. In the short-circuiting, a portion of the flow that enters the reactor during a given time period arrives at the outlet before the bulk of the flow that entered the reactor during the same time period arrives. This non-ideal flow may be caused by density currents due to the temperature difference, wind-driven circulation pattern, inadequate mixing and poor design (Metcalf and Eddy, 2003). Ultimately, the incomplete use of the reactor volume due to above reasons can result in the decrease Δτ

and reduced treatment performance. In this study the values of Δτ were obtained at 33.58 and 4.15 min for V_{up} 0.5 m/h and Q_g 14.87 l/d and V_{up} of 3.0 m/h and Q_g of 7.96 l/d, respectively. From the results, increasing the V_{up} (τ from 21.5 to 128.8 min) resulted in the increase in Δτ (4.15 to 33.58 min). It was attributed to the relatively low up-flow velocity of the liquid within the reactor that may create dead space and inadequate mixing. Inadequate input energy for mixing, non mixing of some portions of the reactor contents with the incoming water, poor design of the reactor at inlet zone caused dead zones to develop within the reactor or allow short circuiting to occur [Levenspiel, 1972; Metcalf and Eddy, 2003]. To elucidate the Δ*τ*, volume of dead zone was also obtained as a response (Eq. 4.12)**.**

$$\Delta\tau = \left(\frac{\bar{t}_{\Delta c} - \theta}{\theta}\right) \times 100 \qquad (4.12)$$

In general, the long tail in the RTD curve shows a discrepancy between the mean residence time and the theoretical residence time. It is possible that stagnant hydraulic zones exist near the inlet and outlet parts of the reactor or in the fixed film zone, where tracer can be trapped and slowly released. It must be noted that, in this UASB-FF reactor, the liquid volume within the fixed film part was 14.5 % of the total liquid volume, likely to promote a relatively high dead volume. The values observed of the response (Δ*τ*) were 26 % and 19.3 % of the total reactor volume at V_{up} of 0.5 m/h and Q_g of 14.87 l/d and V_{up} of 3.0 m/h and Q_g of 7.96 l/d, respectively.

4.7.2 (b) Morrill dispersion index (MDI)

One important factor that indicates the type of the reactor (complete mix or plug-flow) is Morrill Dispersion Index (MDI). MDI can be used as an indicative tool for determining features of flow patterns in reactors. These consist of the regions of stagnant fluid (dead space) and/or the possibilities of bypassing. A ratio of 90 to 10

percent values from the cumulative tracer concentration curve could be used as a measure of the dispersion index. The value for an ideal plug-flow reactor is 1.0 and about 22 for a complete-mix reactor. MDI was computed for both operational conditions studied (Metcalf and Eddy, 2003).

Morrill dispersion index, $MDI = \frac{P_{90}}{P_{10}}$ (4-13)

where P_{90} is 90 percentile value and P_{10} is 10 percentile value from log-probability plot of the cumulative tracer concentration curve.

The values of MDI computed at the minimum and maximum V_{up} and Q_g are identified as 11.33 and 10, respectively, showing that the hydraulic regime in UASB-FF bioreactor is a semi-complete mixing.

In order to further analyze the residence time distribution of the fluid in a reactor the *E*(t) and *F*(t) curves have been developed in the Fig. 4.23. Fluid elements may require differing lengths of time to travel through the reactor. The distribution of the exit times, defined as the *E*(t) curve, is the residence time distribution (RTD) of the fluid. The exit concentration of a tracer species *C*(t) can be used to define *E*(t). That is:

$$E\,(\mathrm{t}) = \frac{C(\mathrm{t})}{\int_0^\infty C(\mathrm{t})\mathrm{dt}} \qquad (2.14)$$

Such that:

$$\int_0^\infty E(t)dt = 1 \qquad (2.15)$$

The *F* curve is defined as

$$F\,(\mathrm{t}) = \int_0^t E(t)dt \qquad (2.16)$$

where *F*(t) is the cumulative residence time distribution function. As shown in the equation (2.16), the *F*(t) curve is the integral of the *E*(t) curve while the *E*(t) curve is the derivative of *F*(t) curve. In the fact, *F*(t) represents the amount of tracer that has been in the reactor for less than the time (t). As can be observed in the Fig.4.23, retention time distribution (RTD) function, *E*(t) and *F*(t) showed a higher initial values at V_{up} 3.0 m/h

compared to the values at the V_{up} 0.5 m/h. The interaction showed that up-flow velocity and gas flow rate played an important role in the MDI of the reactor. As a conclusion, the hydraulic regime in UASB-FF bioreactor is a semi-complete mixing.

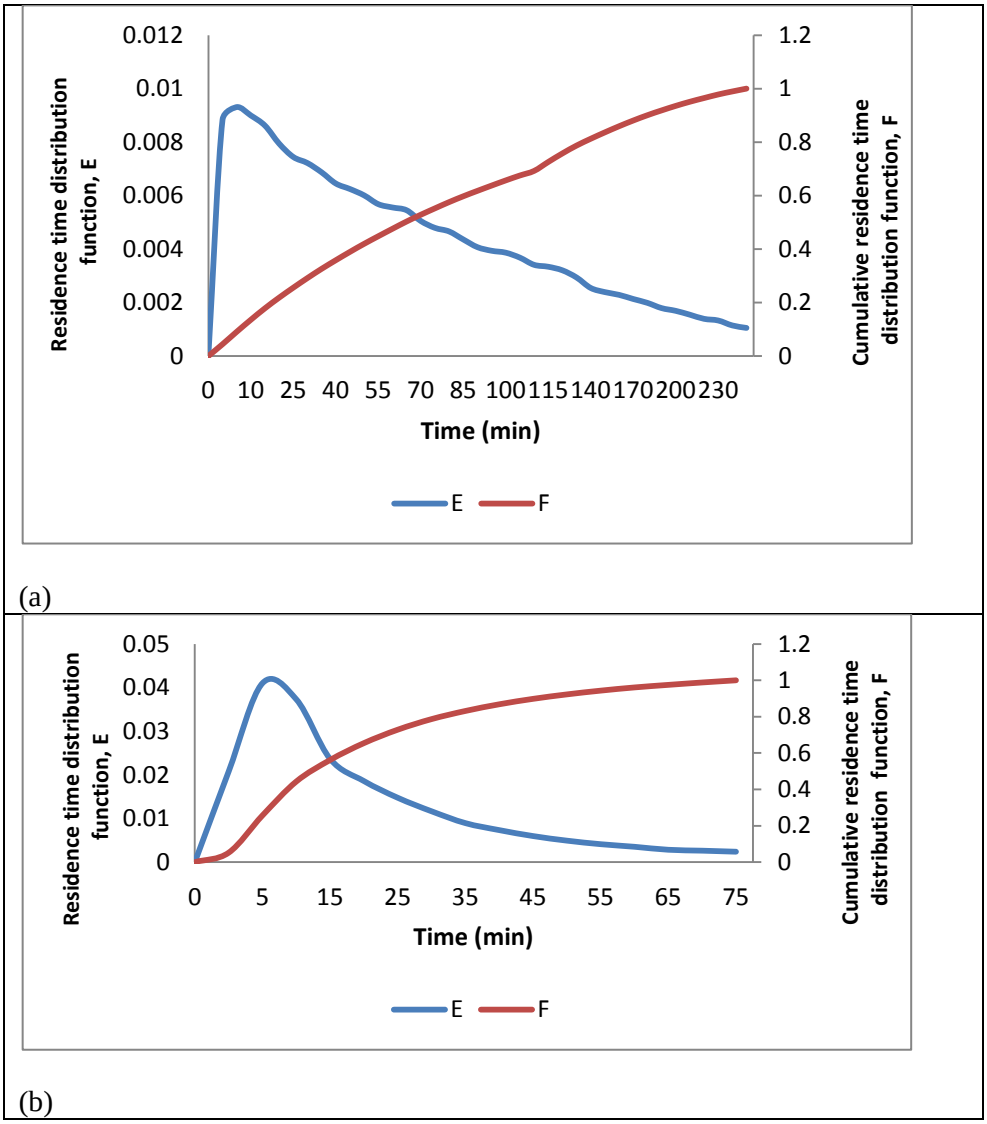

Fig.4.23- *E*(t) and *F*(t) plots with respect to (a) V_{up} 0.5 m/h and Q_g 14.87l/d, (b) V_{up} 3.0 m/h and Q_g 7.96 l/d

4.8. The effect of the fixed film part on UASB-FF bioreactor performance

In order to study the effect of fixed film section on the bioreactor performance, COD and TSS were monitored to determine the quality of the fermented POME sampled from sampling port 4 (S4), below internal packing, and from sampling port 5 (S5), the effluent of the reactor. The COD concentrations in the effluent from S4 and S5

are shown in Figure 4.24. Considerable difference between COD concentrations at S4 and S5 samplings was found at the various conditions (Q_F and V_{up}). The up-flow velocity was ascribed as the main factor in causing the observed differences. As the up-flow velocity increased, the difference between the COD concentrations at S4 and S5 was lower (7.5% at V_{up}=0.5 m/h, 3.3% at V_{up}=3.0 m/h) due to the reduced contact time between the organic matter and immobilized bacteria on the packing bed. The maximum difference of COD concentrations between S4 and S5 was found to be 7.5% at Q_F and V_{up} of 10.2 l/d and 0.5 m/h, respectively. Therefore, at lower V_{up} and HRT, the role of the fixed film reactor in supplementing biological hydrogen production from POME in the UASB-FF bioreactor was expected to be more significant. Washout of biomass, particularly at low up-flow velocities, is undesirable if active biomass within the rector is to be retained, which will subsequently develop as granules (Vadlani and Ramachandran, 2008).

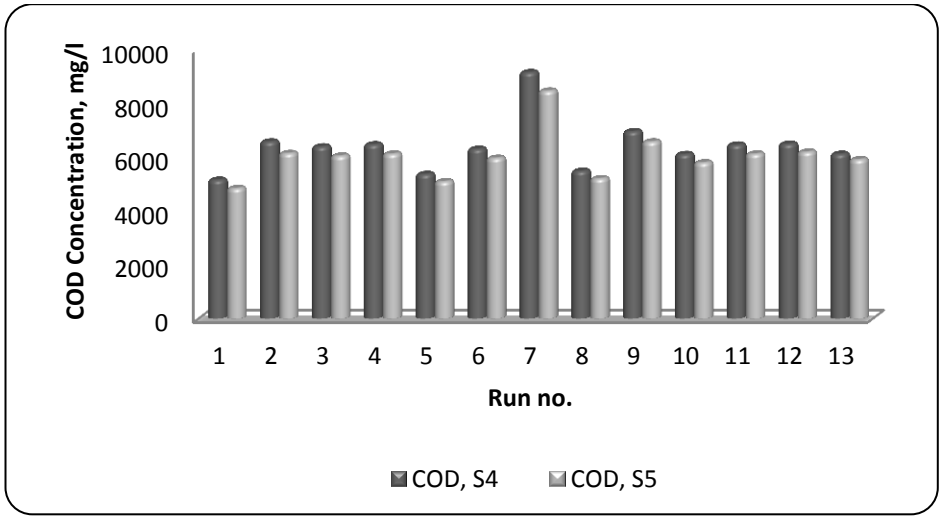

Figure 4.24. Effluent COD concentration at S4 and S5

The main purpose of the fixed film part was to avoid biomass washout. The effluent TSS concentrations at S4 and S5 were shown in Figure 4.25. It can be seen that the fixed film part helped to reduce significant biomass washout and retain them in the UASB reactor. This effect is expected to be more marked at shorter HRT and higher V_{up}

(Borja *et al.*, 1998). The maximum difference of TSS concentrations at S4 and S5 was found to be about 49% at Q_F and V_{up} of 10.2 l/d and 3.0 m/h, respectively.

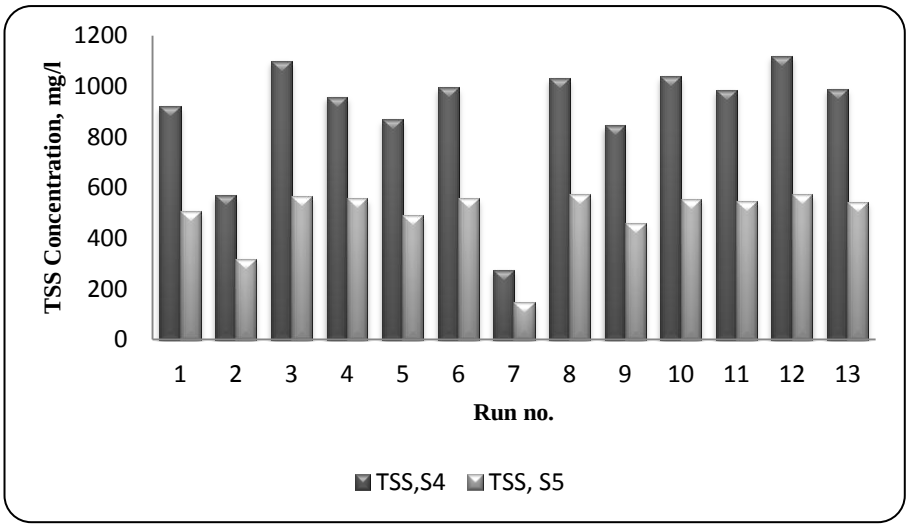

Figure 4.25. Effluent TSS concentration at S4 and S5

As a conclusion, the use of packing media in the middle portion reduced loss of biomass due to flotation associated with poorly performing UASB reactors.

CHAPTER 5

CONCLUSIONS

A lab scale up-flow anaerobic sludge blanket fixed film (UASB-FF) bioreactor with an external settling tank was successfully designed, fabricated and operated for biological H_2 production from palm oil mill effluent (POME). The effects of various pretreatment methods on the enrichment of H_2 evolving bacterial population and their H_2 production efficiency using POME as substrate were studied. Heat shock pretreatment was shown to be the most effective in enhancing the biological H_2 production. The UASB-FF bioreactor was seeded with heat shock pretreatment sludge.

The use of UASB-FF reactor was a good strategy to accelerate anaerobic granulation and to achieve a high COD removal efficiency and H_2 yield in a short period of time. The reactor was efficient in the fermentation of pre-settled POME at high OLR and short HRT. The use of packing media in the middle portion reduced channeling problem and loss of biomass due to flotation associated with poorly performing UASB reactors. Additionally, the packing material caused the flocculated biomass to precipitate over the sludge blanket to serve as suitable and natural hydrophobic core for the development of granular sludge.

The proposed kinetic equations are applicable to anaerobic fermentation of POME in the UASB-FF bioreactor. The hydrogen production rates were between 0.099 to 0.306 l H_2/g $COD_{removed}$.d. The highest value of yield was 0.310 l H_2/g COD at Q_F and V_{up} of 1.7 l/d and 0.5 m/h, respectively. The maximum specific growth rate (μ_{max}) of hydrogenesis bacteria grown on POME as substrate was calculated at 0.371 d^{-1} (38 °C). The half-velocity constant (*K*s) was 10.9 g/L when POME concentration was 15.0 g/L. In this study, the kinetic parameters *Y*, K_d, and *k* were obtained 0.093 g/g, 0.005 d^{-1}, and 3.99 g COD/g VSS.d, respectively.

Effects of three important variables *viz*. initial COD concentration (COD_{in}), biomass concentration and initial bicarbonate alkalinity (BA) on the biological activity of the granulated sludge were also investigated in batch culture. The maximum specific hydrogen production rate (55.42 mmol H_2/g VSS.d) was at the COD_{in}, MLVSS and initial BA of 6500 mg/l, 2000 mg/l and 1100 mg $CaCO_3$/L, respectively. The hydrogen yield (124.5 mmol H_2/g $COD_{removed}$) was also occurred at the COD_{in}, MLVSS and initial BA of 3000 mg/l, 4000 mg/l and 1100 mg $CaCO_3$/L, respectively.

The mathematical model derived from kinetic equations of a consecutive reaction with three constituents gave good fit with the experimental results ($R^2 > 0.93$). All cumulative hydrogen production was well correlated to the modified Gompertz equation with R^2 more than 0.99. The kinetic parameters for total accumulated hydrogen production (ml) were P: 329.8 ml, R_{max}: 83.5 ml H_2/h and λ: 5.45 h. The significant factors affecting sludge activity were initial bicarbonate alkalinity and initial biomass concentration. The required initial bicarbonate alkalinity was determined to be more than 0.083 g $CaCO_3$ per gram initial COD. It was also found that substrate mass transfer into granules was not a limiting factor in the fermentation of POME by the microbial granules.

Response surface methodology was successfully applied to model and analyze the process as well as determination of the optimum operational conditions for the fermentative hydrogen production of pre-settled POME. The optimum conditions for the fermentative hydrogen production of the pre-settled POME were determined between Q_F of 3.71 l/d, V_{up} of 1.48 m/h and Q_F of 2.03 l/d, V_{up} of 2.31m/h, respectively. The experimental findings were in close agreement with the model prediction.

CHAPTER 6

RECOMMENDATIONS FOR FUTURE RESEARCH

1. In the present study, kinetic parameters (μ_m, K_s, K, Y) of POME anaerobic digestion reactions were determined and also operating and process variables (feed flow rate (Q_F), up-flow velocity (V_{up})) in the UASB-FF bioreactor were optimized. Future efforts should be directed towards the application of the kinetic and process data to be incorporated into scale-up of the bioreactor to industrial size as well as economic evaluation.
2. It is recommended that the feasibility of biological hydrogen production applying various industrial wastewaters such as POME, dairy, winery at the same operating conditions (OLR, Q_{in}, HRT, pH, temperature) in an UASB-FF bioreactor be evaluated and compared.
3. It is recommended that the effect of mixing on biological hydrogen production from POME in an UASB reactor be investigated.
4. It is recommended that the effect of Q_{in}, HRT, and temperature on biological hydrogen production from POME in an UASB-FF reactor be investigated.
5. It is recommended that the hydraulic regimes (AnSBR and Continuous) of UASB-FF to biological hydrogen production from POME be compared.

References:

Ahmad, A. L., Ismail, S. & Bhatia, S. (2003). Water recycling from palm oil mill effluent (POME) using membrane technology. *Desalination, 157,* 87-95.

Akutsu, Y., Li, Y. Y., Harada, H. & Yu, H. Q. (2009). Effects of temperature and substrate concentration on biological hydrogen production from starch. *Int J Hydrogen Energy, 34*, 2558-66.

American Public Health Association (APHA). (1999). Standard Methods for the examination of water and wastewater. (20th Ed.). AWWA, Washington DC.

Annachhatre, A. P. (1996). Anaerobic Treatment of industrial wastewaters. *Resources, Conversation and recycling, 16*, 161-166.

Antonopoulou, G., Hariklia, N. G., Ioannis, V. S. & Gerasimos, L. (2011). Effect of substrate concentration on fermentative hydrogen production from sweet sorghum extract. *Int. J. Hydrogen Energy,* 36, 4843–4851.

Atif, A. A. Y., Razia, A. F., Ngan, M. A., Morimoto, M., Iyukec, S. E. & Veziroglu, N. T. (2005). Fed batch production of hydrogen from palm oil mill effluent using anaerobic microflora. *Water Sci Technol., 53,* 271–79.

Azbar, N., Dokgoz, F. T. C., Keskin, T., Korkmaz, K. S. & Syed, H. M. (2009). Continuous fermentative hydrogen production from cheese whey wastewater under thermophilic anaerobic conditions. *Int J Hydrogen Energy, 34*, 7441–47.

Baghchehsaraee, B., Nakhla, G., Karamanev, D. & Margaritis, A. (2010). Fermentative hydrogen production by diverse microflora. *Int J Hydrogen Energy, 35*, 5021-5027.

Baily, J. E. & Ollis, D. F. (1986). Biochemical Engineering Fundamentals (2nd edition). New York, McGraw-Hill: pp. 200-270

Baş, D. & Boyaci, I. H. (2007). Modeling and optimization I: Usability of response surface methodology. *J. Food Eng., 78*(3), 836-845.

Beyenal, H. & Lewandowski, Z. (1999). Combined effect of substrate concentration and flow velocity on effective diffusivity in biofilms. *Wat. Res., 34*, 528-538.

Bhaskar, Y. V., Mohan, S. V. & Sarma, P. N. (2008). Effect of substrate loading rate of chemical wastewater on fermentative biohydrogen production in biofilm configured sequencing batch reactor. *Bioresource Tech., 99*, 6941-6948.

Borja, R., Banks, C. J., Wang, Z. & Mancha, A. (1998). Anaerobic digestion of slaughterhouse wastewater using a combination sludge blanket and filter arrangement in a single reactor. *Bioresource Technol., 65*, 125-133.

Buzzini, A. P. & Pires, E. C. (2002). Cellulose pulp mill effluent treatment in an upflow anaerobic sludge blanket reactor. *Process Biochem., 38*(5), 707-713.

Cai, M. L., Liu, J. X. & Wei, Y.S. (2004). Enhanced biohydrogen production from sewage sludge with alkaline pretreatment. *Environ. Sci. Technol., 38*, 3195–3202.

Cha, G. C. & Noike, T. (1997). Effect of rapid temperature change and HRT on anaerobic acidogensis. *Water Sci. Technol., 36*, 247–253.

Chang, F. Y. & Lin, C.Y. (2004). Biohydrogen production using an upflow anaerobic sludge blanket reactor. *Int J Hydrogen Energy, 29*, 33–39.

Chang, J., Lee, K. & Lin, P. (2002). Biohydrogen production with fixed-bed bioreactors. *Int J Hydrogen Energy, 27*, 1167–74.

Chen, C. C., Lin, C. Y. & Lin, M.C. (2002). Acid–base enrichment enhances anaerobic hydrogen production process. *Appl. Microbiol. Biotechnol., 58*, 224–28.

Chen, C-C., Lin, C-Y. & Chang, J-S. (2001). Kinetics of hydrogen production with continuous anaerobic cultures utilizing sucrose as the limiting substrate. *Appl. Microbiol. Biotechnol., 57*, 56–64.

Chen, W. H., Chen, S. Y., Khanal, S. K. & Sung, S. (2006). Kinetic study of biological hydrogen production by anaerobic fermentation. *Int J Hydrogen Energy, 31*, 2170-2178.

Chen, W. H., Sung, S. & Chen, S. Y. (2009). Biological hydrogen production in an anaerobic sequencing batch reactor: pH and cyclic duration effects. *Int J Hydrogen Energy, 34*, 227-34.

Cheong, D. Y. & Conly, L.H. (2006). Acidogenesis characteristics of natural mixed anaerobes converting carbohydrate-rich synthetic wastewater to hydrogen. *Process Biochemistry, 41*, 1736–45.

Cheong, D. Y. & Hansen, C. L. (2006). Bacterial stress enrichment enhances anaerobic hydrogen production in cattle manure sludge. *Appl. Microbiol. Biotechnol., 72*, 635-643.

Cheong, D. Y. & Hansen, C. L. (2007). Feasibility of hydrogen production in thermophilic mixed fermentation by natural anaerobes. *Bioresour. Technol., 98*, 2229–2239.

Chong, M. L., Sabaratnam, V., Shirai, Y. & Hassan, M. A. (2009). Biohydrogen production from biomass and industrial wastes by dark fermentation. *Int J Hydrogen energy, 34*, 3277-3287.

Chong, M-L., Abdul Rahim, R., Shirai, Y. & Hassan, M. A. (2009). Biohydrogen production by Clostridium butyricum EB6 from palm oil mill effluent. *Int J Hydrogen Energy, 34*, 764-771.

Chookaew, T., Sompong, O. & Prasertsan, P. (2012). Fermentative production of hydrogen and soluble metabolites from crude glycerol of biodiesel plant by the newly isolated thermotolerant Klebsiella pneumoniae TR17. *Int. J. Hydrogen Energy,* 37, 13314–13322.

Chow, M. C. & Ho, C. C. (2000). Surface active properties of palm oil. *Journal of Oil Palm Research, 12*(1), 107-116.

Cohen, A. (1982). Influence of phase separation on the anaerobic digestion of glucose-II. Stability and kinetic responses to shock loadings. *Water Res., 16*, 449–455.

Cohen, A., Zoetemeyer, R. J., Van Deursen, A. & Van Andel, J. G. (1979). Anaerobic digestion of glucose with separated acid production and methane formation. *Water Res.,13*, 571–80.

Cuetos, M. J., Gomez, X., Escapa, A. & Moran, A. (2007). Evaluation and simultaneous optimization of bio-hydrogen production using 32 factorial design and the desirability function. *Power Sources, 169*, 131–39.

Das, D. & Veziroglu, T. N. (2001). Hydrogen production by biological process: a survey of literature. *Int J Hydrogen Energy, 26*, 13–28.

Das, D. & Veziroglu, T. N. (2008). Advances in biological hydrogen production processes. *Int J Hydrogen Energy, 33*, 6046–6057.

Dolfing, J. (1986). Granulation in UASB reactors. *Wat. Sci. and Technol., 18*, 15-25.

Droste, R.L. (1997) Theory and Practice of Water and Wastewater Treatment. New York, John Wiley: pp. 40-200.

Duangmanee, T., Padmasiri, S. I., Simmons, J. J., Raskin, L. & Sung, S. (2007). Hydrogen production by anaerobic microbial communities exposed to repeated heat treatments. *Water Environ. Res. 79*, 975–983.

Economic Planning Unit (EPU). (1999). Support to the development of a strategy for renewable energy as a fifth fuel in Malaysia. Kuala Lumpur, Economic Planning Unit, Prime Minister's Department, Government of Malaysia.

Energy Commission. (2002). Small renewable Energy Power Programme (SREP) Guidelines. Energy Commission, Ministry of Energy, Communications and Multimedia, Kuala Lumpur, Malaysia.

Fabiano, B. & Perego, P. (2002). Thermodynamic study and optimization of hydrogen production by Enterobacter aerogenes. *Int J Hydrogen Energy, 27*, 149-156.

Fan, Y. T., Li, C. L. Lay, J. J., Hou, H. H. & Zhang, G. S. (2004). Optimization of initial substrate and pH levels for germination of sporing hydrogen producing anaerobes in cow dung compost. *Bioresource Technol., 91*, 189–193.

Fang, H. H. P. & Liu, H. (2002). Effect of pH on hydrogen production from glucose by a mixed culture. *Bioresource Tech., 82*, 87–93.

Fang, H. H. P., Li, C. L. & Zhang, T. (2006). Acidophilic biohydrogen production from rice slurry. *Int J Hydrogen Energy, 31*, 683–692.

Fang, H. H. P., Liu, H. & Zhang, T. (2002). Characterization of a hydrogen producing granular sludge. *Biotechnol Bioeng., 78*, 44–52.

Fernandez, J. M., Omil, F., Mendez, R. & Loma, J. M. (2001). Anaerobic treatment of fibreboard manufacturing wastewaters in a pilot scale hybrid UASB reactor. *Wat. Res., 35*(4), 150-158.

Fox, P. & Pohland, F. G. (1994). Anaerobic treatment applications and fundamentals: substrate specificity during phase separation. *Water Environment Research, 66*, 716–724.

Ginkel, S. V. & Sung, S. (2001). Biohydrogen productions a function of pH and substrate concentration. *Environ. Sci. Technol., 35*, 4726–30.

Ginkel, S. W. V., Oh, S. E. & Logan, B. E. (2005). Biohydrogen gas production from food processing and domestic wastewaters. *Int J Hydrogen Energy, 30*, 1535–1542.

Ginkel, V. S., Sung, S. & Lay, J. J. (2001). Biohydrogen production as a function of pH and substrate concentration. *Environ Sci Technol., 35*, 4726–4730.

Gomez, X., Cuetos, M. J., Prieto, J. I. & Moran, A. (2009). Bio-hydrogen production from waste fermentation: Mixing and static conditions. *Renewable Energy, 34*, 970-975.

Gooden, J. A. S., Finlayson, J. M. & Low, E. W. (2001). A further study of the anaerobic bio-treatment of malt whisky distillery pot ale using an UASB system. *Biosource Technol., 78,* 155-160.

Hafez, H., Nakhla, G., Naggar, M. H. E., Elbeshbishy, E. & Baghchehsaraee, B. (2010). Effect of organic loading on a novel hydrogen bioreactor. *Int J Hydrogen Energy, 35*, 81-92.

Hameed, A. & Gondal, M. A. (2005). Production of hydrogen-rich syngas using p-type NiO catalyst: a laser-based photocatalytic approach. *J Mol Catal A: Chem., 233*, 35–41.

Han, H. K. & Shin, H. S. (2004). Performance of an innovative two-stage process converting food waste to hydrogen and methane. *J. Air Waste Manage Assoc., 54*, 242–249.

Han, W., Chen, H., Jiao, A., Wang, Z., Li Y. & Ren, N. (2012). Biological fermentative hydrogen and ethanol production using continuous stirred tank reactor. *Int. J. Hydrogen Energy*, 37, 843–847.

Hart, D. (1997). Hydrogen power: the commercial future of the ‘‘ultimate fuel’’. London: Financial Times Energy Publishing.

Hawkes, F. R., Dinsdale, R., Hawkes, D. L. & Hussy, I. (2002). Sustainable fermentative hydrogen production: challenges for process optimisation. *Int J Hydrogen Energy, 27*, 1339–1347.

Hawkes, F. R., Hussy, I. Kyazze, G. Dinsdale, R. & Hawkes, D. L. (2007). Continuous dark fermentative hydrogen production by mesophilic microflora: Principles and progress. *Int J Hydrogen Energy, 32*, 172–184.

Heuvel, V. J. C., Beeftink, H. H. & Verschuren, P. G. (1988). Inhibition of the acidogenic dissimilation of glucose in anaerobic continuous cultures by free butyric acid. *Applied Microbiology and Biotechnology, 29*, 89–94.

Himmi, E. H., Bories, A., Boussaid, A. & Hassani, L. (2000). Propionic acid fermentation of glycerol and glucose by Propionibacterium acidipropionci and Propionbacterium freudenreichii ssp. Shermanii. *Applied Microbiology and Biotechnology, 53*, 435–440.

Hu, B. & Chen, S. L. (2007). Pretreatment of methanogenic granules for immobilized hydrogen fermentation. *Int J Hydrogen Energy, 32*, 3266–3273.

Huang, G. H., Hsu, S. F., Liang, T. M. & Huang, Y. H. (2004). Study on hydrogen production with hysteresis in UASB. *Chemosphere*, *54*, 815-821.

Hwang, J. H., Choi, J. A., Abou-Shanab, R. A. I., Bhatnagar, A., Min, B.; Song, H. ... & Kumar, E. (2009). Effect of pH and sulfate concentration on hydrogen production using anaerobic mixed microflora. *Int J Hydrogen Energy, 34*, 9702-9710.

Ismail, I., Hassan, M. A., Abdul Rahman, N. A. & Chen, S. S. (2010). Thermophilic biohydrogen production from palm oil mill effluent (POME) using suspended mixed culture. *Biomass and Bioenergy, 34*, 42-47.

Jeong, H. S., Kim, Y. H., Yeom, S. H., Songa, B. K. & Lee, S. I. (2005). Facilitated UASB granule formation using organic-inorganic hybrid polymers. *Process Biochem., 40*(1), 89-94.

Jo, J. H., Lee, D. S. & Park, J. M. (2008b). The effects of pH on carbon material and energy balances in hydrogen-producing Clostridium tyrobutyricum JM1. *Bioresource Tech., 99*, 8485–8491.

Jo, J. H., Lee, D.,S., Park, D. & Park, J. M. (2008a). Biological hydrogen production by immobilized cells of Clostridium tyrobutyricum JM1 isolated from a food waste treatment process. *Bioresource Tech., 99*, 6666–6672.

Kapdan, I. K. & Kargi, F. (2006). Bio-hydrogen production from waste materials. *Enzyme and Microbiol Tech., 38*, 569–582.

Khuri, A.I. and Cornell, J.A. (1996). Response surfaces: design and analyses. (2nd edition). New York, Marcel Dekker: pp. 80-170.

Kim, J., Park, C., Kim, T. H., Lee, M., Kim, S., Kim, S. W. & Lee, J. (2003). Effects of various pretreatments for enhanced anaerobic digestion with waste activated sludge. *J. Biosci. Bioeng., 95*, 271–275.

Kim, D.H. & Kim, M.S. (2012). Thermophilic fermentative hydrogen production from various carbon sources by anaerobic mixed cultures. *Int. J. Hydrogen Energy*, 37, 2021–2027.

Kim, S. H., Han, S. K. & Shin, H. S. (2008). Optimization of continuous hydrogen fermentation of food waste as a function of solids retention time independent of hydraulic retention time. *Process Biochemistry, 43*, 213–218.

Krishnan, V. & Desa, A. (2006). Biohydrogen generation from palm oil mill effluent using anaerobic contact filter. *Int J Hydrogen Energy, 31,* 1284-1291.

Kuehl, R. O. (2000). Design of experiments: statistical principles of research design and analysis. (2nd edition). Duxbury press, Pacific Grove, CA: pp. 2-225.

Lay, J. J. (2000). Modeling and optimization of anaerobic digested sludge converting starch to hydrogen. *Biotechnol. Bioeng., 68*, 269–278.

Lay, J. J. (2001). Biohydrogen generation by mesophilic anaerobic fermentation of microcrystalline cellulose. *Biotechnol Bioeng., 74*, 280–287.

Lay, J. J., Fan, K. S., Chang, J. & Ku, C. H. (2003). Influence of chemical nature of organic wastes on their conversion to hydrogen by heat-shock digested sludge. *Int J Hydrogen Energy, 28*, 1361–1367.

Lay, J. J., Lee, Y. J. & Noike, T. (1999). Feasibility of biological hydrogen production from organic fraction of municipal solid waste. *Water Research, 33*, 2579–2586.

Lay, J. J., Li, Y. Y. & Noike, T. (1998). A mathematical model for methane production from landfill bioreactor. *Environ. Eng., 124*, 730–736.

Lee, K. S., Hsu, Y. F., Lo, Y. C., Lin, P. J., Lin, C. Y. & Chang, J. S. (2008). Exploring optimal environmental factors for fermentative hydrogen production from starch using mixed anaerobic microflora. *Int J Hydrogen Energy, 33,* 1565–1572.

Lee, K. S., Lin, P. J. & Chang, J. S. (2006). Temperature effects on biohydrogen production in a granular sludge bed induced by activated carbon carriers. *Int J Hydrogen Energy, 31,* 465–472.

Lee, K. S., Lo, Y. S., Lo, Y. G., Lin, P. J. & Chang, J. S. (2003). H_2 production with anaerobic sludge using activated-carbon supported packed-bed bioreactors. *Biotechnol., 25,* 133-138.

Lee, M. J., Song, J. H. & Hwang, S. J. (2009). Effects of acid pre-treatment on bio-hydrogen production and microbial communities during dark fermentation. *Biores. Technol., 100,* 1491–1493.

Lee, Y. J., Miyahara, T. & Noike, T. (2001). Effect of iron concentration on hydrogen fermentation. *Bioresour. Technol., 80,* 227–231.

Leite, J. A. C., Fernandes, B. S., Pozzi, E., Barboza, M. & Zaiat, M. (2008). Application of an anaerobic packed-bed bioreactor for the production of hydrogen and organic acids. *Int J Hydrogen Energy, 33,* 579–586.

Lettinga, G. & Hulshoff Pol, L. W. (1991). UASB-process design for various types of wastewaters. *Wat. Sci. and Technol., 24*(8), 87-107.

Lettinga, G. (1995). Anaerobic digestion and wastewater treatment systems. Antonie van Leeuwen hoek. *Int J Gen Mol Biol., 67,* 3-28.

Levenspiel, O. (1972). Chemical reactor engineering. (2nd Ed.) New York: Whiely.

Levin, D. B., Pitt, L. & Love, M. (2004). Biohydrogen production: prospects and limitations to practical application. *Int J Hydrogen Energy, 29,* 173–185.

Li, C. L. & Fang, H. H. P. (2007). Fermentative hydrogen production from wastewater and solid wastes by mixed cultures. *Critical Reviews in Env. Sci. Technol., 37,* 1-39.

Li, J., Ren, N., Li, B., Qin, Z. & He, J. (2008). Anaerobic biohydrogen production from monosaccharides by a mixed microbial community culture. *Bioresource Tech., 99*, 6528-6537.

Lin, C. N., Wu, S. Y., Chang, J. S. & Chang, J. S. (2009). Biohydrogen production in a three-phase fluidized bed bioreactor using sewage sludge immobilized by ethylene–vinyl acetate copolymer. *Bioresource Technology, 100*, 3298–3301.

Lin, C. Y. & Lay, C. H. (2004). Carbon/nitrogen-ratio effect on fermentative hydrogen production by mixed microflora. *Int J Hydrogen Energy, 29*, 41–45.

Lin, C. Y., Wu, C. C. & Hung, C. H. (2008a). Temperature effects on fermentative hydrogen production from xylose using mixed anaerobic cultures. *Int J Hydrogen Energy, 33*, 43–50.

Lin, C. Y., Wu, C. C., Wu, J. H. & Chang, F.Y. (2008b). Effect of cultivation temperature on fermentative hydrogen production from xylose by a mixed culture. *Biomass and Bioenergy, 32*, 1109–1115.

Liu, B. F., Ren, N. Q., Xing, D., Ding, J., Zheng, G. X., Guo, W. Q., ... & Xie, G. J. (2009). Hydrogen production by immobilized R. faecalis RLD-53 using soluble metabolites from ethanol fermentation bacteria E. harbinense B49. *Bioresource Technology, 100*, 2719–2723.

Liu, H., Zang, T. & Fang, H. P. (2003). Thermophilic H_2 production from a cellulose containing wastewater. *Biotechnol. Lett., 23*, 365–369.

Liu, Y. & Tay, J-H. (2004). State of the art of biogranulation technology for wastewater treatment. *Biotechnol. Adv., 22*, 533-563.

Liu, Y., Yang, S., Tay, J., Liu, Q., Qin, L. & Li, Y. (2004). Cell hydrophobicity is a triggering force of biogranulation. *Enz. & Microb. Technol., 34*, 71-374.

Logan, B. E. (2004). Peer revieved: Extacting hydrogen and electricity from renewable resources. *Environ. Sci. Technol., 38*, 160A–7A.

Logan, B. E., Oh, S. E., Kim, I. S. & Ginkel, S. V. (2002). Biological hydrogen production measured in batch anaerobic respirometers. *Environ. Sci. Technol. 36*, 2530–2535.

Ma. A. N. (2000). Environment management for the palm oil industry. *Palm Oil Developments, 30,* 1-10.

Mahmoud, N., Zeeman, G., Gijzen, H. & Lettinga, G. (2003). Solid removal in upflow anaerobic reactors, a review. *Bioresource Technol., 90*(1), 1-9.

Malaysia Palm Oil Board (MPOB) Malaysian Palm Oil Statistics. (2011). Economics and Industry Development Division. MPOB: Kuala Lumpur.

Malaysia palm oil Production Council (MPOPC) (2006). Accessed on 14th April 2006. Available from World Wide Web: http://www.mpopc.org.my.

Malina, J. F. & Pohland, F. G. (1992). Design of anaerobic processes for the treatment of industrial and municipal wastes. Water Quality Management Library, Lancaster: Technomic Publishing Co., USA.

Marone, A., Massini, G., Patriarca, C., Signorini, A., Varrone, C. & Izzo, G. (2012). Hydrogen production from vegetable waste by bioaugmentation of indigenous fermentative communities. *Int. J. Hydrogen Energy*, 37, 5612–5622.

Mason, R. L., Gunst, R. F. & Hess, J. L. (2003). Statistical design and analysis of experiments, eighth applications to engineering and science. (2nd edition). New York: John Wiley.

McHugh, S., Collins, G. & O'Flaherty, V. (2006). Long-term, high-rate anaerobic biological treatment of whey wastewaters at psychrophilic temperatures, *Bioresource Technol., 97*(14), 1669-1678.

Metcalf, L. & Eddy, H. (2003). Wastewater Engineering. (4th edition). New York: McGraw Hill, pp. 800-1200.

Misuno, O., Dinsdale, R., Hawkes, F. R., Hawkes, D. L. & Noike, T. (2000). Enhancement of hydrogen production from glucose by nitrogen gas sparging. *Bioresource Technol., 73*, 59–65.

Mohan, S. V., Babu, V. L. & Sarma, P. N. (2008). Effect of various pretreatment methods on anaerobic mixed microflora to enhance biohydrogen production utilizing dairy wastewater as substrate. *Biores. Technol., 99*, 59–67.

Mohan, S. V., Lalit, V. B. & Sarma, P. N. (2007). Anaerobic biohydrogen production from dairy wastewater treatment in sequencing batch reactor (AnSBR): Effect of organic loading rate. *Enzyme and Microbial Technol. 41*, 506–15.

Montgomery, D. C. (1991). Design and analysis of experiments. 3rd edition, New York: John Wiley, pp. 130-180.

Mu Y., Zheng X-J. & Yu H-Q. (2009). Determining optimum conditions for hydrogen production from glucose by an anaerobic culture using response surface methodology (RSM). *Int J Hydrogen Energy, 34*, 7959-7963.

Mu, Y. & Yu, H. Q. (2007). Simulation of biological hydrogen production in a UASB reactor using neural network and genetic algorithm. *Int J Hydrogen Energy, 32*, 3308-3314.

Mu, Y., Wang, G. & Yu, H.Q. (2006a). Response surface methodological analysis on biohydrogen production by enriched anaerobic cultures. *Enzyme Microb Technol., 38*, 905–913.

Mu, Y., Yu, H. Q. & Wang, G. (2007). Evaluation of three methods for enriching hydrogen producing cultures from anaerobic sludge. *Enzyme Microb. Technol., 40*, 947–953.

Mu, Y., Yu, H. Q. & Wang, Y. (2006b). The role of pH in the fermentative H_2 production from an acidogenic granule-based reactor. *Chemosphere, 64*, 350–358.

Mu, Y., Zheng, X. J., Yu, H. Q. & Zhu, R. F. (2006c). Biological hydrogen production by anaerobic sludge at various temperatures. *Int J Hydrogen Energy, 31*, 780–785.

Muttamara, S., Vigneswaran, S. & Shin, H. S. (1987). Palm oil mill effluent management in Thailand: A preliminary Study. Final report submitted to UNDP/FAO. Asian Institute of Technology, Bankok, Thailand.

Nandi, S. & Sengupta, S. (1998). Microbial production of hydrogen: an overview. *Crit Rev Microbiol., 24*, 61–84.

Nicolau, J. M., Guwy, A., Dinsdale, R., Premier, G. & Esteves, S. (2010). Production of hydrogen from sewage biosolids in a continuously fed bioreactor: Effect of hydraulic retention time and sparging. *Int J Hydrogen Energy, 35*, 469-478.

Ntaikou, I., Kourmentza, C., Koutrouli, E.C., Stamatelatou, K., Zampraka, A., Kornaros, M. & Lyberatos, G. (2009). Exploitation of olive oil mill wastewater for combined biohydrogen and biopolymers production. *Bioresource Tech., 100*, 3724-3730.

Oh, Y. K. Kim, S. H. Kim, M. S. & Park, S. (2004). Thermophilic biohydrogen production from glucose with trickling biofilter. *Biotech. and Bioeng., 88*, 690–698.

Oh, Y. K., Seol, E. H., Kim, J. R. & Park, S. (2003). Fermentative biohydrogen production by a new chemoheterotrophic bacterium Citrobacter sp. Y19. *Int J Hydrogen Energy, 28*, 1353-1359.

Ozmihci, S. & Kargi, F. (2010). Effects of starch loading rate on performance of combined fed-batch fermentation of ground wheat for bio-hydrogen production. *Int J Hydrogen Energy, 35*, 1106-1111.

Ozmihci, S. & Kargi, F. (2011). Dark fermentative bio-hydrogen production from waste wheat starch using co-culture with periodic feeding: Effects of substrate loading rate. *Int. J. Hydrogen Energy*, 36, 7089–7093.

Pakarinen, O., Lehtomaki, A. & Rintala, J. (2008). Batch dark fermentative hydrogen production from grass silage: The effect of inoculum, pH, temperature and VS ratio. *Int J Hydrogen Energy, 33*, 594-601.

Pinto, F. A. L., Troshina, O. & Lindblad, P. (2002). A brief look at three decades of research on cyanobacterial hydrogen evolution. *Int J Hydrogen Energy, 27*, 1209-1215.

Prasertsan P., Sompong O-T. & Nils-Kare B. (2009). Optimization and microbial community analysis for production of biohydrogen from palm oil mill effluent by thermophilic fermentative process. *Int J Hydrogen Energy, 34*, 7448-7459.

Rachman, M. A., Nakashimada, Y., Kakizono, T. & Nishio, N. (1998). Hydrogen production with high yield and high evolution rate by self-flocculated cells of Enterobacter aerogenes in a packed-bed reactor. *Applied Microbiol. Biotechnol*., 49, 450–454.

Rao, A. G. & Bapat, A. N. (2006). Anaerobic treatment of pre-hydrolysate liquor (PHL) from a rayon grade pulp mill: Pilot and full-scale experience with UASB reactors. *Bioresource Technol., 97*(18), 2311-2320.

Ren, N. Q., Liu, B. F., Ding, J. & Xie, G. J. (2009). Hydrogen production with R. faecalis RLD-53 isolated from freshwater pond sludge. *Bioresource Tech., 100*, 484–487.

Ren, N. Q., Tang, J., Liu, B. F. & Guo, W. Q. (2010). Biological hydrogen production in continuous stirred tank reactor systems with suspended and attached microbial growth. *Int J Hydrogen Energy, 35*, 2807-2813.

Ren, N. Q., Wang, B. Z. & Huang, J. C. (1997). Ethanol-type fermentation from carbohydrate in high rate acidogenic reactor. *Biotechnology and Bioengineering, 54*, 428–433.

Rittmann, B. E. & Mac Carty, P. L. (2001). Environmental biotechnology: principles and applications. New York: McGraw-Hill, pp. 569-636.

Ruggeri, B., Tommasi, T. & Sassi, G. (2009). Experimental kinetics and dynamics of hydrogen production on glucose by hydrogen forming bacteria (HFB) culture. *Int J Hydrogen Energy, 34*, 753-763.

Schmidt, J. E. & Ahring, B. K. (1991). Acetate and hydrogen metabolism in intact and disintegrated granules from an acetate-fed, 55°C, UASB reactor. *Appl. Microbiol. Biotechnol., 35*, 681-685.

Schmidt, J. E. & Ahring, B. K. (1996). Granular sludge formation in upflow anaerobic sludge blanket (UASB) reactors. *J. Eng. Appl. Sci., 49*, 229-246.

Shen, L., Bagley, D. M. & Liss, S. N. (2009). Effect of organic loading rate on fermentative hydrogen production from continuous stirred tank and membrane bioreactors. *Int J Hydrogen Energy, 34*, 3689–3696.

Shihwu, S. (2004). Biohydrogen production from renewable organic wastes. Final Technical Report. www.osti.gov/energycitations/servlets/purl/828223.../828223.pdf .

Shivayogimath, C. B. & Ramanujam, T. K. (1999). Treatment of distillery spentwash by hybrid UASB reactor. *Bioprocess Eng., 21*, 255-259.

Show, K. Y., Zhang, Z. P., Tay, J. H., Liang, D. T., Lee, D. J. & Jiang, W. J. (2007). Production of hydrogen in a granular sludge-based anaerobic continuous stirred tank reactor. *Int J Hydrogen Energy, 32*, 4744–4753.

Show, K-Y., Wang, Y., Foong, S-F. & Tay, J-H. (2004). Accelerated Start-up and Enhanced Granulation in Up-flow Anaerobic Sludge Blanket Reactors. *Wat. Res., 38*, 2293-2304.

Soloman, B. D., Barnes, J. R. & Halvorsen, K. E. (2007). Grain and cellulosic ethanol: history, economics and energy policy. *Biomass and Bioenergy, 31*, 416–425.

Sompong, O. T., Prasertsan, P. & Birkeland, N. K. (2009). Evaluation of methods for preparing hydrogen-producing seed inocula under thermophilic condition by process performance and microbial community analysis. *Biores. Technol. 100*, 909–918.

Sompong, O. T., Prasertsan, P., Karakashev, D. & Angelidaki, I. (2008). Thermophilic fermentative hydrogen production by the newly isolated Thermoanaerobacterium thermosaccharolyticum PSU-2. *Int J Hydrogen Energy, 33*, 1204–1214.

Speece, R.E. (1996). Anaerobic Biotechnology for Industrial Wastewaters. Tennessee: Archaea Press, Nashville.

Su, H., Cheng, J., Zhou, J., Song, W. & Cen, K. (2009). Improving hydrogen production from cassava starch by combination of dark and photo fermentation. *Int J Hydrogen Energy, 34*, 1780-1786.

Subudhi, S. & Lal, B. (2011). Fermentative hydrogen production in recombinant *Escherichia coli* harboring a [FeFe]-hydrogenase gene isolated from *Clostridium butyricum. Int. J. Hydrogen Energy*, 36, 14024–14030.

Suwansaard, M., Choorit, W., Zeilstra-Ryalls, J. H. & Prasertsan, P. (2009). Isolation of anoxygenic photosynthetic bacteria from Songkhla Lake for use in a two-staged biohydrogen production process from palm oil mill effluent. *Int J Hydrogen Energy, 34*, 7523-7529.

Tang, G. L., Huang, J., Sun, Z. J., Tang, Q. Q., Yan, C. H. & Liu, G. Q. (2008). Biohydrogen Production from Cattle Wastewater by Enriched Anaerobic Mixed Consortia: Influence of Fermentation Temperature and pH. *Bioscience and Bioeng., 106*, 80–87.

Tao, Y., Chen, Y., Wu, Y., He, Y. & Zhou, Z. (2007). High hydrogen yield from a two-step process of dark- and photo-fermentation of sucrose. *Int J Hydrogen Energy, 32*, 200-206.

Tay, J. H. & Zhang, X. (2000). Stability of high-rate anaerobic systems. I. performance under shocks. *J. Environm. Eng., 30*(12), 43-53.

Thani, M. I., Hussin, R., Ibrahim, W. W. R. & Sulaiman, M. S. (1999). Industrial process the environment: crude palm oil industry. Handbook no. 3, Department of Environment, Kuala Lumpur, pp. 7-54.

Thaveesri, J., Gernaey, K., Kaonga, B., Boucneau, A. & Verstraete, W. (1994). Organic and ammonium nitrogen and oxygen in relation to granular sludge growth in lab-scale UASB reactors. *Wat. Sci. and Technol., 30*(12), 43-53.

Torkian, A., Eqbali, A. & Hashemian, S. J. (2003). The effect of organic loading rate on the performance of UASB reactor treating slaughterhouse effluent. *Resource, Conversation and Recycling, 40*, 1-11.

Vadlani, P. V. & Ramachandran, K. B. (2008). Evaluation of UASB reactor performance during start-up operation using synthetic mixed-acid waste. *Bioresource Technology,* 99(17), 8231–8236.

Ugoji, E. O. (1997). Anaerobic digestion of palm oil mill effluent and its utilization as fertilizer for environmental protection. *Renewable Energy, 10*(23), 291-294.

Wang, G., Mu, Y. & Yu, H. Q. (2005). Response surface analysis to evaluate the influence of pH, temperature and substrate concentration on the acidogenesis of sucrose-rich wastewater. *Biochem. Eng. J., 23*, 175-184.

Wang, J. & Wan, W. (2008). Effect of temperature on fermentative hydrogen production by mixed cultures. *Int J Hydrogen Energy, 33*, 5392–5397.

Wang, J. & Wan, W. (2009). Factors influencing fermentative hydrogen production: A review. *Int J Hydrogen Energy, 34*, 799–811.

Wang, X. & Jin, B. (2009). Process optimization of biological hydrogen production from molasses by a newly isolated Clostridium butyricum W5. *Bioscience and Bioeng., 107*,138–144.

Wu, K. J. & Chang, J. S. (2007). Batch and continuous fermentative production of hydrogen with anaerobic sludge entrapped in a composite polymeric matrix. *Process Biochem., 42*, 279–284.

Wu, S. Y., Lin, C. N. & Chang, J. S. (2003). Hydrogen production with immobilized sewage sludge in three-phase fluidized-bed bioreactors. *Biotech. Progress, 19*, 828-832.

Wu, S. Y., Lin, C. N., Chang, J. S. & Chang, J. S. (2005). Biohydrogen production with anaerobic sludge immobilized by ethylene-vinyl acetate copolymer. *Int J Hydrogen Energy, 30*, 1375–1381.

Xing, D. F., Ren, N. Q., Wang, A. J., Li, Q. B., Feng, Y. J. & Ma, F. (2008). Continuous hydrogen production of auto-aggregative Ethanoligenens harbinense YUAN-3 under non-sterile condition. *Int J Hydrogen Energy, 33*, 1489–1495.

Yang, M. & Yu, H. Q. (2007). Simulation of biological hydrogen production in a UASB reactor using neural network and genetic algorithm, *Int J Hydrogen Energy, 32*, 3308-3314.

Yang, P., Zhang, R., McGarvey, J. A. & Benemann, J. R. (2007). Biohydrogen production from cheese processing wastewater by anaerobic fermentation using mixed microbial communities. *Int J Hydrogen Energy, 32*, 4761–4771.

Yang, S. & Lewandowski, Z. (1995). Measurement of local mass transfer coefficient in biofilms. *Biotechnol. and Bioeng., 48*, 737-746.

Yokoi, H., Saitsu, A., Uchida, H., Hirose, J., Hayashi, S. & Takasaki, Y. (2001). Microbial hydrogen production from sweet potato starch residue. *Bioscience and Bioeng., 91*, 58–63.

Younesi, H., Najafpour, G., Syahidah, K. K. I., Abdul Rahman, M. & Azlina, H. K. (2008). Biohydrogen production in a continuous stirred tank bioreactor from

synthesis gas by anaerobic photosynthetic bacterium: *Rhodopirillum rubrum*. *Bioresource Technology, 99*, 2612-2619.

Yu, H. Q. & Mu, Y. (2006). Biological hydrogen production in a UASB reactor with granules. II: Reactor performance in 3-year operation. *Biotech. Bioeng., 94*, 988-995.

Yu, H., Zhu, Z., Hu, W. & Zhang, H. (2002). Hydrogen production from rice winery wastewater in an upflow anaerobic reactor by using mixed anaerobic cultures. *Int J Hydrogen Energy, 27*, 1359–1365.

Zadariana, J., Annuar, M. S. M., Shaliza, I. & Vikineswary, S. (2009). Optimization of phototrophic hydrogen production by Rhodopseudomonas palustris PBUM001 via statistical experimental design. *Int J Hydrogen Energy, 34*, 7502-7512.

Zhang, H., Bruns, M. A. & Logan, B. E. (2006). Biological hydrogen production by clostridium acetobutylicum in an unsaturated flow reactor. *Water Res., 40*,728-734.

Zhang, Y. & Shen, J. (2006). Effect of temperature and iron concentration on the growth and hydrogen production of mixed bacteria. *Int J Hydrogen Energy, 31*, 441–446.

Zhang, Z. P., Show, K. Y., Tay, J. H., Liang, D. T. & Lee, D. J. (2008). Biohydrogen production with anaerobic fluidized bed reactors-A comparison of biofilm-based and granule-based systems. *Int J Hydrogen Energy, 33*, 1559–1564.

Zhang, Z. P., Tay, J. H., Show, K. Y., Liang, D. T., Lee, D. J. & Jiang, W. J. (2007). Biohydrogen production in a granular activated carbon anaerobic fluidized bed reactor. *Int J Hydrogen Energy, 32*, 185–191.

Zhao B-H., Yue Z-B., Zhao Q-B., Mu Y., Yu H-Q., Harada H. & Li Y-Y. (2008). Optimization of hydrogen production in a granule-based UASB reactor. *Int J Hydrogen Energy, 33*, 2454-2461.

Zhao, Q. B. & Yu, H. Q. (2008). Fermentative H_2 production in an upflow anaerobic sludge blanket reactor at various pH values. *Bioresource Tech., 99*, 1353–1358.

Zhou, J. B., Wang, K. S., Shen, H. T. & Wang, S. B. (2004). Dynamic equations of impurity hydrogen during heavy water electrolysis. *Int J Hydrogen Energy, 29*, 1393–96.

Zhu, H. G. & Beland, M. (2006). Evaluation of alternative methods of preparing hydrogen producing seeds from digested wastewater sludge. *Int J Hydrogen Energy, 31*, 1980–1988.

Zhu, J., Li, Y., Wu, X., Miller, C., Chen, P. & Ruan, R. (2009). Swine manure fermentation for hydrogen production. *Bioresource Tech., 100*, 5472-5477.

Zinatizadeh, A. A. L., Mohamed, A. R., Abdullah, A. Z., Mashitah, M. D., Hasnain Isa, M. & Najafpour, G. D. (2006). Process modeling and analysis of palm oil mill effluent treatment in an up-flow anaerobic sludge fixed film bioreactor using response surface methodology (RSM). *Water Research, 40*, 3193–3208.

Zinatizadeh, A. A. L., Mohamed, A. R., Mashitah, M. D., Abdullah, A. Z. & Hasnain Isa, M. (2007). Optimization of pre-treated palm oil mill effluent digestion in an up-flow anaerobic sludge fixed film bioreactor: A comparative study. *Biochemical Engineering Journal, 35*, 226–37.

Zoetemeyer, R. J., Matthijsen, A. J. C. M., Cohen, A. & Boelhouwer, C. (1982). Product inhibition in the acid forming stage of the anaerobic digestion process. *Water Research, 16*, 633–639.